University of Pisa
Department of Pharmacy

Doctoral School
Clinical Pathophysiology and Science of Medicine
Research Program
Medical Pathophysiology and Pharmacology

New pharmacological strategies for cutaneous malignant melanoma

Candidate:
Sara Carpi
(sara.carpi@for.unipi.it)

Tutor:
Prof.ssa Paola Nieri

Dean
Prof.ssa Maria Cristina Breschi
Cycle
XXVII
Scientific Area
BIO/14
Academic year
2013/2014

Scientific products

Publications:

1 "Theranostic properties of a survivin-directed molecular beacon in human melanoma cells"
S. Carpi, S. Fogli, A. Giannetti, B. Adinolfi, S. Tombelli, E. Da Pozzo, A. Vanni, E. Martinotti, C. Martini, M. C. Breschi, M. Pellegrino, P. Nieri, F. Baldini
Plos One, 2014 Dec 11;9(12):e114588.

2 "Complex nanostructures based on oligonucleotide optical switches and nanoparticles for intracellular mRNA sensing and silencing"
B. Adinolfi, S. Carpi, A. Giannetti, P. Nieri, M. Pellegrino, G. Sotgiu, S. Tombelli, C. Trono, G. Varchi, F. Baldini
Procedia Engineering 87 (2014) 751 – 754.

3 "Selection of a human butyrylcholinesterase-like antibody single-chain variable fragment resistant to AChE inhibitors from a phage library expressed in E. coli."
Podestà A, Rossi S, Massarelli I, Carpi S, Adinolfi B, Fogli S, Bianucci AM, Nieri P.
MAbs. 2014 Jul-Aug;6(4):1084-93.

4 "AM251 induces apoptosis and G2/M cell cycle arrest in A375 human melanoma cells"
S. Carpi, S. Fogli, A. Romanini, M. Pellegrino, B. Adinolfi, A. Podestà, B. Costa, E. Da Pozzo, C. Martini, M.C. Breschi, P. Nieri
Submitted to British Journal of Pharmacology, manuscript ID: 2014-BJP-1571-RP.

5 "New quinolone- and 1,8-naphthyridine-3-carboxamides as selective CB2 receptor agonists with anticancer and immuno-modulatory activity"
C. Manera; A. M. Malfitano; T. Parkkari; V. Lucchesi; S. Carpi; S. Fogli; S. Bertini; C. Laezza; A. Ligresti; G. Saccomanni; J. R. Savinainen; E. Ciaglia; S. Pisanti; P. Gazzerro; V. Di Marzo; P. Nieri; M. Macchia; M. Bifulco
Submitted to European Journal of Medicinal Chemistry, manuscript ID: EJMECH-S-14-02633-1.

Oral communications:

1 S. Carpi, S. Fogli, A. Giannetti, B. Adinolfi, S. Tombelli, F. Baldini, E. Da Pozzo, A. Vanni, E. Martinotti, C. Martini, M. C. Breschi, M. Pellegrino, P. Nieri. *Theranostic properties of a survivin-directed molecular beacon in human melanoma cells*. "XVII Seminario Società Italiana di Farmacologia" September 16-18, 2014 Rimini (Italy).

2 B. Adinolfi, S. Carpi, A. Giannetti, P. Nieri, M. Pellegrino, G. Sotgiu, S. Tombelli, C. Trono, G. Varchi, F. Baldini. *Complex nanostructures based on oligonucleotide optical switches and nanoparticles for intracellular mRNA sensing and silencing*. "Eurosensors" September 7-10, 2014 Brescia (Italy).

3 B. Adinolfi, S. Tombelli, A. Giannetti, C. Trono, M. Pellegrino, S. Carpi, P. Nieri, G. Sotgiu, G. Varchi, F. Baldini. *Complex nanostructures based on a specific molecular beacon and PMMA nanoparticles for the detection and silencing of survivin mRNA in human cancer cells*. "Nanomedicine" September 17-19, 2014 Viterbo (Italy).

4 S. Tombelli,, B. Adinolfi, A. Giannetti, C. Trono, M. Pellegrino, S. Carpi, P. Nieri, G. Sotgiu, G. Varchi, F.Baldini. *Molecular beacons and PMMA nanoparticles for the detection and silencing of mRNA in human cancer cells.* "Functional DNA Nanotechnology Workshop" June 19-20, 2014 Rome (Italy).

5 B. Adinolfi , A. Giannetti, S. Tombelli, C. Trono, F. Chiavaioli, S. Carpi, P. Nieri, S. Fogli, M. Pellegrino, G. Sotgiu, G. Varchi, F. Baldini. *Detection and silencing of survivin mRNA by bi-color imaging based on PMMA nanoparticles/molecular beacon in human cancer cells*. "5th International BioNanoMed" March 26-28, 2014 Krems (Austria).

6 F. Baldini, M. Ballestri, S. Carpi, S.G. Conticello, G. Giambastiani, A. Giannetti, A. Guerrini, R. Mercatelli, P. Nieri, F. Quercioli, F. Severi, G. Sotgiu, S. Tombelli, C. Trono, G. Tuci, G. Varchi. *Molecular beacon as oligonucleotide nanosensors for intracellular mRNA*. "The Italian National Conference on Condensed Matter Physics (Including Optics, Photonics, Liquids, Soft Matter) FisMat" September 9-13, 2013 Milan (Italy).

7 F. Baldini, M. Ballestri, S. Carpi, S.G. Conticello, G. Giambastiani, A. Giannetti, A. Guerrini, R. Mercatelli, P. Nieri, F. Quercioli, F. Severi, G. Sotgiu, S. Tombelli, C. Trono, G. Tuci, G. Varchi. *Oligonucletide Switches and Nanomaterials for Intracellular mRNA Sensing.* "European Conferences on Biomedical Optics (ECBO)" May 12-16, 2013 Messe Munchen (Germany).

8 Adinolfi B, Carpi S, Fogli S, Giannetti A, Baldini F, Pellegrino M, Vanni A, Martinotti E, Breschi MC, Nieri P. *Survivin mRNA detection and silencing by a Molecular Beacon Oligodeoxynucleotide in living cutaneous melanoma cells.* "VI Convegno Monotematico SIF, Gruppo di Lavoro Farmacologia Oncologica, La Farmacologia oncologica tra innovazione ed evidenza clinica" November 30, December 1, 2012 Siena (Italy).

9 F. Baldini, M. Ballestri, S. Carpi, S.G. Conticello, G. Giambastiani, A. Giannetti, A. Guerrini, R. Mercatelli, P. Nieri, F. Quercioli, F. Severi, G. Sotgiu, S. Tombelli, C. Trono, G. Tuci, G. Varchi. *Molecular beacon-coated PMMA nanoparticles for the intracellular detection of tumour associated mRNA*. "Nanotechitaly2012" November 21-23, 2012 Venezia (Italy).

Poster:

1 S. Carpi, B. Adinolfi, S. Fogli, A. Giannetti, S. Tombelli, F. Baldini, E. Da Pozzo, A. Vanni, E. Martinotti, M.C. Breschi, M. Pellegrino, P. Nieri. *Survivin-directed molecular beacon as potential theranostic agent in melanoma cells*. "Global Biotechnology Congress" June 16-19, 2014 Boston MA (USA).

2 S. Tombelli, A. Giannetti, C.Trono, B. Adinolfi, M. Pellegrino, S. Carpi, P. Nieri, G. Sotgiu, G. Varchi, F.Baldini. *Complex nanostructures based on oligonucleotide optical switches and nanoparticles for intracellular sensing*. "EUROPT(R)ODE XII" April 13-16, 2014 Athens (Greece).

3 S. Carpi, B. Adinolfi, S. Fogli, A. Giannetti, S. Tombelli, F. Baldini, A. Vanni, E. Martinotti, M.C. Breschi, M. Pellegrino, P. Nieri. *Survivin directed molecular beacon as potential "theranostic agent" in melanoma cells*. "36° Congresso Nazionale SIF" October 23-26, 2013 Torino (Italy).

4 A.Giannetti, S.Tombelli, C.Trono, M.Ballestri, G.Giambastiani, S.Carpi, S.G.Conticello, A.Guerrini, R.Mercatelli, P.Nieri, F.Quercioli, F Severi, G Sotgiu, G.Tuci, G.Varchi, F.Baldini. *PMMA nanopaticles and carbon nanotubes as intracellular carriers of molecular beacons for mRNA sensig and imaging*. "3rd Conference on Innovation in Drug Delivery: Advances in Local Drug Delivery (Apgi and Adritelf)" September 22-25, 2013 Pisa (Italy).

5 S. Carpi, A. Giannetti, F. Baldini, M. Pellegrino, B. Adinolfi, A. Vanni, E. Martinotti, P. Nieri. *Survivin mRNA detection and silencing by a molecular beacon oligodeoxynucleotide in living melanoma cells*. "XVI Seminario SIF Dottorandi e Assegnisti di Ricerca" September 16-19, 2012 Rimini (Italy).

Abstract

Human cutaneous melanoma is an aggressive and chemotherapy resistant type of cancer. Although the development of new targeted therapies and immunologic agents has completely changed the treatment guidelines, one of the most important tasks for the future will be to overcome acquired resistance. In this thesis we investigated different pharmacological strategies against human melanoma cells. Particularly, we demonstrated the theranostic properties (i.e., the ability of imaging and pharmacological silencing activity) of a molecular beacon-oligodeoxynucleotide (MB) that targets survivin mRNA. This may represent an innovative approach for cancer diagnosis and treatment in melanoma patients because survivin is an inhibitor of apoptosis overexpressed in tumor cells and almost undetectable in human melanocytes. We also provide evidence of the pro-apoptotic effect and cell cycle arrest ability of AM251, a cannabinoid type 1 receptor antagonist/inverse agonist with an anticancer potency comparable to that observed for cisplatin. This compound may be a potential prototype for the development of promising diarylpyrazole derivatives to be evaluated in human cutaneous melanoma. Finally, we demonstrated that the cannabinoid type 1 receptor is markedly expressed in stem-like cells and not expressed in the BRAF-wild type parental cells. Otherwise, both primary BRAF-mutated melanoma cultures and their correspondent melanoma-initiating cells expressed high levels of this receptor subtype. These findings suggest a possible role of the endocannabinoid system in determining the phenotype of melanoma cells and their potential to cause central nervous system metastases.

Sommario

Il melanoma è un tumore aggressivo e resistente alla chemioterapia. Lo sviluppo di nuove terapie mirate e immunoterapie ha completamente cambiato le linee guida del trattamento del melanoma ma, il compito più importante per il futuro è quello di superare la resistenza. In questa tesi abbiamo studiato diverse strategie farmacologiche contro le cellule di melanoma umano. In particolare, abbiamo dimostrato le proprietà teranostiche (cioè, capacità di imaging coniugata con attività farmacologica di silenziamento) di un oligodesossinucleotide antisenso molecular beacon (MB) diretto verso l'mRNA codificante per la survivina. Questo può rappresentare un approccio innovativo per la diagnosi ed il trattamento in pazienti affetti da melanoma perché la survivina è un inibitore dell'apoptosi sovraespresso in diversi tipi di tumore e non rilevabile nella maggior parte dei tessuti sani (melanociti). Abbiamo anche valutato le capacità di blocco del ciclo cellulare e pro-apoptotica di AM251, un antagonista/agonista inverso del recettore dei cannabinoidi di tipo 1 (CB1) con una potenza antitumorale paragonabile a quella osservata per il cisplatino. Questo composto può pertanto rappresentare un potenziale prototipo per lo sviluppo di derivati diaril-pirazolici con attività nel melanoma cutaneo umano. Infine, abbiamo dimostrato la marcata espressione del recettore CB1 in cellule simil-staminali derivanti da pazienti e la sua non espressione nelle cellule parentali tipo BRAF non mutato. Invece, le culture primarie di melanoma con mutazione BRAF e le cellule simil-staminali derivanti esprimono alti livelli di questo sottotipo recettoriale. Questi risultati suggeriscono un possibile ruolo del sistema endocannabinoide sia nel determinare il fenotipo di melanoma sia nel causare metastasi a livello del sistema nervoso centrale.

Contents

List of Figures

Chapter 1

Introduction

1.1 Definition of melanoma

Melanoma is a form of cancer that begins in melanocytes, cells that make the pigment melanin (Fig. 1.1). It may begin in a mole (skin melanoma), but can also begin in other pigmented tissues, such as in the eye or in the intestines (National Cancer Institute, Melanoma, 2014). It is called also malignant melanoma, melanocarcinoma, melanoepithelioma, melanosarcoma (Merriam-Webster, 2014).

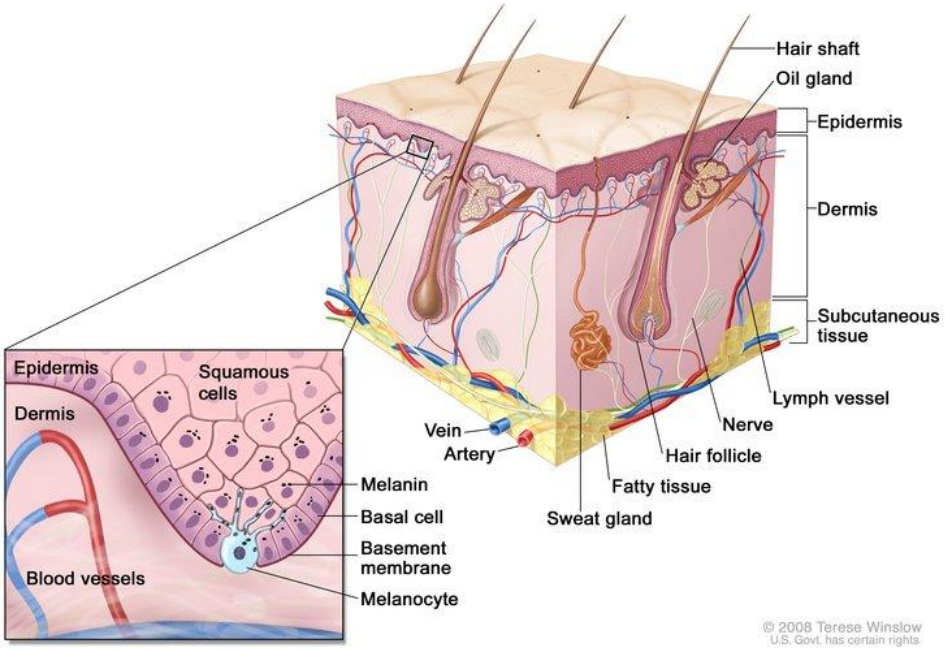

Figure 1.1 Schematic representation of normal skin. The pullout shows a close-up of the squamous cell and basal cell layers of the epidermis, the basement membrane in between the epidermis and dermis, and the dermis with blood vessels. Melanin is shown in the cell (National Cancer Institute, Melanoma Anatomy, 2014).

1.2 Epidemiology

Until a few years ago, melanoma was considered a tumor rare, and very rare until adolescence, while currently it represents an incidence in continued growth (Tsao et al., 2004) and the second most common cancer in adolescents (Kauffmann et al., 2014).

It is estimated that in the last decade, melanoma skin has reached the 132,000 new cases a year worldwide: an increase of about 15% compared to the previous decade (Tsao et al., 2004). Its incidence varies considerably between different areas of the world. Melanoma affects predominantly caucasians, but there are significant geographical differences: the highest rates are observed in populations of Australia and New Zealand, which have values 2-3 times higher than North America and Europe. In Europe there is a gradual reduction from north to south. Incidence rates are low in Asian and black people (Globacan 2012, 2014). About 80% of cutaneous melanomas that arise annually in the world affects the populations of North America, Europe and Oceania (Fig. 1.2) (Globacan 2012, 2014). The current melanoma risk for Australian and New Zealander populations may be as high as 1 out of 50 (Rigel, 2010).

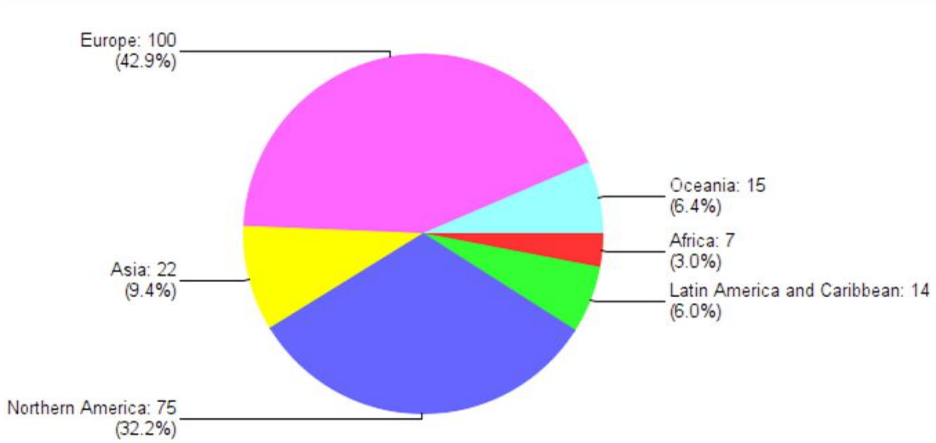

Figure 1.2 Estimated number of cancer cases (x1000) of melanoma of skin in all ages and both sexes (Globacan 2012, 2014).

In 2014, an estimated, 76,100 patients will be diagnosed and about 9700 patients will die of melanoma in the United States (Siegel et al., 2014). In Italy, an estimated 11,000 new cases in 2014 (with a slight predominance in males) (Aiom-airtum, 2014). Melanoma is increasing in men more rapidly than any other malignancy except lung cancer (Fig. 1.3) (Jemal et al., 2011). Although melanoma can affect persons of essentially any age, it is mainly a disease of adulthood, with median ages of diagnosis and death between 61 and 68 years, respectively (Weinstock, 2012).

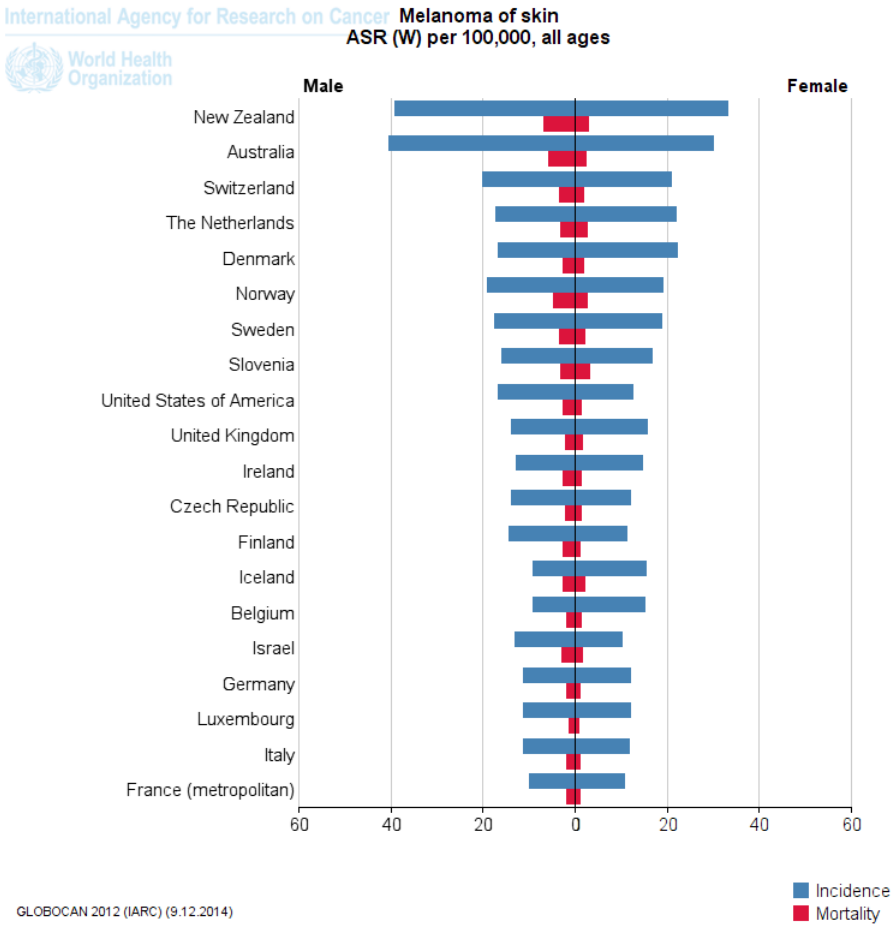

Figure 1.3 Incidence and mortality of melanoma worldwide in all ages (Globacan 2012, 2014).

The 5-year survival rate for localized (stage I and II) melanoma is 98%; however, this drops to 16% in cases where cancer has metastasized to distant sites or organs (Wolchok, 2014).

1.3 Risk Factors

The risk of developing melanoma is highly dependent on the interaction between endogenous risk factors and environmental risk factors. The recognition of groups of individuals with different risk and the application of appropriate strategies for prevention, are the key points to reduce morbidity and mortality from melanoma (Tsao et al., 2004). The skin phototype, the total number of nevi and in particular of dysplastic nevi, indices of solar exposure, the family history of melanoma which has been cited for the hereditary mutation of the tumor suppressor gene CDKN2A (cyclin-dependent kinase inhibitor type 2A) (Aitken et al., 1999) and a long series of genetic alterations (Gudbjartsson et al., 2008) as well as the states of immunodeficiency are personal risk factors. These factors (Tab. 1.1)

contribute independently in the development of cutaneous melanoma (Gandini et al., 2005).

Risk Factors
Fitzpatrick skin type I or II (blond or red hair, clear skin and clear eyes)
UV exposure
Genetic factors
Higher number of nevi
Nevi that develop in adulthood
Histologically displkastic nevi
Personal or family history of melanoma
Personal or family history of basal cell or squamous cell carcinomas
Depressed immune system
Sex
Age

Table 1.1 Risk factors for melanoma (Helfand et al., 2001).

Exposure to UV rays, which generally gives double the risk of developing melanoma in exposed with respect to non-exposed individuals, increases markedly in phototype clear people (Vainio et al., 2000). Moreover, it was shown that advanced age and male sex are associated with a higher incidence and a poorer prognosis (Fig. 1.3) (Lasithiotakis et al., 2008). Retrospective studies on a large scale have shown that a previous melanoma is the most important predictor for a subsequent melanoma. It was also calculated that the cumulative probability of developing a second melanoma at 5 and 10 years of distance is 2.8% and 3.6%, respectively (Goggins et al., 2003).

Several molecular genetic studies have shown the relevant role of some genes as risk factors for susceptibility to melanoma (Fig. 1.6). To date, two high penetrance susceptibility genes, the CDKN2A and CDK4 (cyclin-dependent kinase type 4), and a low-penetrance susceptibility gene, the MC1R (melanocortin 1 receptor) have been identified (Fargnoli et al., 2006; Meyle et al., 2009).

1.4 Melanoma pathogenesis

Melanoma is characterized by complex changes in multiple signaling pathways that control cell proliferation and ability to evade the cell death processes. Impairment or hyper-activation of some components of these

pathways may lead to malignant transformation and cancer development. The most relevant signaling pathways involved in development and progression of melanoma are Rb/E2F, MAPK/ERK, PI3K/Akt/, NF-kB, Wnt/β-catenin, Notch, Jak/STAT, cyclin/CDK, JNK/c-Jun/AP-1, MITF and some growth factors.
In the following sub-paragraphs further insights on the principal pathways are given for their relevance in the comprehension of the action mechanism of drugs cited in the 1.6 paragraph.

1.4.1 Rb/E2F

E2F is a transcription factor involved in the cell cycle regulation and synthesis of DNA in eukaryotic cells through binding site in the target promoter sequence (Halaban et al., 2005). G1/S transition is controlled by transcription factor E2F, which triggers expression of target genes that encode proteins involved in DNA synthesis and its regulation (Uzdensky et al., 2013). Rb (retinoblastoma) is a tumor suppressor that represses the expression of E2F regulated genes required for cell cycle progression. Rb is inactivated in melanomas and other cancer cells by phosphorylation catalyzed by persistent cyclin dependent kinase (CDK) activity (Fig.1.4).

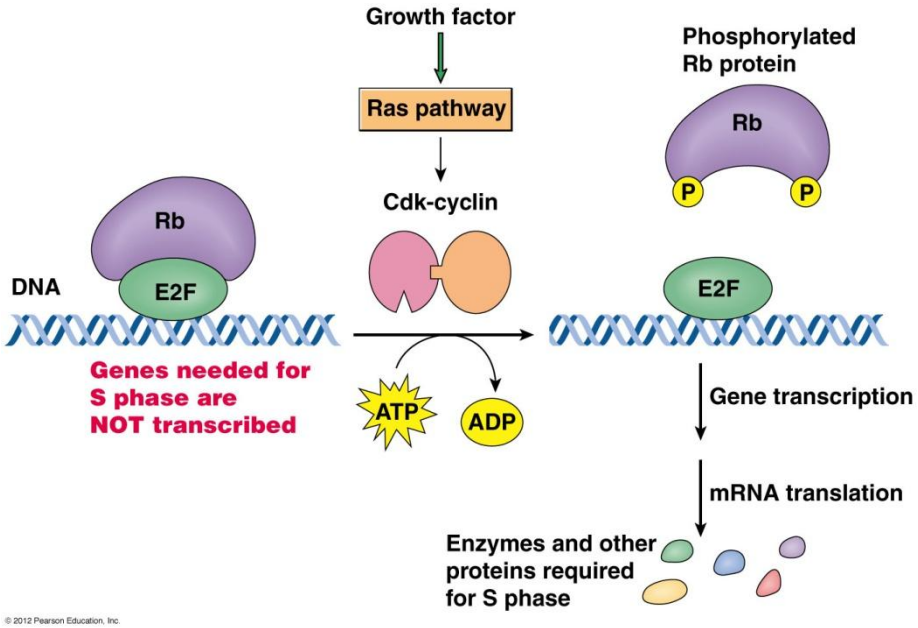

Figure 1.4 Pathway Rb/E2F (Hardin et al. 2012).

The molecular events that lead to autonomous proliferation of melanoma cells include sustained activity of CDK2 (cyclin dependent kinase type 2), CDK4 and CDK6 (cyclin dependent kinase type 6) as a result of mutations or loss of CDK inhibitors such as $p16^{INK4}$ (cyclin-dependent kinase inhibitor 2A) and $p27^{KIP1}$ (cyclin-dependent kinase inhibitor 1B) (Fig. 1.5).

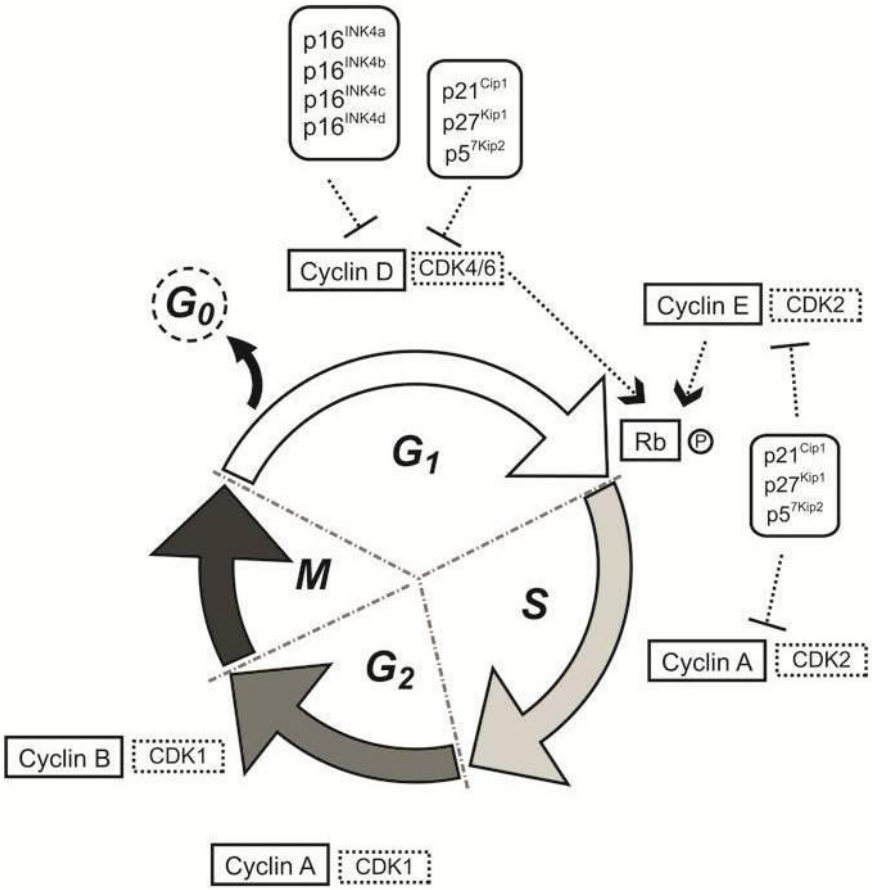

Figure 1.5 Schematic representation of the eukaryotic cell cycle with cyclins playing a role in the different stages (Currais et al., 2009).

In melanoma cells Rb is permanently and highly phosphorylated (Carnero, 2002). This prevents their binding to E2F and so E2F result activated and mantains the transcription of target genes involved in G1/S transition, that is a key event in malignant melanocyte transformation (Ibrahim et al., 2009).

1.4.2 CDKN2A

The gene CDKN2A simultaneously encodes two tumor suppressor proteins, $p16^{INK4a}$ and $p14^{ARF}$ (ARF tumor suppressor) (Fig. 1.5). In pathogenesis of both sporadic and familial melanoma CDKN2A is often inactivated due to deletion, mutation or promoter hypermethylation. CDKN2A is the principal target in UV mediated melanoma (Harland et al., 2014). Its mutations were found in 20-40% of familial cutaneous melanomas (Fig.1.6).

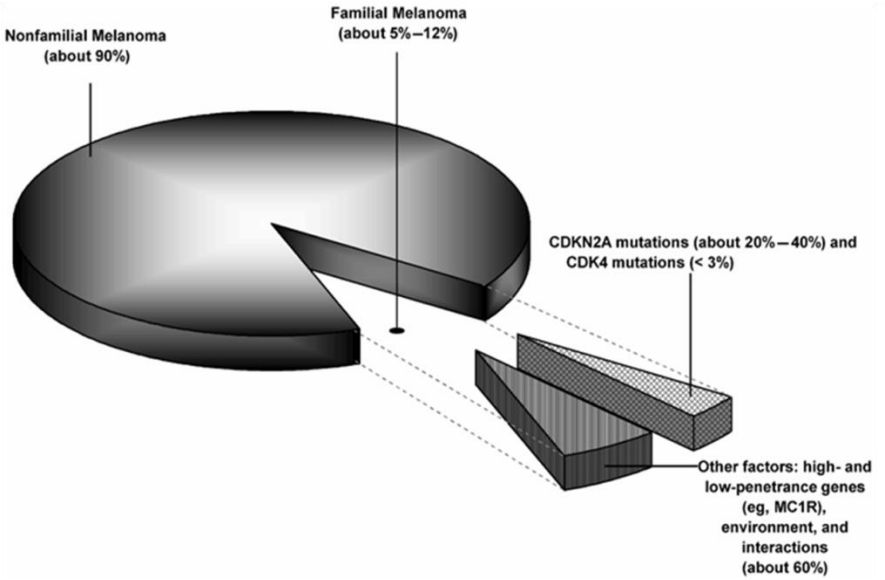

Figure 1.6 Prevalence of CDKN2A mutations in hereditary melanoma (Harland et al., 2014).

Protein $p16^{INK4a}$ prevents interaction of CDK4/6 with cyclin D1(Fig. 1.5) that leads to decrease in pRb phosphorylation, sequestration of E2F, and G1/S arrest (Fig. 1.4). The mutations levels are low in normal proliferating cells but rapidly increases under stressful genotoxic impacts such as UV (Giles et al., 2012). These alterations correspond to melanoma progression and poor prognosis.

Protein $p14^{ARF}$ boosts p53-mediated apoptosis and thereby prevents reproduction of tumor cells. Inactivation of p53 is the most common molecular injury in human cancer cells. However, in melanoma the TP53 gene that encodes p53 mutates rather seldom (only 9%) (Mihic et al., 2010).

1.4.3 MAPK/ERK

MAPK (mitogen-activated protein kinase)/ERK (extracellular signal-regulated kinases) pathway is also known as Ras-Raf-MEK-ERK pathway from the proteins involved. Constitutive activation of the this pathway mediates critical events in melanoma growth, progression, regulation of apoptosis, adhesion, migration, and melanoma vascularization (Eisenmann et al., 2003; Woods et al., 2001).

Ras identifies a class of proteins called small GTPases, located at the plasma membrane which are involved in cellular signal transduction, whereas the downstream kinases Raf, MEK and ERK are cytosolic residents (Fig. 1.7).

After binding of some ligands, such as growth factors to their respective receptor (tyrosine kinase, RTK), receptor dimerization triggers the intrinsic

tyrosine-kinase, activating MAPK pathway. Like other GTPase proteins, Ras cycles between the GDP (guanosine diphosphate) -bound inactive form and the GTP (guanosine -5'triphosphate) -bound active form. In the quiescent state, Ras exists in the GDP-bound form. The binding of SOS (Son Of Sevenless, a small GTPase) to Ras causes a change in the Ras conformation and leads to the dissociation of GDP and binding of GTP. GTP-bound Ras is the activator of this signaling module. It initiates the signal cascade by phosphorylating Raf. Raf, in turn, phosphorylates the MEK (MEK1 and MEK2), which then phosphorylates ERK (extracellular signal-regulated kinases, ERK1 and ERK2). Activated ERKs then translocate into the nucleus where they phosphorylate specific substrates that are involved in the regulation of various cellular responses (Chin, 2003) ERK induced production of various transcription factors involved in regulation of proliferation and apoptosis prevention and G1/S transition as cyclin D (Fig. 1.6) (Uzdensky et al., 2013).

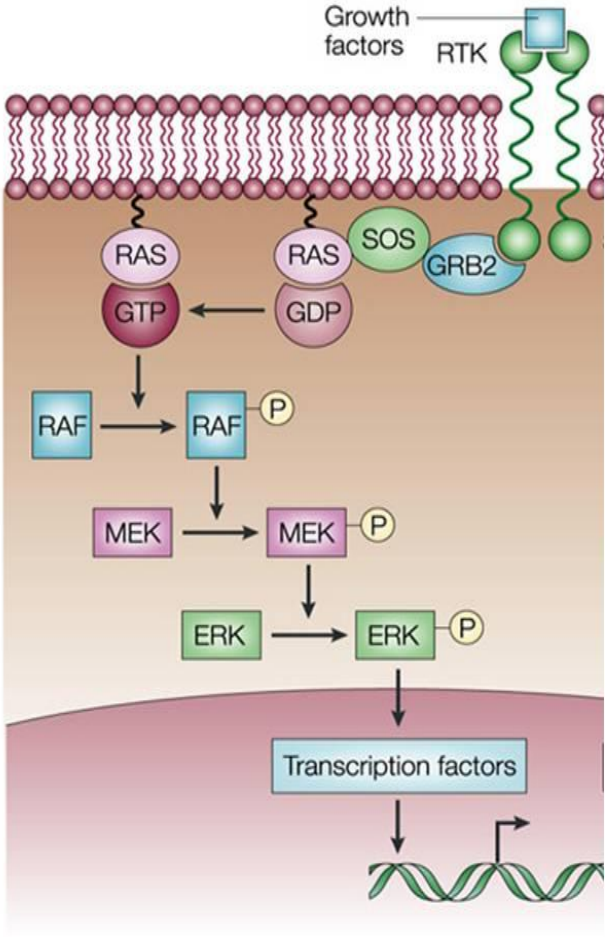

Figure 1.7 Activation of the MAPK/ERK signaling pathway (Chin, 2003).

Mutated Ras or Raf proteins permanently stimulate cell proliferation, tumor invasion and metastasis. Such mutations were observed in >90% of clinical cases of melanoma (Smalley, 2010).
The Ras subfamily consists of three isoforms: H-Ras, K-Ras and N-Ras. NRAS is mainly related to melanoma pathogenesis. NRAS mutations were found in 15-30% of melanoma cases (Sekulic et al., 2008).
The Raf subfamily consists of isoforms A-Raf, B-Raf and C-Raf (also called Raf-1). Braf mutations are the most relevant in melanoma and have been found in 60-70% of primary melanoma but also in a high % of cutaneous melanocyte nevi; it is considered a risk factor involved in initiation rather than in progression of melanomas. Although more than 40 different mutations in BRAF gene have been described, the most clinically relevant mutation is the BRAF T1799A, which results in the substitution of valine by glutamic acid (V600E) in the kinase domain of the protein. Mutated Braf protein permanently activates ERK and stimulates proliferation. The mutation V600E, is found in 80-90% of all BRAF mutations in melanoma. ARAF and CRAF are found seldom in melanoma and actually are not considered relevant (Platz et al., 2008).

1.4.4 PI3K/Akt/mTOR

The phosphatidylinositol-3-kinase (PI3K)/ protein kinase B (Akt) and the mammalian target of rapamycin (mTOR) signaling pathways (Fig. 1.8) make a crucial network to many aspects of cell growth and survival, in physiological as well as in pathological conditions (e.g., cancer) (Porta et al., 2014).
The PI3K/Akt pathway is a key regulator of survival during cellular stress (Datta et al., 1999). Since tumors exist in an intrinsically stressful environment (characterized by limited nutrient and oxygen supply, as well as by low pH), the role of this pathway in cancer appears to be crucial.

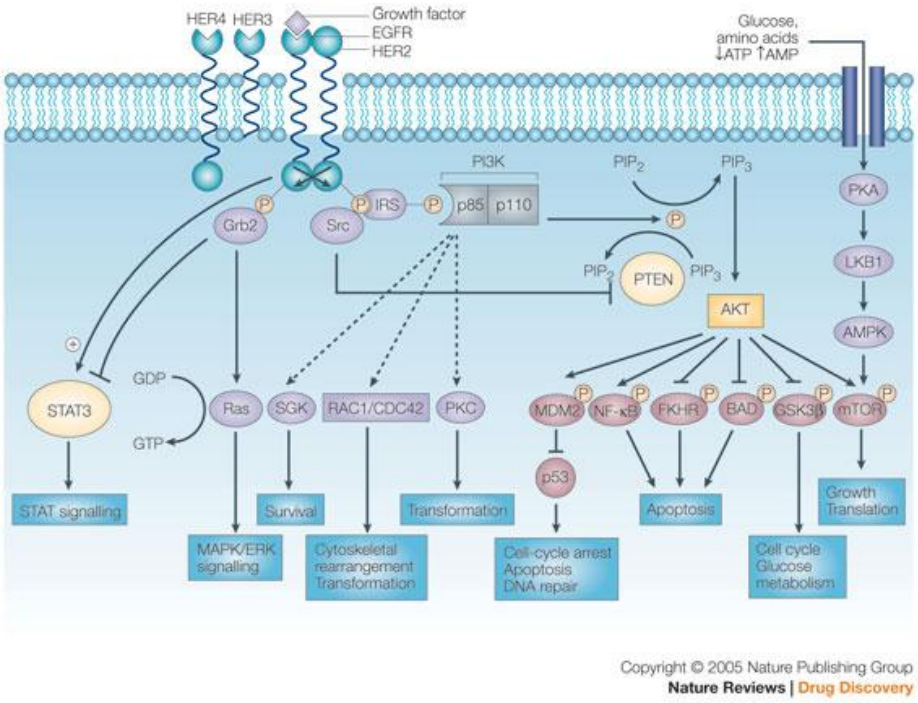

Figure 1.8 Schematic of signaling through the PI3K/AKT pathway (Hennessy et al., 2005).

PI3Ks constitute a lipid kinase family enzymes capable of phosphorylating the 3 position hydroxyl group of the inositol ring of phosphatidylinositol. The PI3K/AKT and related pathways are important in internalizing the effects of external growth factors and of membrane tyrosine kinases. Activation of growth factor receptor protein tyrosine kinases results in autophosphorylation on tyrosine residues (Fig. 1.8) and subsequent events to activate these intracellular pathways. This leads to activation of PI3K and this leads to the production of the second messenger phosphatidylinositol-3,4,5-triphosphate (PIP3) from the substrate phosphatidylinositol-4,4-bisphosphate (PIP2). This provides anchoring of Akt at the plasma membrane, where it is phosphorylated by phosphoinositide dependent protein kinase-1 (PDK1) that is also activated by PI3K.

Activation of Akt regulates several cell processes involved in cell survival and cell cycle progression. Akt phosphorylates and thereby inactivates the pro-apoptotic proteins Bad (Bcl-2-associated death promoter), Bim, Bax (Bcl-2-associated X protein) and caspase-9. Moreover, Akt- activates the protein MDM2 (Mouse double minute 2*)*, which down-regulates p53 (tumor suppressor). Akt also activates the transcription factors CREB (cAMP response element-binding protein), E2F and NF-κB (Nuclear factor

kappa-light-chain-enhancer of activated B cells) involved in cell protection and survival. Activated Akt stimulates proliferation and tumorigenesis through up-regulation of cyclin D1, which controls G1/S transition, and inhibition of p21 (cyclin-dependent kinase inhibitor 1) and p27, which prevent G1/S transition (Fig. 1.5). Akt-mediated activation of mTOR also suppresses apoptosis and stimulates protein synthesis, proliferation and angiogenesis. Other effects of PI3K/Akt/mTOR is mediated by the transcription factor HIF1 (hypoxia-inducible factor-1) and VEGF (vascular endothelial growth factor) (Madhunapantula et al, 2009).

The Akt family comprises three isoforms: Akt1, Akt 2 and Akt3, but only Akt3 is the predominant isoform in melanoma cells. Overexpression and overactivation of Akt3 are characteristic for 60-70% of sporadic melanomas. Significant phosphorylation of Akt3 was registered in 17%, 43%, 49% and 77% of biopsies from normal nevi, dysplastic nevi, primary melanoma and melanoma metastases, respectively (Stahl et al., 2004).

The PI3K/Akt pathway is regulated by the lipid phosphatase PTEN, (phosphatase and tensin homolog) that acts as a tumor suppressor by inhibiting cell growth and enhancing cellular sensitivity to apoptosis. PTEN removes phosphate groups from PIP3 and converts it into PIP2 (Fig. 1.8), preventing Akt binding and activation. PTEN also inhibits the Raf/ERK pathway (Stahl et al., 2003) and its impairment has been found related to about 40-50% cases of sporadic melanoma (Stahl et al., 2003). Sun ultraviolet radiation, the major risk factor for skin cancer, induces PTEN mutations that promote melanoma promotes melanoma growth (Hocker et al., 2007). The PTEN and NRAS or BRAF mutations cooperate in melanoma development and metastasis (Dankort et al., 2009).

mTOR is a bioenergetic sensor and it is a master regulator of protein synthesis, proliferation, autophagy, apoptosis and other cellular processes. It serves as a sensor of abundance of metabolites and energy depletion in the cell (Fig. 1.8). It is stimulated by protein Rag, which is activated by free amino acids. AMP-activated protein kinase (AMPK) inhibits mTOR and thereby mTOR-mediated protein synthesis, when ATP (adenosine triphosphate) depletion induces accumulation of AMP (adenosine monophosphate). Activation of the PI3K/Akt pathway by growth factors stimulates mTOR (Fig. 1.9). mTOR forms two signaling complexes: mTORC1 and mTORC2. mTORC1 contains proteins mTOR, GβL (G protein β-like) and RAPTOR (regulatory-associated protein of mTOR), whereas in mTOR2 RAPTOR is substituted by RICTOR (rapamycin-insensitive companion of mammalian target of rapamycin). mTORC1 stimulates protein synthesis and inhibits autophagy. mTORC2 regulates remodeling of the actin cytoskeleton and the cell shape. It also activates

Akt thereby creating the regulatory feedback, which results in Akt-mediated inhibition of the pro-apoptotic protein GSK3 (glycogen synthase kinase 3), and stimulates proliferation through activation of cyclin D1 and inhibition of p27. The activity of Akt and cell survival depends on the fine balance between mTORC1 and mTORC2 activities because the two different mTORC complexes have opposite effects on Akt signaling, with mTORC1 suppressing Akt signaling and mTORC2 directly activating Akt through a phosphorylation event at Ser473 (Sarbassov et al., 2004; Uzdensky et al., 2013).

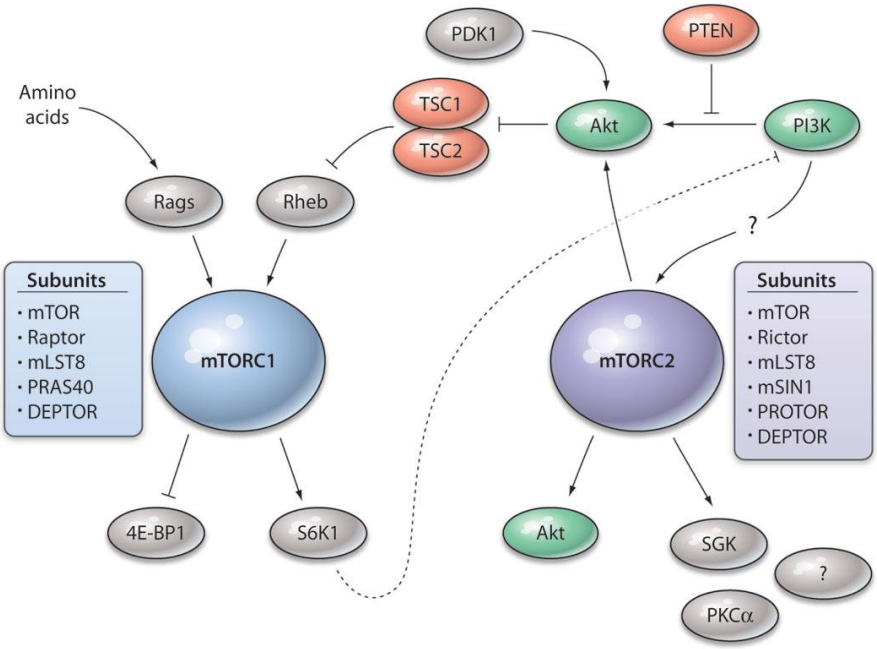

Figure 1.9 mTOR signaling pathways (Guertin, 2009).

mTOR involvement in melanoma development has been suggested since it is activated in 73% of malignant melanomas versus 4% in benign nevi (Karbowniczek et al., 2008). Activation of the mTOR pathway in cutaneous melanoma is associated with poor prognosis (Populo et al., 2011). Activation of mTOR in response to growth, nutrient and energy signals leads to an increase in protein synthesis, which is required for tumor development (Dancey, 2010).

1.4.5 NF-kB

NF-κB is a transcriptional factor consisting of two subunits: p50 and RelA/p65 (Fig. 1.10). In the cytoplasm, NF-kB forms the inactive complex with the inhibitory protein IkB (nuclear factor of kappa light polypeptide gene enhancer in B-cells inhibitor) that prevents its translocation into the nucleus. In response to external factors or under stress conditions, different

signaling proteins such as Akt, ERK, p38 (mitogen-activated protein kinases) and NIK (NF-kappa-B-inducing kinase) phosphorylate IkB kinase (IKK, inhibitor of nuclear factor kappa-B kinase) that induces detachment and proteasomal degradation of IkB. Free NF-kB (p50/p65), which may be additionally phosphorylated/activated by a variety of other enzymes, is transferred into the nucleus, where it initiates transcription of more than 150 target genes involved in regulation of apoptosis, proliferation, inflammation, immune reactions, metastasis and tumor angiogenesis (Uzdensky et al., 2013; Madonna et al., 2012). Constitutive activation of Akt3 in melanoma leads to up-regulation of NF-kB and contributes to tumor progression. Akt3 phosphorylates and activates NF-kB either directly or through phosphorylation of IKKα. This is followed by IKKα-mediated phosphorylation of p65 that stimulates nuclear localization and DNA-binding of NF-kB (Amiri et al., 2005).

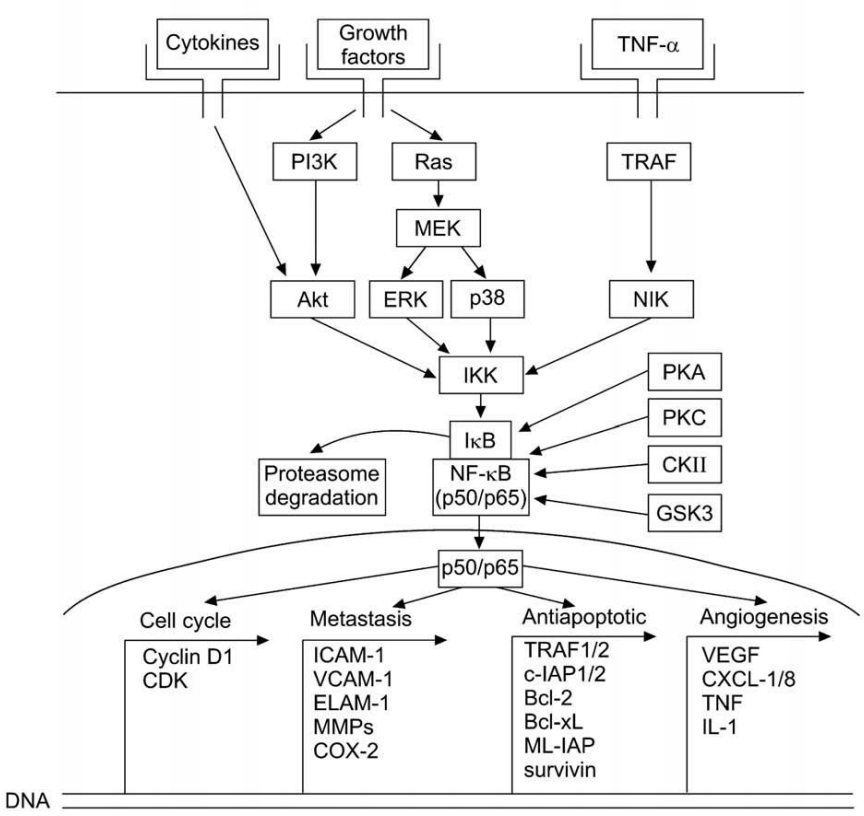

Figure 1.10 The NF-kB-related signaling pathway (Uzdensky et al., 2013).

Up-regulation and constitutive activation of various components of the NF-kB pathway have been found related to progression and metastasis of melanoma. The NF-kB-mediated expression of anti-apoptotic proteins such as IAP (Inhibitor of apoptosis), survivin, TRAF1/2 (tumor necrosis factor

receptor associated factor 1/2), and Bcl-2 (B-cell lymphoma 2) family members increases along with melanoma progression to invasive and metastatic phases. NF-kB also controls the expression of cyclin D1 and CDK2 that regulate proliferation. Overexpression of these proteins allows melanoma cells to escape the cell-cycle control and initiate tumor growth. The activation of NF-kB in melanoma cells is associated with deregulation of upstream signaling pathways, such as Ras/Raf/MAPK, PI3K/Akt, and TRAF/NIK/NF-κB. In melanoma tumorigenesis and progression, in addition to the role played by specific melanoma cell pathways, as above reported, there are other features which must be considered, i.e. the relevance of stem cells and the role played by the immune system.

1.4.6 Melanoma stem cells

Cancer stem cells (CSC) are the subset of cells found in a malignancy that is responsible not only for the formation of tumors, but also for their inexorable progression. These primitive melanoma cells (Fig. 1.11) are not only capable of self-renewal (produce new stem cells), reprogramming and phenotype-switching capability but also it gives rise to a diversity of cells that differentiate and after a finite number of divisions, eventually succumb to programmed cell death (differentiation plasticity). Cancer stem cells may also confer virulence via immune evasion and multidrug resistance, and potentially via vasculogenic mimicry and transition to migratory and metastasizing derivatives (Girouard et al., 2011).

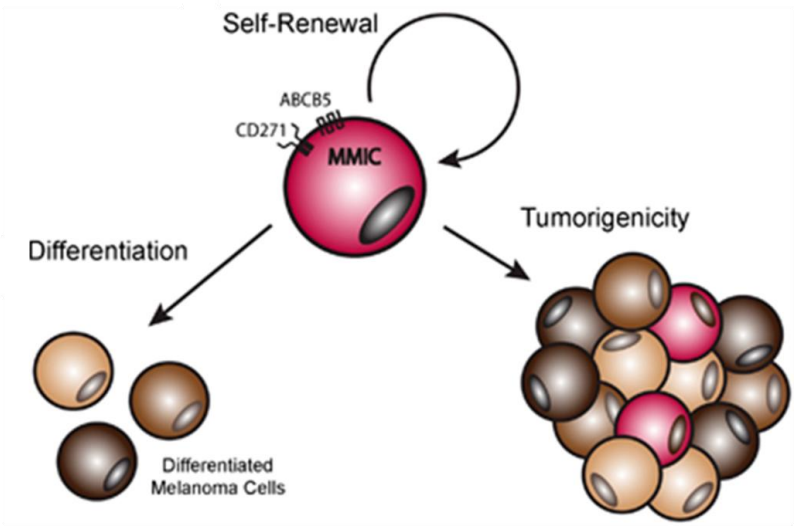

Figure 1.11 Malignant melanoma-initiating cells (MMICs) (Lee et al., 2014).

The presence of a minor subpopulation of CSC is observed in the melanoma tissue and drives tumor initiation and progression. Chemotherapy and/or radiotherapy of a tumor kills a bulk of rapidly proliferating cancer cells but not quiescent CSC that are more resistant and

can survive and reinitiate tumor growth (Schatton et al., 2008). Melanoma biopsies contain from 1 to 20% of melanoma stem cells (Na et al., 2009; Schatton et al., 2008). Quintana and collaborators (2008) have shown that 1 in 4 melanoma cells can initiate a new tumor in immune-deficient animals, i.e. up to 25% melanoma cells are potentially tumorigenic.
The future development of the anti-melanoma therapy will involve the searches of specific markers of melanoma-initiating cells different from markers of normal stem cells.

1.4.7 Melanoma immune escape

The immune system's natural capacity to detect and destroy abnormal cells may prevent the development of many cancers. However, some cancers, as melanoma, are able to avoid detection and destruction by the immune system. The hypothesis is that tumor variants become more resistant to identification and/or elimination by the immune system with a consequent tumor growth. This process has been called "cancer immunoediting". This hypothesis explains the observation that tumors often become clinically evident years after their molecular origin. At the end of this equilibrium between the immune system and tumor growth, the immune response allows for the outgrowth of a subpopulation of tumor cells (Herrera-Gonzalez, 2013). For deepening also Gajewski et al., 2013.

1.5 Cancer staging

Staging is based on detailed information regarding the histologic subtype, Clark level, Breslow depth, dermal mitotic rate per square millimeter, degree of atypia, presence of lymphocytic invasion, presence of ulceration or tumor regression, presence of lymphovascular or perineural invasion, microsatellitosis, and margin assessment (Fig. 1.12) (Kauffmann et al., 2014).

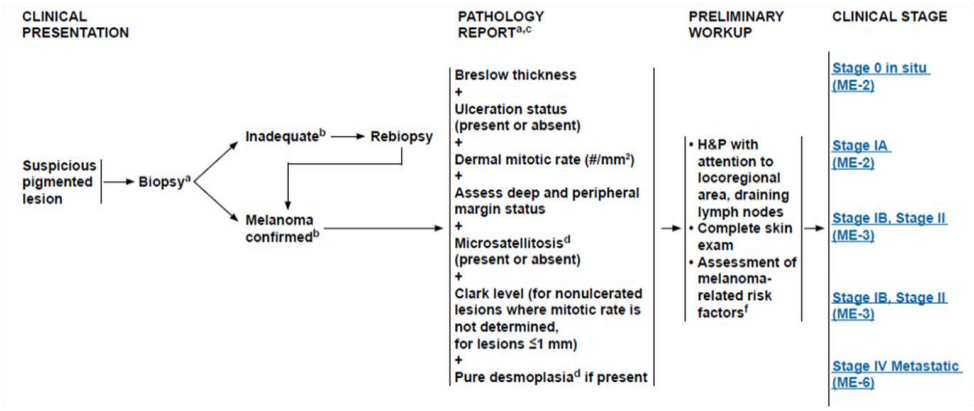

Figure 1.12 Overview of cancer staging (NCCN Guidelines–Melanoma, 1.2015).

Staging of melanoma is based on the 2010 American Joint Committee on Cancer (AJCC) seventh edition TNM (Tumor-Node-Metastasis) system (AJCC, Cancer staging, 2014) (Tab. 1.2).

Stage	Description	5-y Survival
Stage 0	In situ	99.9%
Stage I (A/B) T1a: 1.0 mm thick, no ulceration, mitosis <1/mm2 T1b: 1.0 mm thick, with ulceration or mitoses 1/mm2 T2a: 1.01–2.0 mm thick, no ulceration	Invasive	89%–95%
Stage II (A, B, C) T2b: 1.01–2.0 mm thick, with ulceration T3a: 2.01–4.0 mm thick, without ulceration T3b: 2.01–4.0 mm thick, with ulceration T4a: >4.0 mm thick, without ulceration T4b: >4.0 mm thick, with ulceration	High risk	45%–79%
Stage III (A, B, C) N1: Single positive lymph node N1a: Micrometastasis N1b: Macrometastasis N2: Two to 3 positive lymph nodes or regional in-transit metastases N2a: Micrometastasis N2b: Macrometastasis N2c: In-transit metastasis/satellites without metastatic nodes N3: Four positive lymph nodes, matted nodes, or in-transit metastases/satellites with metastatic nodes	Regional metastases	24%–70%
Stage IV M1a: Metastases to skin, subcutaneous or distant lymph nodes, normal LDH M1b: Lung metastases, normal LDH M1c: Other visceral metastases or any distant metastases with elevated LDH	Distant metastases	7%–19%

Table 1.2 AJCC, seventh edition, staging criteria for cutaneous (Kauffmann et al., 2014).

The T category is based on the thickness of the melanoma, mitotic rate and ulcerations seen in the biopsy. N stands for spread to nearby lymph nodes. The M indicates distant metastasis. The presence of tumor in the lymph nodes is a key prognostic indicator, and accurate identification is

paramount for both accurate staging and decision-making on further therapy.
Understanding the cancer's stage is also critical to identifying clinical trials that may be appropriate for particular patients (AJCC, Cancer staging, 2014).

1.6 Treatment

Surgical excision is the primary treatment for melanoma (Dummer et al., 2012). The surgical treatment of melanoma may be completed by the enlargement of the excision, based on the thickness of the histological lesion. Sentinel lymph node biopsy (SLNB) is a minimally invasive staging procedure developed to identify patients with subclinical nodal metastases at higher risk of recurrence, who could be candidates for complete lymph node dissection or adjuvant systemic therapy (NCCN Guidelines– Melanoma, 1.2015). In Fig. 1.13 the recommendations of National Comprehensive Cancer Network (NCCN) 1-2015 that put in relationship clinical stage, primary treatment and adjuvant treatment, are reported.

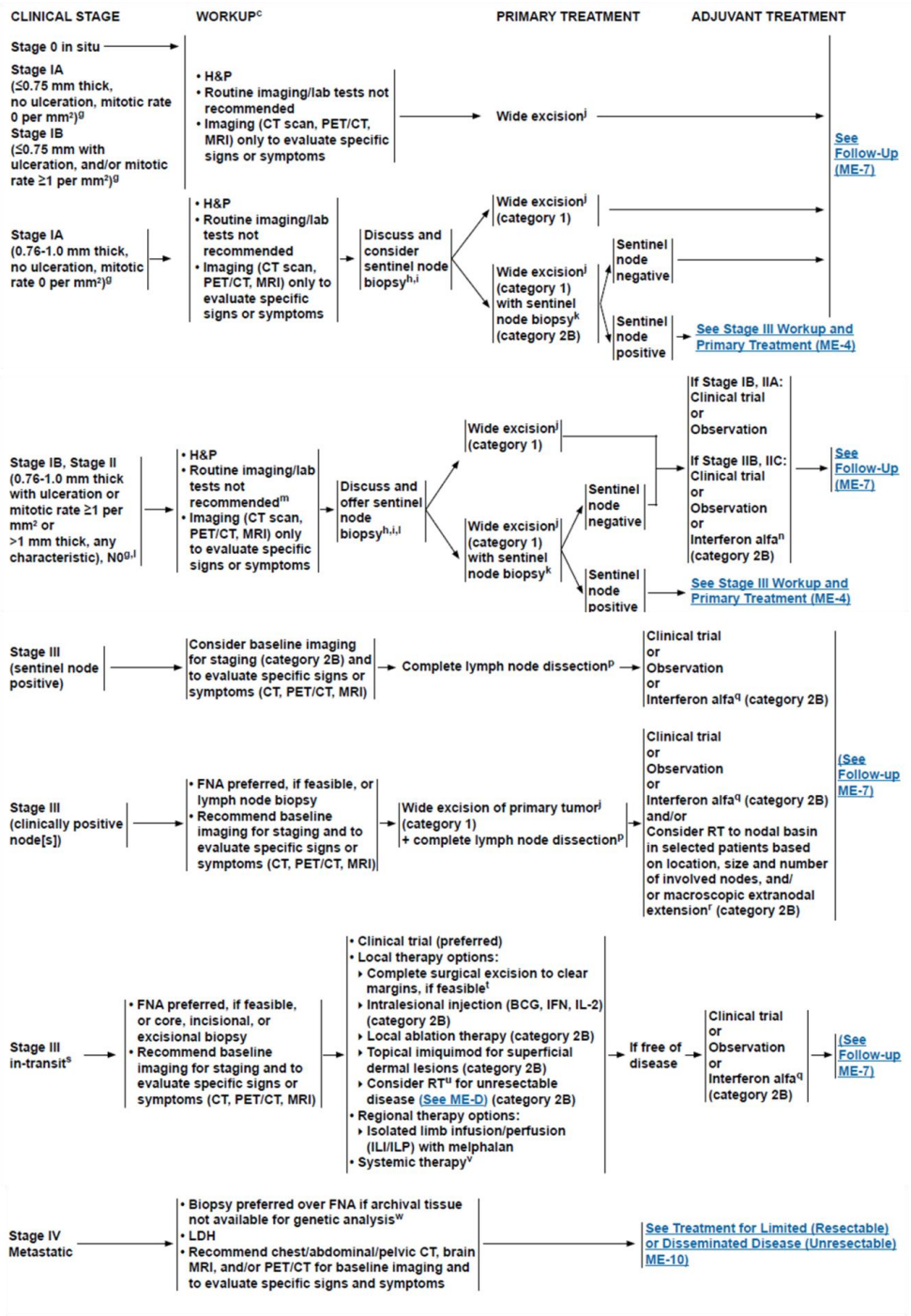

Figure 1.13 Guidelines for treatment of melanoma (NCCN 1-2015).

As regards melanoma pharmacological therapy, it is radically changed after key molecular and immunological insights over the past decade. Whereas 5 years ago, treatment for advanced melanoma was restricted to the alkylating agent dacarbazine and the immunostimulants interleukin-2 (IL-2) and interferon-α 2b (INF-α2b), today the therapeutic menu includes

precise therapies (Fig. 1.14) that target key determinants in oncogenic pathways and immune checkpoints (Miller et al., 2014).

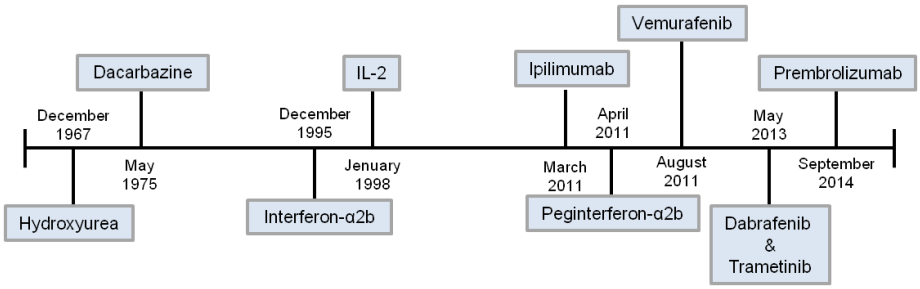

Figure 1.14 Timeline of FDA-approved medications for melanoma (Miller et al., 2014).

1.6.1 Chemotherapy

Chemotherapy with cytotoxic agents has been used for the treatment of metastatic melanoma for over three decades. Among the antitumoral agents, efficacy is modest in metastatic melanoma including alkylating agents (dacarbazine, temozolomide, nitrosoureas), analogues of platinum (cisplatin, carboplatin) and microtubular toxins (vincas and taxanes), which have been used alone or in combination (Bhatia et al., 2009). Specifically in relation to cytotoxic chemotherapy, dacarbazine used as a chemotherapeutic agent still represents the single most common option. It was demonstrated that combinations of cytotoxic agents can produce low response rates, although higher than monotherapy with dacarbazine, which are associated with increased toxicity and do not extend significantly the survival of patients (Bhatia et al., 2009).

1.6.2 Immunotherapy

Melanoma is characterized as one of the most immunogenic tumors because of the presence of tumor-infiltrating lymphocytes in resected melanoma, occasional spontaneous regression, and clinical responses to immune stimulation (Mouawad et al., 2010). For these reason, melanoma has long been considered a promising target for immunotherapeutic approaches. In 1998, the FDA (US Food and Drug Administration) approved the use of the immune molecule IL-2 to treat advanced melanoma (Fig. 1.14). This provided the first proof-of-principle that an immune-based treatment could provide durable control of the disease. The immune molecule IFNα has also been used alone after surgery or in combination with other agents to treat advanced melanoma (Wolchok, 2014). Furthermore, the immunogenicity of melanoma has led investigators to study novel immune strategies for overcoming immune system evasion by tumors (Mouawad et al., 2010).

A promising avenue of clinical research in melanoma is the use of immune checkpoint inhibitors. By blocking inhibitory molecules or, alternatively, activating stimulatory molecules, these treatments are designed to unleash or enhance pre-existing anti-cancer immune responses. Several checkpoint inhibitors, targeting multiple different checkpoints, are currently in development (Wolchok et al., 2014). T cells self-regulate their activation through CTLA-4 (Cytotoxic T-Lymphocyte Antigen 4) expression. CTLA-4 functions as a negative co-stimulatory molecule for the T cell; therefore, therapies that antagonize CTLA-4 remove the brakes from T cells leading to a net effect of T cell hyper-responsiveness (Melero et al., 2007). Several human monoclonal antibodies, i.e. ipilimumab (Yervoy®, MDX-010; Bristol-Myers Squibb, Medarex, Princeton, NJ), tremelimumab (CP-675,206; Pfizer Pharmaceuticals, New York), and others. These antibodies have been demonstrated to induce tumor regression and may prolong time to disease progression free and are in clinical development.

Ipilimumab (Fig. 1.15) is a fully human monoclonal IgG1κ antibody against CTLA-4, an immune inhibitory molecule expressed in activated T cells and suppressor T regulatory cells. Activation of the cellular immune response involves the interaction of T cell receptors with major histocompatibility complex molecules on antigen-presenting cells (APCs). This requires costimulation where ligand B7 on APC binds to CD28 (Cluster of Differentiation 28) on T cells, which triggers T cell proliferation. A negative co-stimulation signal is transduced by CTLA-4, which is present in T cells, and interaction of CTLA-4 with the same B7 ligand inhibits T cell activation and proliferation (Chambers et al., 2001; (Melero et al., 2007; Garber, 2010).

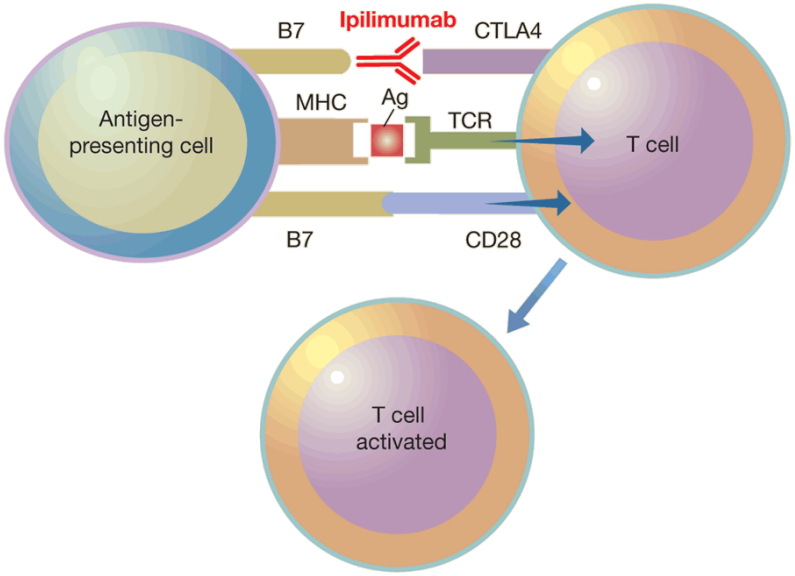

Figure 1.15 Ipilimumab stimulates antitumor immunity by blocking CTLA4, a natural brake on T cells, and allowing their unimpeded 'costimulation' (Garber, 2010).

Ipilimumab was approved by the FDA in February 2011 (Fig. 1.14) and by the European Medicines Agency in July 2011 for use in the treatment of advanced malignant melanoma in patients not responding to chemotherapy, with or without previous exposure to immunotherapy (Hanaizi et al., 2012); moreover,multiple clinical trials using this drug for the treatment of other malignancies are ongoing.

In 2011, the immunotherapy Ipilimumab (Yervoy®) became the first drug ever shown to extend survival for patients with metastatic melanoma. Results from a large, phase III trial of Ipilimumab demonstrated that it reduced the risk of death by 32% and nearly doubled the patients surviving to 1 and 2 years, with some patients experiencing complete and durable clinical regressions lasting for years (Wolchok, 2014). Ipilimumab induces a significant increase in the frequency of circulating regulatory T cells (Tregs) and increase in the induction of tumor infiltrating Tregs at 6 weeks (Tarhini et al., 2012). Ipilimumab is the first agent that has been demonstrated to improve overall survival (OS) in patients with metastatic melanoma, which has a very poor prognosis, in randomized phase III clinical trials (Graziani et al., 2012).

Tremelimumab is a fully human IgG2 antibody, which is directed against human CTLA-4, as ipilimumab. Tremelimumab did not produce a statistically significant advantage in overall survival compared to first-line standard-of-care chemotherapy in a phase III randomized trial reported in the Journal of Clinical Oncology in patients with advanced melanoma (Ribas et al, 2013).

Urelumab is a humanized agonistic monoclonal antibody targeting the CD137 receptor with potential immunostimulatory and antineoplastic activities. CD137 is a member of the tumor necrosis factor receptor (TNFR) family and functions as a costimulatory molecule. Urelumab specifically binds to and activates CD137-expressing immune cells, stimulating an immune response, in particular a cytotoxic T cell response against tumor cells (Molckovsky et al., 2008).

Pembrolizumab is a humanized monoclonal IgG4 antibody directed against human cell surface receptor PD-1 (programmed death-1 or programmed cell death-1) with immune-potentiating activity. Upon administration, pembrolizumab binds to PD-1, an inhibitory signaling receptor expressed on the surface of activated T cells, and blocks the binding of PD-1 by its ligands, which results in the activation of T-cell-mediated immune responses against tumor cells (Fig. 1.16). The ligands for PD-1 include PD-

L1 (programmed death-ligand 1), which is expressed on APCs and overexpressed on certain cancer cells, and PD-L2 (programmed death-ligand 2), which is primarily expressed on APCs. Activated PD-1 negatively regulates T-cell activation through the suppression of the PI3K/Akt pathway (Fig. 1.9).

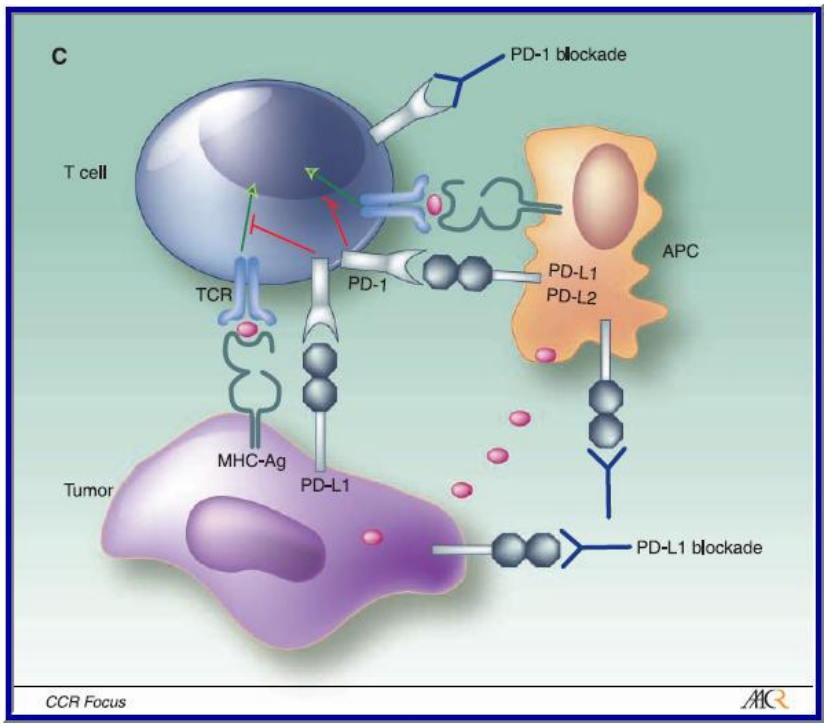

Figure 1.16 PD-1 checkpoints (Brahmer et al., 2010).

In July 2014, Bristol-Myers Squibb anti-PD-1 antibody, Nivolumab received its first regulatory approval for use in inoperable melanoma in Japan, under the name Opdivo, making it the first anti-PD-1 cancer therapy.

In September 2014, Merck's anti-PD-1 antibody, Keytruda (pembrolizumab, MK-3475), was FDA approved for the treatment of advanced or unresectable melanoma (Fig. 1.14) in patients failing prior treatment with ipilimumab and/or , if they have a BRAF V600E mutation, a BRAF or MEK inhibitor (Wolchok, 2014).

There are also other anti-PD1 antibody under investigation: 1) MEDI4736**,** an anti-PD-L1 antibody made by MedImmune/AstraZeneca, is being tested in a phase I/II trial for melanoma and 2) MPDL3280A, an anti-PD-L1 antibody developed by Roche/Genentech, that is being tested in a phase I trial in melanoma as well as numerous other cancers (Wolchok, 2014).

Since melanoma is well known to be an immunogenic tumor, there have been many efforts to develop vaccines that induce an anti-melanoma

response (Ozao-Choy et al., 2014). Vaccine strategies are highly varied and options vary from the simplest peptide vaccines to the most complex autologous whole-tumor cells.
After several decades of failed attempts at developing potent therapeutic cancer vaccines, the first was approved in prostate cancer by FDA in 2010 Sipuleucel-T (Provenge, Dendreon Corporation). A trial of gp100:209-217(210M) peptide vaccination in melanoma showed a response rate higher and progression-free survival longer with vaccine and IL-2 than with IL-2 alone. Nevertheless, additional work is required to optimize vaccine strategies using peptides (Schwartzentruber et al., 2011).

1.6.3 Targeted Therapy

The main characteristics of targeted antineoplastic treatment is that the drugs act specifically on their intended target which have specific effects on the tumor (Martí et al., 2012). The number of possible therapeutic targets in melanoma is increasing with an improvement in our understanding of the biology of melanoma.

c-KIT inhibitors

c-KIT(tyrosine-protein kinase or CD117) is a growth factor receptor in epidermal melanocytes and has an essential role in the differentiation and migration of melanocytic cells during embryonic development. The ligand for KIT (tyrosine-protein kinase) is stem cell factor (SCF) and binding of SCF to c-KIT induces the activation of downstream signaling pathways that mediate growth and survival signals within the cell, including the PI3K-Akt-mTOR (Fig. 1.9) and Ras-Raf-MEK-ERK (Fig. 1.8) pathways.
C-KIT is mutated in approximately 20% of sun-induced skin damage. For these reasons, c-KIT has been considered a potential therapeutic target in melanoma and two c-KIT inhibitors, i.e., imatinib (Gleevec, Novartis Pharmaceuticals Corporation) and dasatinib (Bristol-Myers Squibb), are under evaluation for treating melanoma. Imatinib (Gleevec) have shown promise in improving clinical outcomes in patients with advanced melanoma (Miller et al., 2014).

Braf/ERK inhibitors

One of the most common signaling pathways affected by mutations in melanoma is the Braf/ERK pathway (paragraph 1.4.3 of the present manuscript) (Fig. 1.8). The V600E mutation, which comprises nearly 90% of the observed mutations in Braf obviates the need for activation by Ras and results in constitutive activation and unregulated phosphorylation of downstream effectors such as MEK (Cantwell-Dorris et al., 2011). As

shown in Table 1.3, six BRAF inhibitors are under evaluation for melanoma.

Name	Mechanisms
Sorafenib	Multi-target BRAF inhibitors
RAF265	Multi-target BRAF inhibitors
Dabrafenib	Selective BRAF inhibitors
Vemurafenib	BRAF V600E inhibitor
Selumetinib	MEK inhibitor
Trametinib	MEK inhibitor

Table 1.3 Clinical trials of Braf/MEK inhibitors for treating melanoma (Tseng et al, 2013).

Vemurafenib was launched in 2011 in the US after FDA approval for BRAF V600E mutation positive unresectable or metastatic melanoma and in the UK after EMA (European Medicine Agency) approval in 2012 (Fig. 1.14).

In a phase III randomized controlled trial of patients with metastatic melanoma and BRAF mutation, vemurafenib significantly reduced the risks of death and disease progression by 63% and 74%, respectively, compared with dacarbazine (Fig. 1.17). The response rate in patients who received vemurafenib was 48.4%, which was almost 9 times higher than that in patients who received chemotherapy (5.5%). Furthermore, 84% of the patients who received vemurafenib were alive after 6 months compared with 64% who received chemotherapy: the median over survival with vemurafenib (10.5 months) was longer than that with dacarbazine (Chapman et al., 2011).

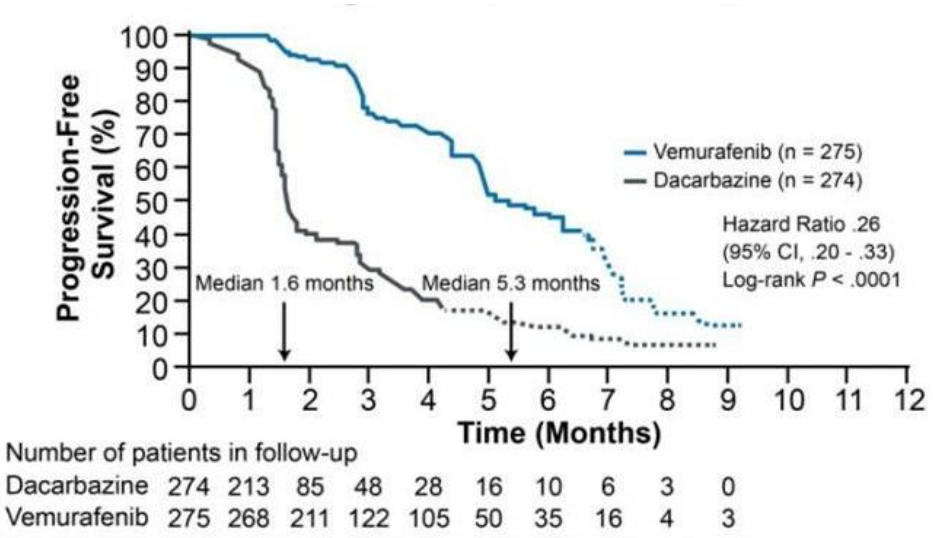

Figure 1.17 Progression-free survival from a trial comparing vemurafenib

with dacarbazine in patients with BRAFV600E-mutated melanoma (Chapman et al.,2011).

Despite this initial success, numerous challenges remain with selective Braf inibithors. For example, only half of melanomas possess activating mutations in BRAF gene. In addition, the duration of response to Braf-inhibitor is relatively short secondary to acquired and adaptive resistance. Lastly, selective Braf inhibition has been associated with rare, but serious, adverse effects such as the rise of secondary malignancies (Sullivan et al., 2013).

Trametinib specifically binds to and inhibits MEK 1 and 2, resulting in an inhibition of growth factor-mediated cell signaling and cellular proliferation. Trametinib was found to improve progression free survival compared to dacarbazine (4.8 months vs 1.5 months) in a phase III trial suggesting that MEK could be a valid therapeutic target in BRAF-mutant melanoma. There were no reports of cutaneous squamous cell carcinoma or hyperproliferative skin lesions, such as those seen with the Braf inhibitors. Based on the clinical benefit of the MEK-inhibitor, the FDA (Fig. 1.14) approved trametinib (Mekinist) in May of 2013 (Miller et al., 2014).

The resistance to Braf-inhibitors is associated with reactivation of the MAPK pathway; so future strategies will include rationally designed, triple and quadruple therapeutic regimens targeting complementary oncogenic pathways. Additional targets include PI3K, mTOR, MDM2, BCL-2, PDGF (platelet-derived growth factor), HSP90 (Heat-shock protein 90), IGF (insulin-like growth factor), MITF (microphthalmia-associated transcription factor), Notch and several other cyclin-dependent kinases (Miller et al., 2014).

Chapter 2

Experimental Section: Theranostic properties of a survivin-directed molecular beacon in human melanoma cells

2.1 Introduction

Survivin is a member of the inhibitor of apoptosis family (Ambrosini et al., 1997) that plays a key role in the regulation of cell division, apoptosis, cell migration and metastasis (Altieri, 2008; Groner et al., 2014; Mita et al., 2008). Furthermore, survivin is involved in the promotion of angiogenesis and chemoresistance (Mita et al., 2008). Unlike other anti-apoptotic proteins, survivin is undetectable in most terminally differentiated normal tissues, while it is overexpressed in human cancer (Altieri, 2001). For instance, survivin is highly overexpressed in malignant melanoma cells compared with normal melanocytic nevi and normal differentiated skin tissues (Grossman et al., 1999). Furthermore, a retrospective analysis performed in melanoma patients has revealed that survivin up-regulation is correlated with decreased survival rate, increased relapse, and chemoresistance occurrence (Hartman et al., 2013; Takeuchi et al., 2005; Chen et al., 2009). These features make survivin a promising target against which novel anti-cancer drugs could be developed.

Pharmacological modulation of survivin was tagged with its evolving functional complexity associated with various cell-signaling cascades including PI3K/AKT, mTOR, ERK, MAPK, signal transducer and activator of transcription (STAT), hypoxia-inducible factor-1α, HSP90, p53, Bcl2, epidermal growth factor receptor (EGFR), VEGF etc (Kanwar et al., 2013). It is widely recognised that therapeutic strategies targeting surviving or surviving expression (e.g., antisense oligonucleotides and short interfering RNA, siRNA) can induce tumor cell death, circumvent drug resistance and sensitize cancer cells to chemotherapeutic drugs (Mita et al., 2008).

More recently, much attention has been directed to molecular beacons (MBs) as potential theranostic agents (Wang et al., 2013). MBs are stem-

loop-folded oligodeoxyribonucleotides with fluorophore and quencher dyes conjugated to the opposite ends of the hairpin (Fig. 2.1).

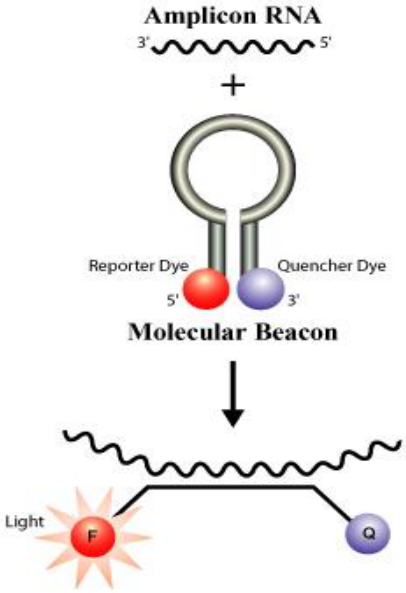

Figure 2.1 Molecular beacon structure and mechanism of action.

In the absence of the complementary nucleic acid target (mRNA, in the case of this work), the fluorescence of the fluorophore is quenched by the closely located quencher (Kolpashchikov et al., 2012). Otherwise, the hybridization with target nucleic acid opens the hairpin, generates probe-analyte duplex that physically separates the fluorophore from quencher, allowing a fluorescence signal to be emitted upon excitation (Santangelo et al., 2006; Giannetti et al., 2013).

It has been reported that MB technology may allow assessing gene expression in vivo with high sensitivity and low background signal and may help to noninvasively detect cancer in its early stages. Furthermore, MB can also produce therapeutic effect by binding and down-regulating its target gene (Han et al., 2013). Several lines of evidence provided by the antisense therapy research, demonstrate that complementary pairing of a short segment of an exogenous oligonucleotide to mRNA can have a profound impact on protein expression levels and even cell fate. In fact, binding of MB to mRNA can trigger RNase H mediated mRNA degradation (Santangelo et al., 2006).

In the current study, we provide evidence of the simultaneous imaging and pro-apoptotic activities of a previously described MB (Nitin et al., 2004) and demonstrate that such effects are associated with selective targeting of survivin mRNA in human melanoma cells. This approach may represent an innovative strategy for the development of novel theranostic drugs in human cancer.

2.2 Materials and Methods

2.2.1 Cell cultures

The human malignant melanoma A375 cell line (American Type Culture Collection, Rockville, MD, USA) was cultured at 37°C in a humidified atmosphere containing 5% CO2 in DMEM (Dulbecco's modified Eagle's medium) supplemented with l-glutamine (2 mM), 10% heat-inactivated fetal bovine serum (FBS) and 1% (w/v) penicillin/streptomycin (Sigma-Aldrich, Milan, Italy). The human metastatic melanoma 501 Mel cell line was a kind gift from Dr. Poliseno (Oncogenomics Unit, Core Research Laboratory, Istituto Toscano Tumori c/o IFC-CNR, Pisa, Italy). 501 Mel cells were cultured in the same condition of A375 with glucose supplement. Human bronchial smooth muscle cells (BSMC; Lonza, Walkersville, MD, USA) were maintained exactly as recommended by the manufacturer in an optimized medium containing 5% fetal bovine serum, 5.5 mM glucose, 50 μg/ml gentamicin, 50 ng/ml amphotericin-B, 5 ng/ml insulin, 2 ng/ml basic fibroblast growth factor and 0.5 ng/ml epidermal growth factor (SmGM-2 Bullet Kit, Lonza). Human melanocytes (PromoCell GmbH, Germany) were cultured at 37°C in a humidified atmosphere containing 5% CO2 in Melanocyte Growth Medium M2 (PromoCell GmbH, Germany). Human monocytes were a kind gift from Dr. Celi (Department of Surgery, Medical, Molecular, and Critical Area Pathology). Monocyte isolation was performed as described previously (Neri et al., 2012). The procedure was approved by the local ethics committee at the University of Pisa and was in accordance with the Declaration of Helsinki. A signed consent was obtained from all donors.

2.2.2 Drugs

Docetaxel (DTX) and Cisplatin (CisPt) were purchased from Sigma–Aldrich, Milan, Italy. DTX was dissolved in dimethyl sulfoxide (DMSO) and diluted with culture medium (DMSO final concentration of 0.0001%, v/v), while CisPt was dissolved in water.

2.2.3 Transfection

Cells were transfected with 100 nM antisense oligodeoxynucleotides using Lipofectamine 2000 (Ref. 11668-027, Invitrogen Life Technologies, Carlsbad, CA, USA), which has been reported to yield high transfection efficiency (≈70%) in A375 cells (Zhou et al., 2013). A molecular beacon (MB), which targets nucleotides 149–163 of survivin mRNA, and the other oligodeoxynucleotides were synthesized by IBA (Göttingen, Germany) (Nitin et al., 2004). ATTO647N (λ_{abs} 644 nm, λ_{em} 669 nm) and Blackberry

Quencher 650 (λ_{max}~650 nm, useful absorbance between 550 and 750 nm) were used as fluorophore/quencher pair. A fluorescent DNA probe, with the same oligonucleotide sequence of MB but not structured as a molecular beacon and labelled only with the ATTO647N dye, was used as control. Oligonucleotide sequences are listed in Table 2.1.

Name	Sequences
MB	5'-ATTO647N-CGACGGAGAAAGGGCTGCCACG/thiol-(C6)-dT/CG–BBQ-3'
Probe	5'-ATTO647N-GAGAAAGGGCTGCCA/thiol-3'

BBQ: BlackBerry Quencher; ATTO647N: fluorescent label (report). Underlined bases are the ones forming the loop.

Table 2.1 Oligonucleotide sequences of Molecular Beacon (MB) and probe.

2.2.4 In vitro confocal microscopy in living cells

Laser scanning confocal microscopy was carried out by using a microscope RadiacePLUS (Bio-Rad). Briefly, cells were plated on 35 mm µ-dishes (Ibidi Giemme Snc, Milan, Italy) and treated with 100 nM antisense oligodeoxynucleotides (MB or probe). All observations were done with an oil immersion x 40 Nikon objective lens (Numerical aperture NA=1.3). Fluorescence was evaluated at different time points during the transfection (excitation and emission wavelengths of 644 and 669 nm, respectively). Acquired images were processed using the open source Image-J software.

2.2.5 RT-PCR and quantitative real-time PCR analyses

Total RNA from cells was extracted by using the RNeasy® Mini kit, following manufacturer's instructions, and reverse-transcribed by the QuantiTect® Reverse Transcription kit (Qiagen, Valencia, CA, USA). RT-PCRs (Reverse transcriptase polymerase chain reaction) were performed by the HotStartTaq Master Mix kit (Qiagen, Valencia, CA, USA). Primer sequences are listed in Table 2. Thermal cycle conditions were as follows: 95°C for 15 min, 35 cycles of denaturation at 95°C for 1 min followed by annealing and extension at 72°C for 1 and 10 min, respectively. Detection of the RT-PCR products was performed by agarose gel electrophoresis and ethidium bromide staining.

Real-time PCR (polymerase chain reaction) was performed with SsoFast Eva Green Supermix (Ref. 172-5201, Bio-Rad, CA, USA). Samples were amplified using the following thermal profile: 95°C for 30 s, 40 cycles of denaturation at 95°C 15 s followed by annealing for 30 s and 72°C for 30 s, with a final step at 65°C for 5 s. GAPDH (glyceraldehyde 3-phosphate dehydrogenase) and β-actin were used as housekeeping genes.

Protein	Primer nucleotide sequences	Ta (°C)	Amplicon length
β-actin	5'- AACTGGAACGGTGAAGGTGAC-3' (F) 5'-GACTTCCTGTAACAACGCATCTC-3' (R)	61	138
GAPDH	5'-GTGAAGGTCGGAGTCAACG-3'(F) 5'GGTGAAGACGGCCAGTGGACT-3' (R)	59	301
Survivin	5'-ACCAGGTGAGAAGTGAGGGA-3' (F) 5'-AACAGTAGAGGAGCCAGGGA-3' (R)	59	309

Table 2.2 Primer nucleotide sequences, Ta (annealing temperature) and amplicon length used for PCR experiments.

2.2.6 Western blot analysis

Cell lysates were collected after treatments at different time points. Samples containing the same amount of protein (40 μg) were separated on a 15% SDS (sodium dodecyl sulfate) -polyacrylamide gel electrophoresis, transferred to a nitrocellulose membrane (Sigma–Aldrich, Milan, Italy), blocked with 5% non-fat milk in TBE (buffer tris-borate-EDTA) and probed with specific antibodies. Incubation was performed at 4°C overnight with anti-survivin (Ref. sc-17779, Santa Cruz Biotechnology, Santa Cruz, CA, USA) and anti-β-actin (Ref. A2228, Sigma–Aldrich, Milan, Italy) antibodies. Membranes were then washed with blocking solution and incubated with secondary antibodies conjugated with horseradish peroxidase (Ref. sc-2005, Santa Cruz Biotechnology, Santa Cruz, CA, USA). Chemiluminescence detection was performed using Western Blotting Luminol Reagent (Ref. sc-2048, Santa Cruz Biotechnology, Santa Cruz, USA), according to the manufacturer's instructions. Quantification of proteins on SDS-PAGE gels was performed using ImageJ densitometry software and signal intensities were normalized to those for β-actin.

2.2.7 Internucleosomal DNA fragmentation

The Cell Death Detection ELISA (enzyme-linked immunosorbent assay) Kit (Ref. 11774452001, Roche, Mannheim, Germany) was used for assessing apoptosis in A375 cells treated with MB, according to the manufacturer's protocol. Briefly, A375 cells were treated with 100 nM MB at different times. After treatment, 10^4 cells were lysed and centrifuged at 200 × g for 10 min and the supernatant placed into a streptavidin-coated microplate. A mixture of anti-histone-biotin and anti-DNA-POD (horseradish peroxidase) was added and incubated at room temperature for 2 h. After incubation, unbound antibodies were removed from the solution and the nucleosomes were quantified by colour development with substrate. Optical density was measured at 405 nm with the Infinite® M200 NanoQuant instrument (Tecan, Salzburg, Austria).

2.2.8 Mitochondrial membrane potential (ΔΨm)

Changes in mitochondrial membrane potential (ΔΨm) during the early stages of apoptosis were assayed using the Muse™ MitoPotential assay (Ref. MCH 100110, Merck Millipore; Darmstadt, Germany) in A375 cells treated with MB alone or in combination with Cis-Pt or DTX. Briefly, cells were harvested and the cell pellet was suspended in assay buffer (10^5 cells/100µl). MitoPotential dye working solution was added and the cell suspension incubated at 37 °C for 20 min. After the addition of Muse MitoPotential 7-AAD dye (propidium iodide) and incubation for 5 min, changes in ΔΨm and in cellular plasma membrane permeabilization were assessed using the fluorescence intensities of both the dyes analysed by flow cytometry (Muse™ Cell Analyzer, Merck Millipore; Darmstadt, Germany).

2.2.9 Determination of nuclear morphology

Changes in nuclear morphology were assessed after transfection with MB and in lipofectamine-treated cells for 48 and 72 h. Cells were fixed with 4% paraformaldehyde on 8-well chamber slides. After washing with PBS, cells were incubated with DAPI (4',6-diamidino-2-phenylindole) 300 nM (Invitrogen Life Technologies, Carlsbad, CA, USA). Life fluorescence analysis was realized with Eclipse E600FN Nikon microscope. The fluorophore DAPI is a fluorescent label for the blue spectral region (excitation and emission wavelengths of 360 and 460 nm, respectively) (magnification 40 × WD).

2-2-10 Statistical analysis

All experiments were performed in triplicate and results were analyzed by GraphPad Prism 5 (GraphPad Software, San Diego, CA, USA). Data were shown as mean values ± standard error of the mean (SEM) obtained from at least three independent experiments. Statistical analyses were performed by Student's *t*-test or one-way ANOVA followed by the Bonferroni's multiple comparison test.

2.3 Results

2.3.1 Survivin mRNA expression in different cell types

RT-PCR experiments followed by densitometry and quantification of electrophoresis bands clearly demonstrated that survivin was differentially expressed in human melanoma cells compared to normal cells. Specifically, survivin mRNA levels were significantly higher in A375 and 501 Mel cells than in BSMC ($p<0.001$), while human melanocytes and

monocytes did not express survivin (Fig. 2.2). β-actin was used as housekeeping gene because its expression levels did not significantly change in all of our experimental conditions.

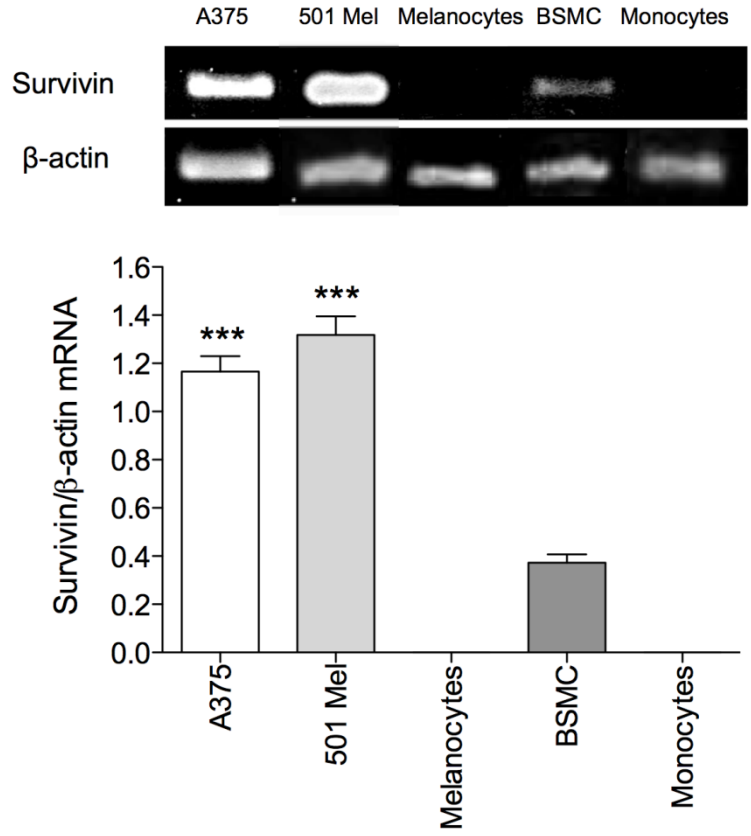

Figure 2.2 Survivin gene espression in A375, 501 Mel, melanocytes, BSMC, and monocytes. Values were expressed as mean ± standard error of the mean (SEM) from three separate experiments. ***$p<0.001$, compared with melanocytes (ANOVA followed by the Bonferroni's multiple comparison test).

2.3.2 MB specific binding to survivin mRNA

In *vitro* bioimaging was used to assess transfection of the MB via Lipofectamine into different cell types tested and its target-specific structure opening with fluorescence emission. Confocal microscopy of living cells clearly demonstrated that MB transfection generated a fluorescence signal according to survivin expression levels and time of exposure. Specifically, confocal microscopic images of A375 (Fig. 2.3) and 501 Mel (Fig. 2.4) cells showed high signal intensity in these specific cell types indicating that MB could cross the cell membrane, bind to survivin mRNA and generate high fluorescence emission.

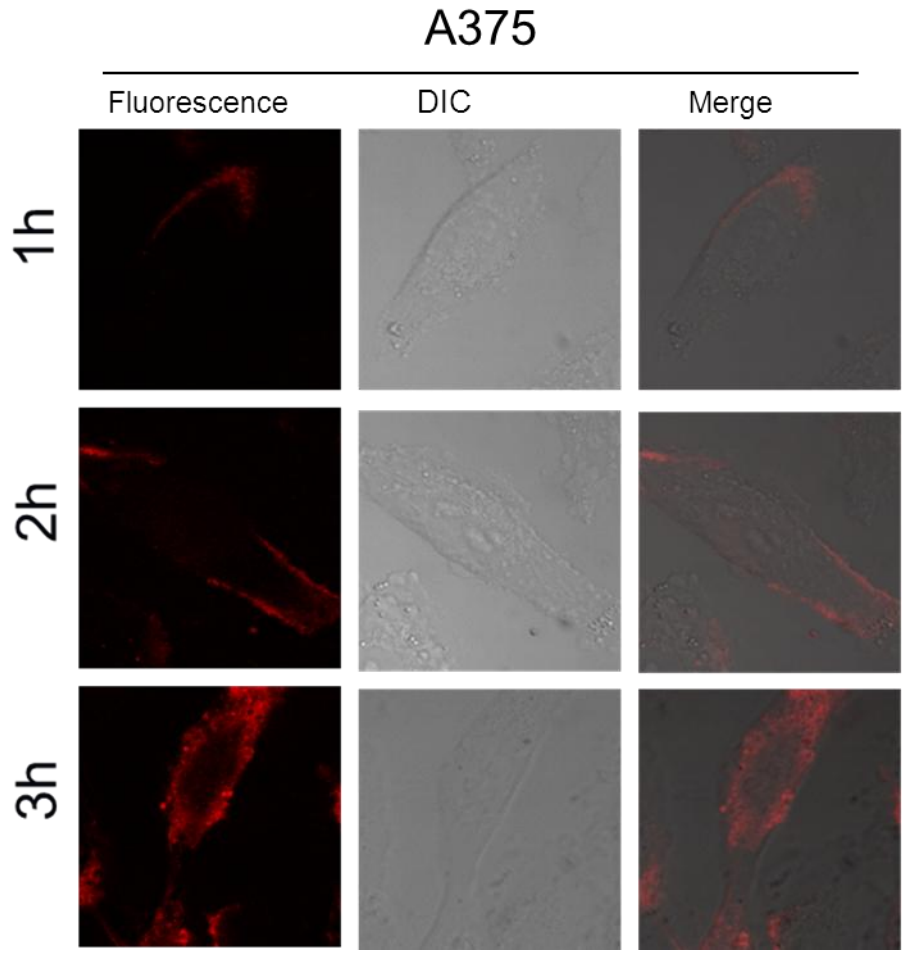

Figure 2.3 Confocal microscopy images of survivin expression in the cytoplasm of A375 living cells. Cells were treated with 100 nM MB (red) and fluorescence was measured at 1, 2 and 3 h following start of transfection. Confocal fluorescent images are shown in the left column, transmission DIC (differential interference contras) images in the central column, while the merged images are also shown in the right column. The fluorescence images were obtained by using excitation and emission wavelengths of 645 and 669 nm, respectively and an oil immersion objective (x40, NA=1.3).

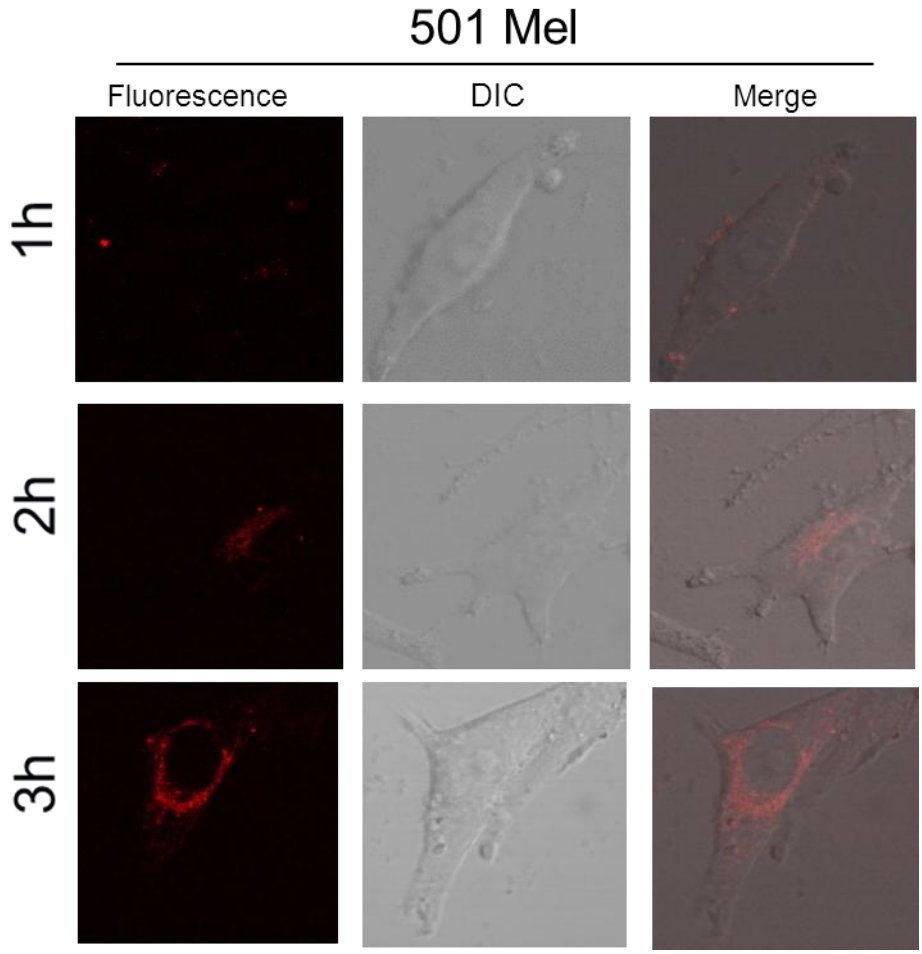

Figure 2.4 Confocal microscopy images of survivin expression in the cytoplasm of 501 Mel living cells. Cells were treated with 100 nM MB (red) and fluorescence was measured at 1, 2 and 3 h following start of transfection. Confocal fluorescent images are shown in the left column, transmission DIC images in the central column, while the merged images are also shown in the right column. The fluorescence images were obtained by using excitation and emission wavelengths of 645 and 669 nm, respectively and an oil immersion objective (x40, NA=1.3).

Otherwise, the fluorescence signal was significantly lower in the case of BSMC cells (Fig. 2.5), while no fluorescence could be detected in human melanocytes (Fig. 2.6) and monocytes (Fig. 2.7).

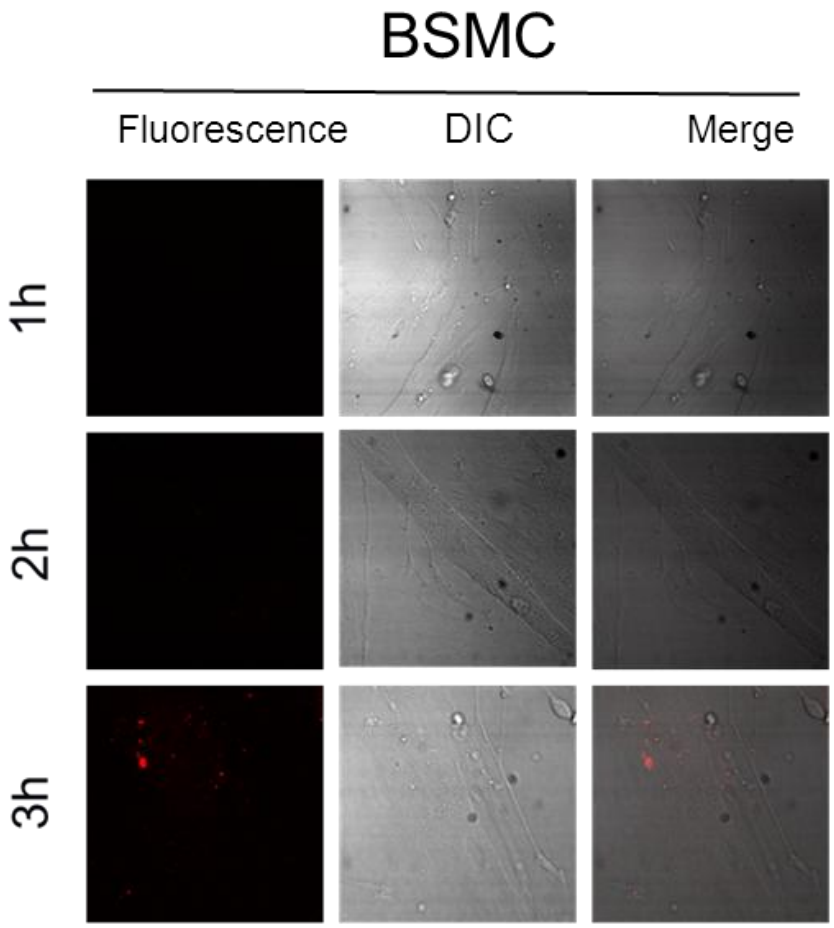

Figure 2.5 Confocal microscopy images of survivin expression in the cytoplasm of BSMC living cells. Cells were treated with 100 nM MB (red) and fluorescence was measured at 1, 2 and 3 h following start of transfection. Confocal fluorescent images are shown in the left column, transmission DIC images in the central column, while the merged images are also shown in the right column. The fluorescence images were obtained by using excitation and emission wavelengths of 645 and 669 nm, respectively and an oil immersion objective (x40, NA=1.3).

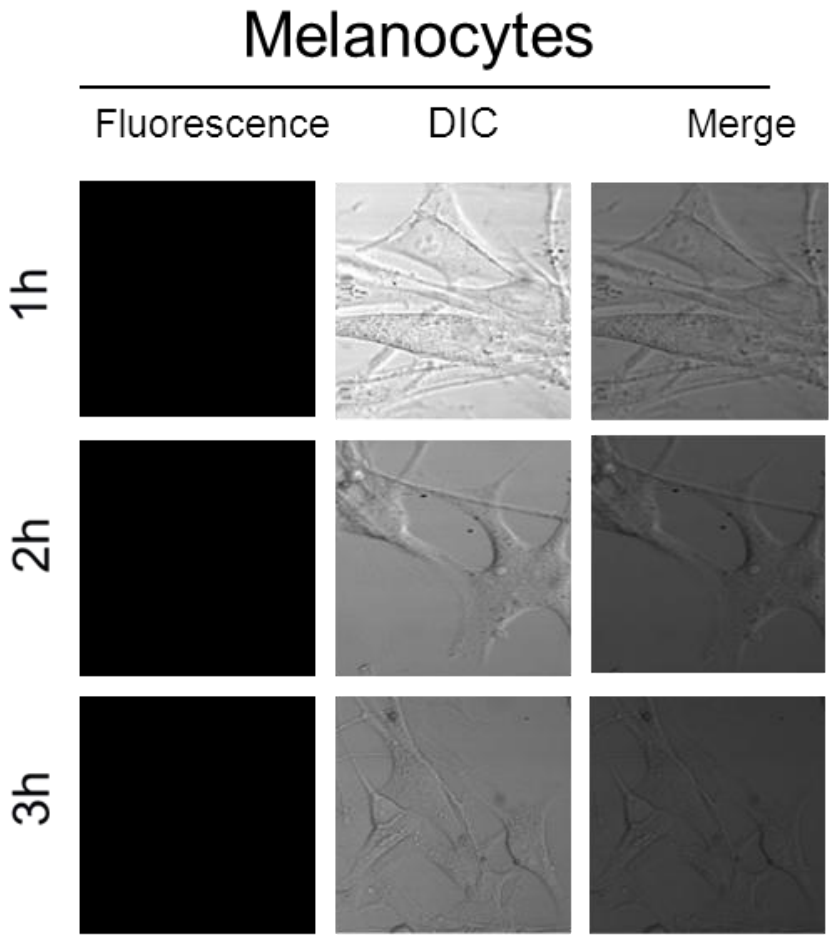

Figure 2.6 Confocal microscopy images of survivin expression in the cytoplasm of melanocytes living cells. Cells were treated with 100 nM MB (red) and fluorescence was measured at 1, 2 and 3 h following start of transfection. Confocal fluorescent images are shown in the left column, transmission DIC images in the central column, while the merged images are also shown in the right column. The fluorescence images were obtained by using excitation and emission wavelengths of 645 and 669 nm, respectively and an oil immersion objective (x40, NA=1.3).

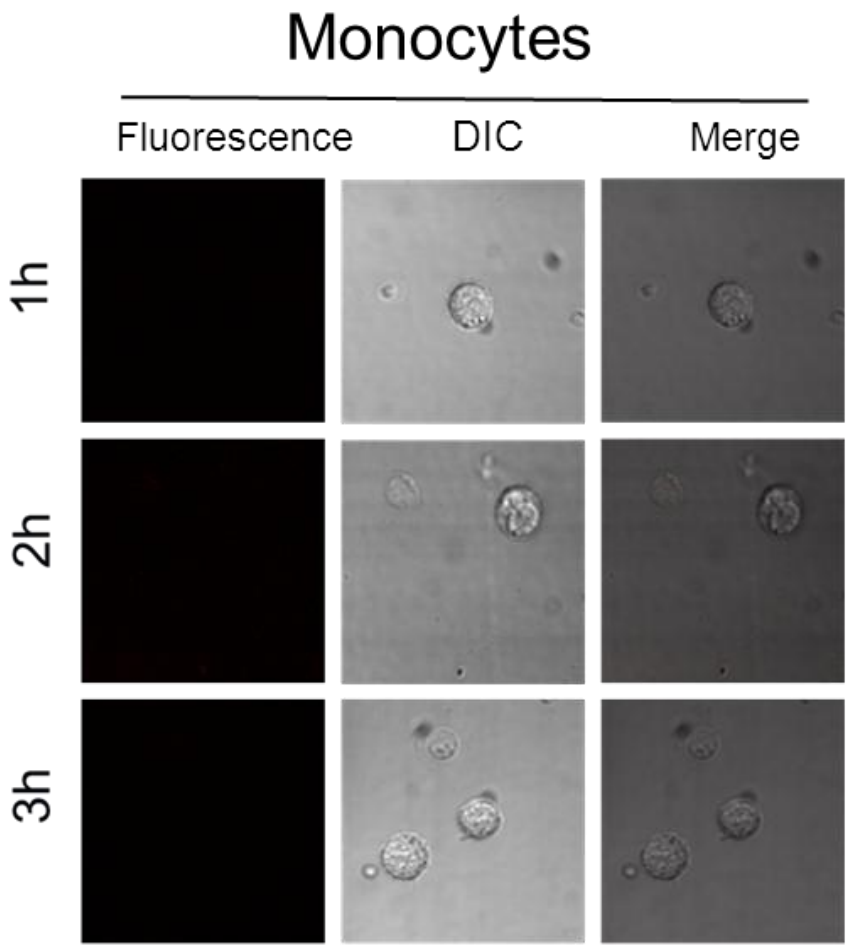

Figure 2.7 Confocal microscopy images of survivin expression in the cytoplasm of monocytes living cells. Cells were treated with 100 nM MB (red) and fluorescence was measured at 1, 2 and 3 h following start of transfection. Confocal fluorescent images are shown in the left column, transmission DIC images in the central column, while the merged images are also shown in the right column. The fluorescence images were obtained by using excitation and emission wavelengths of 645 and 669 nm, respectively and an oil immersion objective (x40, NA=1.3).

Noteworthy, an intense red fluorescent signal was observed (Fig. 2.8) when human monocytes were transfected with the fluorescent probe. This demonstrated that Lipofectamine was able to transfect both melanoma cells and normal cells (i.e., melanocytes and monocytes), and that the MB specifically opened with fluorescence emission only in survivin mRNA positive cells (i.e., A375 and 501 Mel cells). Specificity of the bases forming the MB loop for survivin versus other members of the IAP family was confirmed by BLAST analysis.

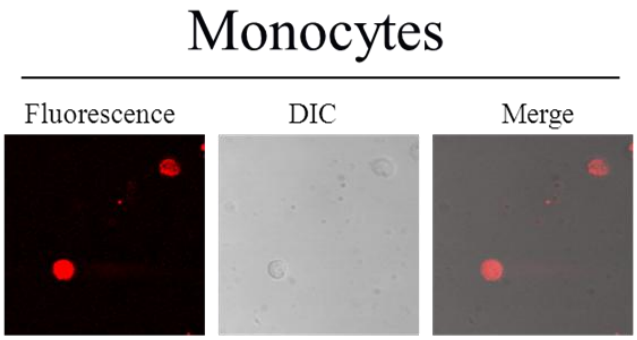

Figure 2.8 Confocal microscopy images of probe in the cytoplasm of monocytes living cells. Cells were treated with 100 nM probe (red). Confocal fluorescent images are shown in the left column, transmission DIC images in the central column, while the merged images are also shown in the right column. The fluorescence images were obtained by using excitation and emission wavelengths of 645 and 669 nm, respectively and an oil immersion objective (x40, NA=1.3).

2.3.3 MB downregulation of survivin expression and protein synthesis

We performed real-time PCR experiments to quantitatively assess the effect of MB on survivin gene expression in different cell types. Treatment with MB for 24 h significantly decreased survivin expression by 79.3±7.6 % ($p<0.01$), as compared to cells transfected with control (only lipofectamine) in A375 cells (Fig. 2.9).

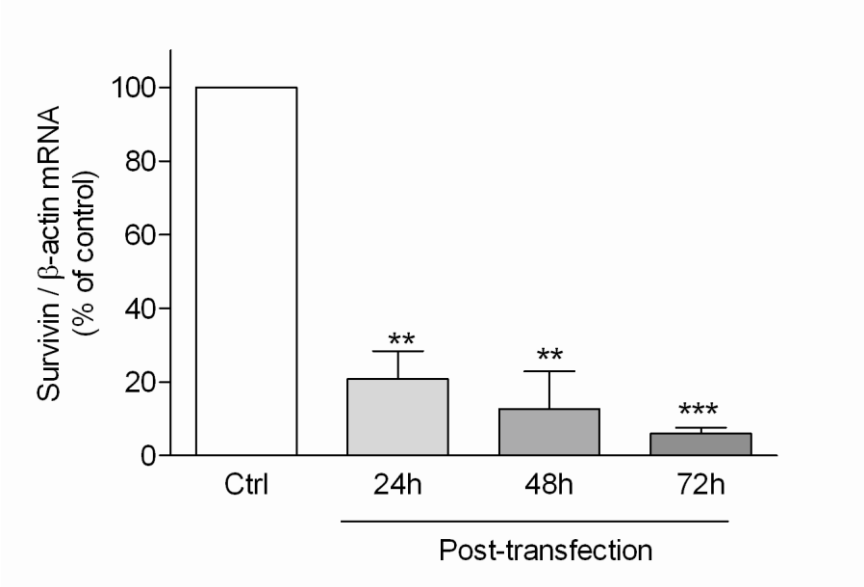

Figure 2.9 Real-time PCR assessment of survivin gene expression in A375 cells. Cells were transfected with lipofectamine-MB or treated with lipofectamine alone (Ctrl) and analyzed after 24, 48 and 72 hours. Values were expressed as mean ± standard of the mean (SEM) from three separate experiments. **$p<0.01$, ***$p<0.001$, (ANOVA followed by the Bonferroni's multiple comparison test).

Prolonged cellular exposure to MB further decreased expression of survivin and the maximum effect was reached after 72 h (-94±1.6 %, as compared to control). These findings were also confirmed in 501 Mel cells in the same experimental conditions (Fig. 2.10).

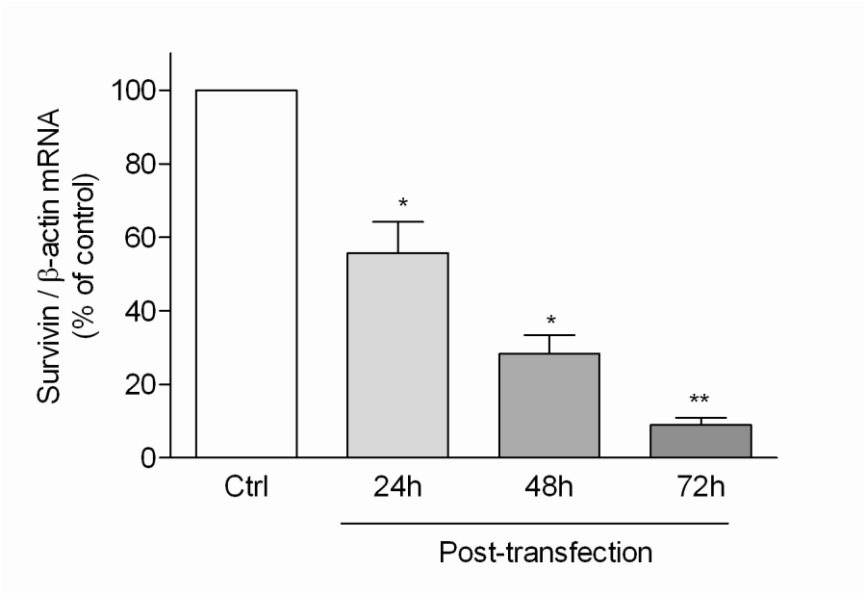

Figure 2.10 Real-time PCR assessment of survivin gene expression in 501 Mel cells. Cells were transfected with lipofectamine-MB or treated with lipofectamine alone (Ctrl) and analyzed after 24, 48 and 72 hours. Values were expressed as mean ± standard of the mean (SEM) from three separate experiments. *p<0.05, **p<0.01 (ANOVA followed by the Bonferroni's multiple comparison test).

Expression levels of survivin protein in A375 cells was assessed by western blot and the bands on the blot image were analysed by densitometry. In A375 lysates, the survivin antibody mainly labelled a band corresponding to an apparent molecular weight of 16.5 KDa. Cell treatment with MB time-dependently inhibited survivin protein expression by 44.3±2.4, 66.1±1.1, and 90.1±1.8 % after 24, 48 and 72 h, respectively, as compared to control (Fig. 2.11).

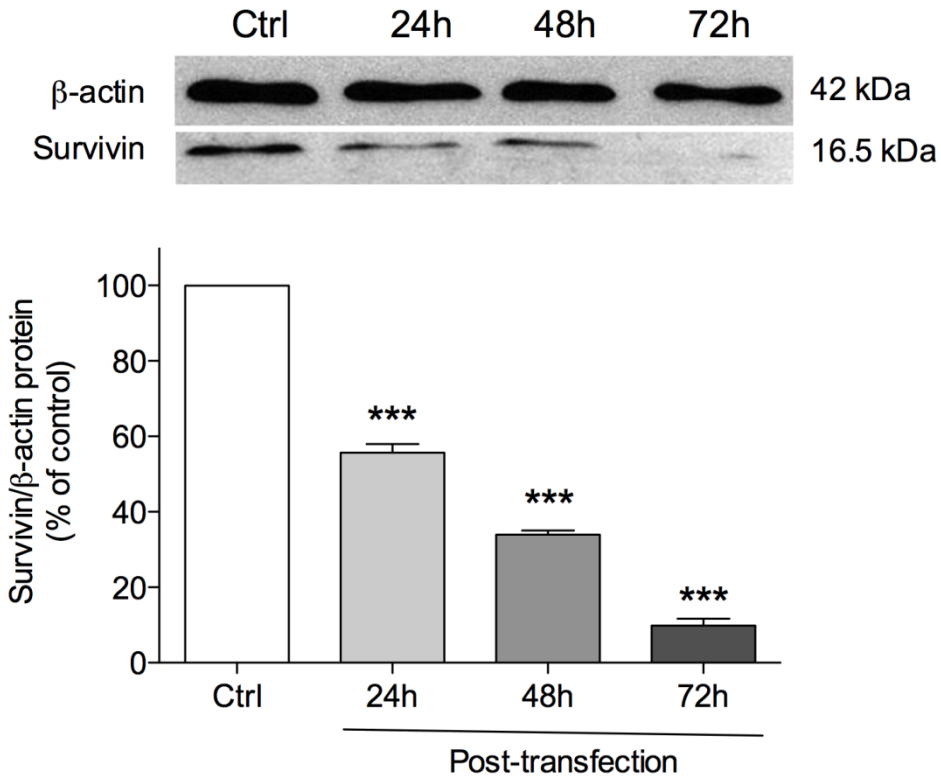

Figure 2.11 Detection of survivin protein levels by Western Blot analysis in A375 cells. Cells were transfected with lipofectamine-MB or treated with lipofectamine alone (Ctrl) and analyzed after 24, 48 and 72 hours. Values were expressed as mean ± standard of the mean (SEM) from three separate experiments. ***$p<0.001$, (ANOVA followed by the Bonferroni's multiple comparison test).

2.3.4 MB induction of apoptosis

The ability of MB to induce apoptosis in human melanoma cells was investigated by evaluating dissipation of mitochondrial membrane potential ($\Delta\Psi m$), internucleosomal DNA fragmentation, and nuclear morphological changes.

Treatment with MB for 48 h induced a significant ($p<0.001$) variation in $\Delta\Psi m$ in about 35% of total cells in A375, suggesting the involvement of the intrinsic pathway in the molecular mechanism of MB action. Otherwise, control experiments demonstrated the absence of significant changes in $\Delta\Psi m$ (Fig. 2.12). A representative dot plots in live, depolarized/live, depolarized/dead and dead phase is showed in the upper panel in Fig. 2.12.

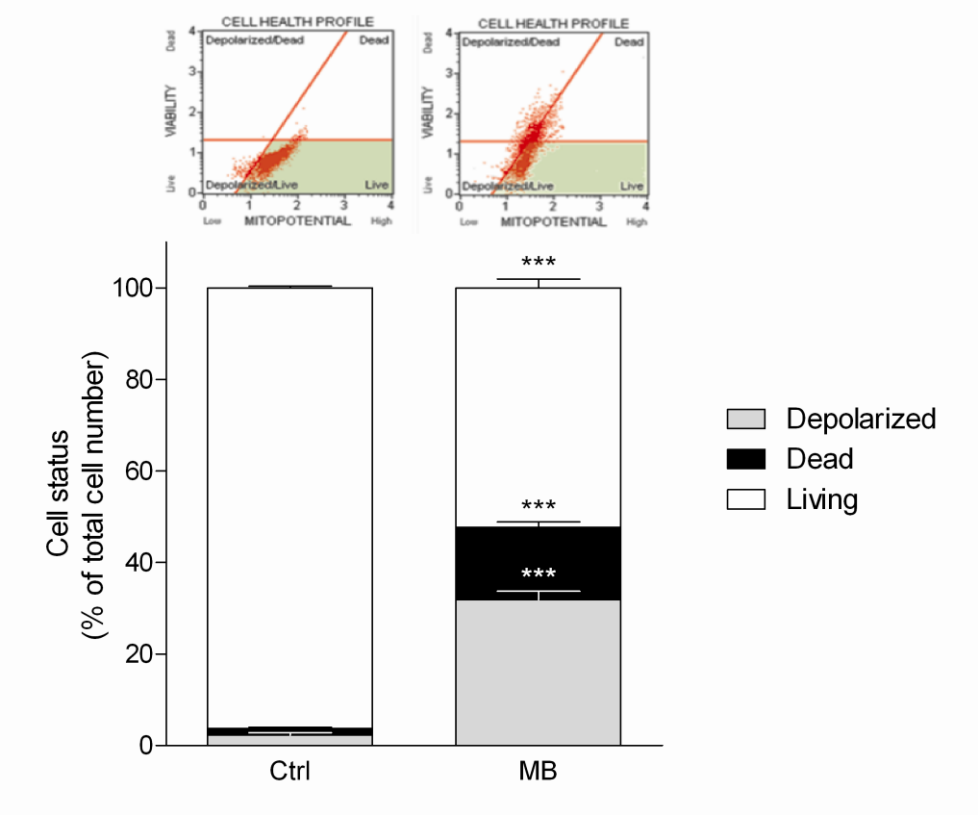

Figure 2.12 Dissipation of the mitochondrial membrane potential (ΔΨm) in A375 cells at 48 h. A representative dot plots in live, depolarized/live, depolarized/dead and dead phase is showed in the upper panel, whereas the mean percentages of the total cell number for each cell status are reported in the lower panel. Values were expressed as mean ± standard of the mean (SEM) from three separate experiments. ***$p<0.001$, as compared to control (Student's *t*-test).

MB induced accumulation of histone-complexed DNA fragments in the cytoplasmic fraction of A375 cell lysates after 48 and 72 h, while after 24 h it did not significantly induce cell death (Fig. 2.13). This is probably due to the fact that major DNA fragmentation is a late event in apoptosis.

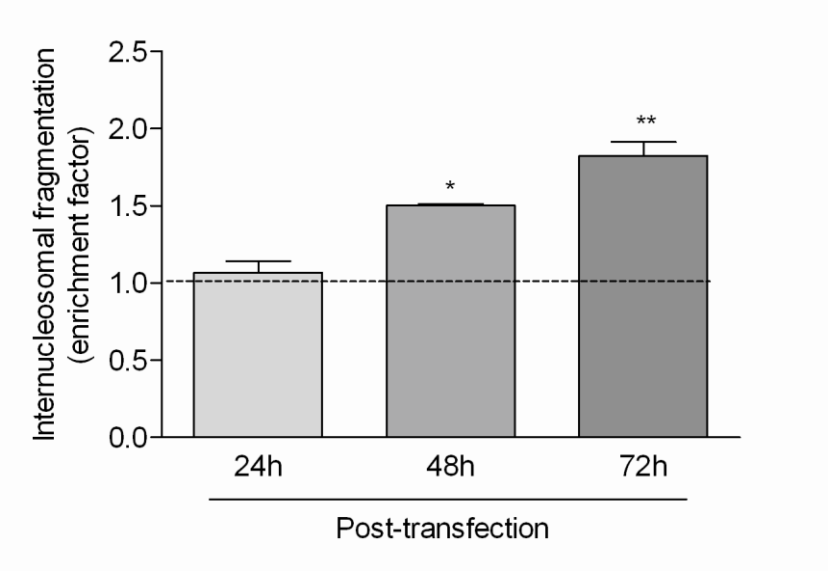

Figure 2.13 Time-dependent fragmentation of internucleosomal DNA in A375 cells after MB treatment at 100 nM for 24, 48 and 72 h. Values were expressed as mean ± standard of the mean (SEM) from three separate experiments. *$p<0.05$, **$p<0.01$, as compared to 24 h (ANOVA followed by the Bonferroni's multiple comparison test).

According to this, DAPI staining experiments showed that many A375 and 501 Mel cells exposed to MB for 48 and 72 h exhibited nuclear condensation and chromatin fragmentation, while human melanocytes did not (Fig. 2.14). Noteworthy, increased formation of multinucleated cells was observed in MB-treated cells, whereas control cells showed normal nuclear morphology (data not shown).

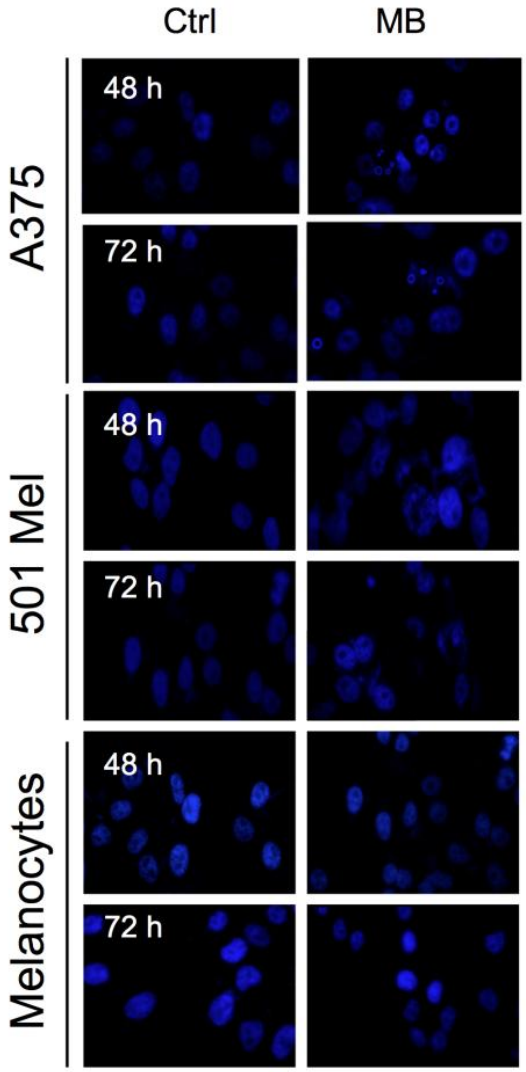

Figure 2.14 Nuclear morphology revealed by DAPI staining of A375, 501 Mel cells and human melanocytes transfected with MB or treated with lipofectamine alone (Ctrl) at 48 and 72 h.

2.3.5 MB enhancement of chemotherapy-induced apoptosis

To assess the ability of MB to increase the proapoptotic effects induced by DTX and CisPt, A375 cells were pre-incubated with MB at 100 nM for 48 h, followed by DTX at 10 nM or CisPt at 1 μM for 24 h. Apoptosis after single agent or combination treatments was analyzed by measuring ΔΨm. The combination of MB with DTX or CisPt at low concentrations produced an effect greater than that of each drug alone (Fig. 2.15; Fig. 2.16). Specifically, the percentage mean values of depolarized A375 cells after single DTX and MB treatments were 1.64±0.72 % and 16.34±4.24%,

respectively, as compared to control. It is worth mentioning that MB *plus* DTX significantly ($p<0.001$) increased the percentage of depolarized cells up to 33.28±4.59 %, compared to control (Fig. 2.15).

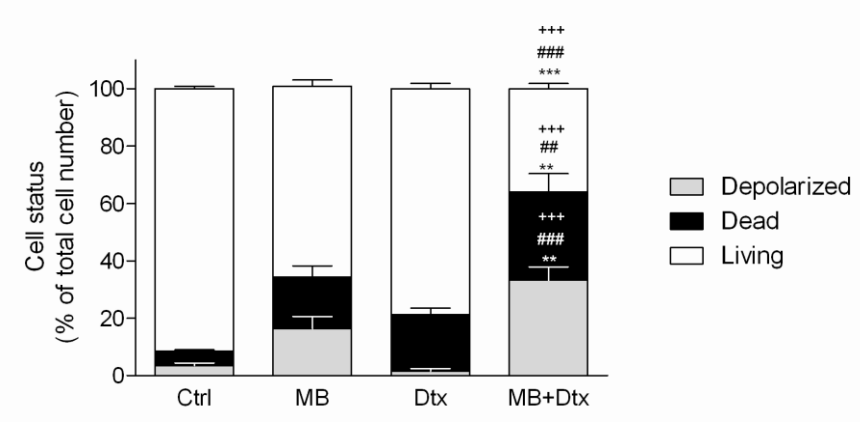

Figure 2.155 Dissipation of the mitochondrial membrane potential (ΔΨm) induced by MB and docetaxel (DTX), alone or in combination schedules, in A375 cells. Cells were pre incubated with MB at 100 nM for 48 h in the presence or absence of DTX at 10 nM for 24 h. Values were expressed as mean ± standard of the mean (SEM) from three separate experiments. **p<0.01, ***p<0.001, compared with MB alone; ##p<0.01, ###p<0.001, compared with DTX alone; +++p<0.001, compared with control (Ctrl), (ANOVA followed by the Bonferroni's multiple comparison test).

The statistical analysis also highlighted a significant ($p<0.01$) ΔΨm increase in combination *versus* single agent treatments. In a similar manner, the percentage of depolarized cells after treatment with single CisPt and MB was 10.64±0.92 % and 11.93±2.76 %, respectively, whereas it was of 29.98±4.09 % after combination treatment (Fig. 2.16).

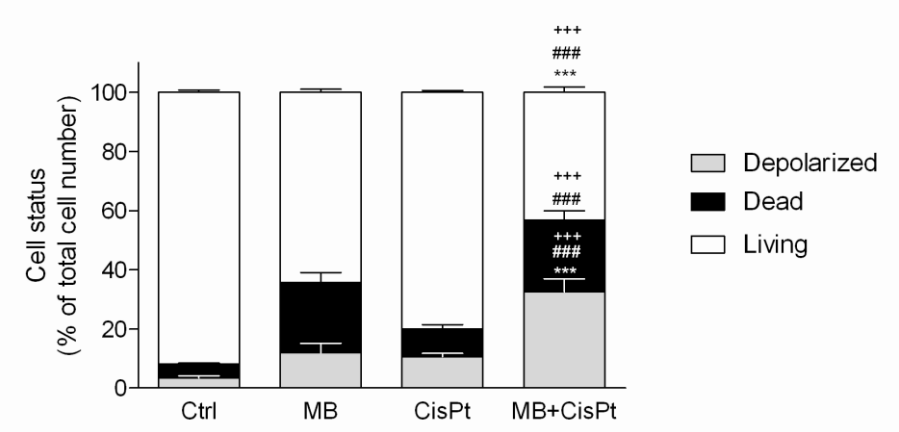

Figure 2.16 Dissipation of the mitochondrial membrane potential (ΔΨm) induced by MB and cisplatin (CisPt), alone or in combination schedules, in A375 cells. Cells were preincubated with MB at 100 nM for 48 h in the presence or absence of CisPt at 1 µM for 24 h. Values were expressed as mean ± standard of the mean (SEM) from three separate experiments. ***p<0.001, compared with

MB alone; ###p<0.001, compared with CisPt alone; +++p<0.001, compared with control (Ctrl), (ANOVA followed by the Bonferroni's multiple comparison test).

2.4 Discussion

Although depletion of survivin by siRNA has been previously reported to increase the sensitivity of cancer cells to chemotherapy *in vivo* (Li et al., 2013; Ryan et al., 2009), siRNA-based therapeutics targeting survivin per se does not have the potential to detect cancer cells. Our findings provide evidence of a novel potential strategy for both cancer diagnosis and treatment. Specifically, we deeply characterized in vitro a MB that conjugates the ability of imaging of survivin with the pharmacological silencing activity in human melanoma cells (Fig. 2.17).

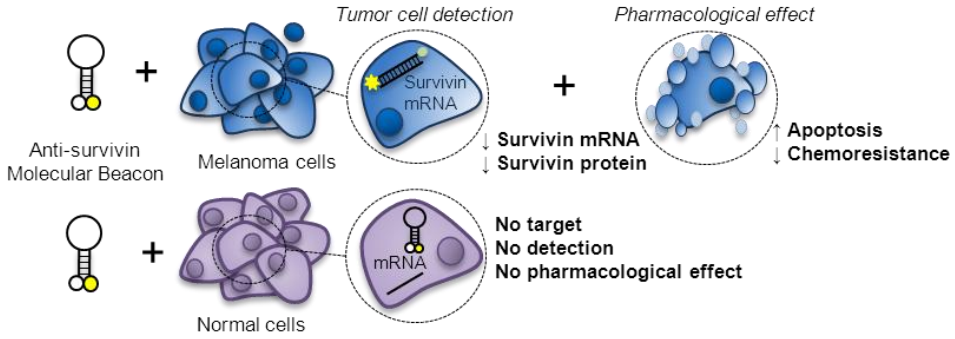

Figure 2.17 Overview of theranostic properties of anti-survivin moleular beacon.

The ability of the MB-lipofectamine system to cross the cell membrane and to penetrate into the cytoplasm of A375 and 501 Mel cells was clearly demonstrated in the current study by confocal microscopy. Transfection of MB into human melanoma cells generated high signal intensity from the cytoplasm, while no signal was detected in the extracellular environment or in survivin-negative cells (i.e., human melanocytes and monocytes). These findings demonstrate the diagnostic capability of the MB that may have great potential to translate into clinical applications. In this regards, a tumor-specific accumulation in the in vivo setting could be reached via nanoparticle-delivered transfection, therefore permitting enhanced permeability and retention effect in cancer tissues (Sinha et al., 2006).

It is widely recognized that survivin expression in melanoma is inversely correlated with patient survival (Cheung et al., 2013). Furthermore, high survivin expression is associated with resistance to chemotherapeutic agents (Groner et al., 2014) and survivin-overexpressing melanoma cells have been reported to have a potential role in lung metastasis (McKenzie et al., 2010; McKenzie et al., 2013). Therefore, the development of targeted

contrast agents (such as fluorescent probes) coupled with optical imaging techniques could allow to characterize tumor progression *in vivo* with great sensitivity and selectivity.

The current study demonstrated the therapeutic potential of the tested MB. This MB was already described in literature (Nitin et al., 2004) for the detection and quantification of survivin mRNA. However, no evidence was provided on its silencing activity in pancreatic cancer cells (Nitin et al., 2004; Santangelo et al., 2004), whereas other works showed that a partially homologous MB did not induce any variation in survivin expression in human breast cancer cells (Peng et al., 2005).

Concerning the molecular beacon tested in this work, we found that treatment with MB markedly decreased survivin mRNA and protein expression associated with activation of apoptosis and vitality reduction. In line with evidence highlighting the central role of mitochondrial survivin in the apoptotic machinery (Dohi et al., 2004), we demonstrated that MB, at nanomolar concentrations, induced a significant loss of mitochondrial transmembrane potential in A375 cells. Furthermore, the increased formation of multinucleated cells observed in the current study after transfection with MB is also consistent with the critical role of survivin in the regulation of cytokinesis (Vong et al., 2005; Szafer-Glusman et al., 2011). Indeed, survivin is a component of the chromosomal passenger complex, which plays a role in chromosome condensation, interaction between kinetochores and microtubules at metaphase and midzone microtubule organization at anaphase (Szafer-Glusman et al., 2011).

Concerning the mechanism of action, MB is a stem-loop hairpin-structured oligonucleotide that works as an antisense oligonucleotide. In agreement with this notion, selective inhibition of survivin expression by the antisense oligonucleotide LY2181308 induced apoptosis, cell cycle arrest in the G2-M phase, and multinucleated cells (Carrasco et al., 2011).

Another interesting point that needs to be discussed regards the role of survivin in chemoresistance (Pennati et al., 2008). For example, it has been reported that both docetaxel and cisplatin induced accumulation of survivin in different types of tumors including melanoma (Yamanaka et al., 2011; Li et al., 2006), lung (Yang et al., 2008), breast (Kaneko et al., 2013), and gastric (Zheng et al., 2012; Ikeguchi et al., 2002) cancer. We have found that *in vitro* combination treatment of MB and docetaxel or cisplatin induced a greater rate of apoptosis than the sum of the single-treatment rates in A375 cells, suggesting that targeting survivin has the potential to increase the sensitivity of cancer cells to chemotherapeutics. The effect induced by combination schedules appears to be additive because it is approximately the sum of the percentage obtained from single treatments,

both in terms of depolarized cells (i.e., cells committed to die) and dead cells. Moreover, it is also possible that survivin silencing may restore sensitivity to targeted therapy. In line with this notion, it has been recently demonstrated that blood survivin mRNA positivity was strongly related to a poor treatment outcome of EGFR-tyrosine kinase inhibitors in non-small cell lung cancer patients (Shi et al., 2014).

Although general transfection techniques (including those employing liposomes or dendrimers) might result in false positive signals, we demonstrated that cellular lipofection of tested MB was specific with no false positive results. Indeed, a bright red fluorescent signal was observed when cells that did not express survivin (i.e., monocytes) were transfected with the linear probe (the same fluorescent antisense oligonucleotide of MB lacking the quencher molecule), while no signal was detected after MB transfection.

Taken together, our findings provide evidence of a novel potential anticancer strategy for the simultaneous imaging and targeted therapy in human cutaneous melanoma. The ability to image specific RNAs *in vivo* may offer new opportunities in terms of development of clinical diagnostic procedure for the early detection of cancer, pharmacological monitoring of silencing effect, and follow-up after surgery or chemotherapy treatment.

Chapter 3

Experimental Section: AM251 induces apoptosis and G2/M cell cycle arrest in A375 human melanoma cells

3.1 Introduction

AM251 (N-(Piperidin-1-yl)-5-(4-iodophenyl)-1-(2,4-dichlorophenyl)-4-methyl-1H-pyrazole-3-carboxamide) (Fig.3.1) is prevalently used as cannabinoid 1 receptor CB1R antagonist/inverse agonist but several lines of evidence demonstrated that the pharmacological profile of the diarylpyrazole derivative is also characterized by CB-independent biological actions (Fogli et al., 2006; Patil et al., 2011; Fiori et al., 2011; Raffa and Ward, 2012; Seely et al., 2012; Baur et al., 2012; Krzysik-Walker et al., 2013).

AM251 is also recognized as agonist/partial agonist of GPR55 receptor (Kapur et al., 2009; Sharir and Abood, 2010; Anavi-Goffer et al., 2012) however the pharmacology of GPR55 is not completely clear but rather sometimes controversial (Ross, 2009; Sharir and Abood, 2010; Anavi-Goffer et al., 2011) since GPR55 (G protein-coupled receptor 55) ligands are lipid molecules able to bind different targets as occurs for cannabinoid compounds (Pertwee, 2010).

Noteworthy, a remarkable anticancer activity of AM251 has been documented in pancreatic (Fogli et al., 2006; Fiori et al., 2011) and colon cancer cells (Fiori et al., 2011).

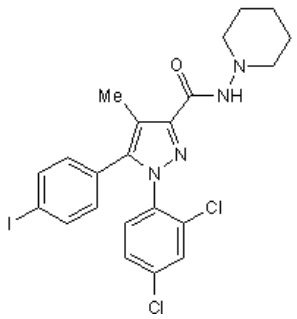

Figure 3.1 Molecular structure of AM251.

The aim of the present study was to characterize the anti-melanoma activity of AM251 against the BRAF V600E mutant cell line, A375, in terms of proapototic activity and mechanism of action.

3.2 Materials and Methods

3.2.1 Cell cultures

The human melanoma A375 cell line (American Type Culture Collection, Rockville, MD, USA) was cultured at 37°C in a humidified atmosphere containing 5% CO_2 in DMEM supplemented with l-glutamine (2 mM), 10% FBS and 1% penicillin/streptomycin (Sigma-Aldrich, Milan, Italy). Adult human dermal fibroblasts (HDFa; Ref. C-013-5C, Gibco, Life Technologies, CA, USA) were cultured in an optimized medium containing 10% FBS and 1% (w/v) penicillin/streptomycin, as recommended by the manufacturer.

3.2.2 Drugs

AM251 (selective CB1 receptor antagonist/inverse agonist and GPR55 agonist), CID16020046 (selective GPR55 antagonist) and forskolin (adenylyl cyclase activator) were obtained from Tocris Bioscience (Northpoint, UK). Cisplatin (CisPt), L-α-lysophosphatidylinositol (LPI), celecoxib, rofecoxib and indomethacin were purchased from Sigma–Aldrich, Milan, Italy. Compounds were dissolved in their specific solvents (DMSO for AM251, CID16020046, LPI and rofecoxib, water for Cis-Pt, and ethanol for others) and further diluted in sterile culture medium immediately before their use. DMSO did never exceed 0.33% v/v in the culture medium.

3.2.3 Cell viability assay

Cell viability was measured using a method based on the cleavage of the 4-(3-(4-iodophenyl)-2-(4-nitrophenyl)-2H-5-tetrazolium)-1,3-benzene disulfonate (WST-1) to formazan by mitochondrial dehydrogenase activity following manufacturer's instructions (Cell proliferation reagent WST-1; Roche, Mannheim, Germany). Briefly, cells (5×10^4/well) were seeded in 96-well plate in 10% FBS medium; after 24 h, the complete medium was replaced with compound-containing 1% FBS medium. Each compound was dissolved in its specific solvent and then diluted in medium up to the concentrations to be tested. Freshly stock solutions were prepared. AM251 was tested in a concentration range of 0.1–50 μM and its effects evaluated in the presence or absence of different antagonists added 2 h before. After drug treatment, WST-1 was added and, after 1 h, the absorbance was

measured at 450 nm using Infinite® M200 NanoQuant instrument (Tecan, Salzburg, Austria). Optical density values from vehicle-treated cells were considered as 100% cell viability.

3.2.4 Transfection

Cells were transfected with GPR55 siRNA (Santa Cruz Biotechnology, Inc., Santa Cruz, CA, USA, sc-75183) according to the manufacturer's instructions. Briefly, cells were transfected with 100 nM siRNA using Lipofectamine 2000 (Ref. 11668-027, Invitrogen Life Technologies, Carlsbad, CA, USA) which has been reported to yield high transfection efficiency (≈70%) in A375 cells (Zhou et al., 2013). A scrambled non-specific siRNA fluorescent conjugate (Santa Cruz Biotechnology, Inc., Santa Cruz, CA, USA, sc-36869) was used as control and for preliminary confirmation of transfection efficiency through microscope analysis.

3.2.5 RT-PCR and quantitative real-time PCR analyses

Total RNA from cells was extracted by using the RNeasy® Mini kit, following manufacturer's instructions, and reverse-transcribed by the QuantiTect® Reverse Transcription kit (Qiagen, Valencia, CA, USA). RT-PCRs were performed by the HotStartTaq Master Mix kit (Qiagen, Valencia, CA, USA). Primer sequences are listed in Table 3.1.

Protein	Primer nucleotide sequences	Ta (°C)	Amplicon length
β-actin	5'- AACTGGAACGGTGAAGGTGAC-3' (F) 5'-GACTTCCTGTAACAACGCATCTC-3' (R)	61	138
GAPDH	5'-GTGAAGGTCGGAGTCAACG-3'(F) 5'GGTGAAGACGGCCAGTGGACT-3' (R)	59	301
TRPA1	5'-TCACCATGAGCTAGCAGACTATTT-3' (F) 5'-GAGAGCGTCCTTCAGAATCG-3' (R)	55	74
Bax	5'-TCTGACGGCAACTTCAACTG-3' (F) 5'-TTGAGGAGTCTCACCCAACC-3' (R)	56.6	188
Bcl-2	5'-TCCATGTCTTTGGACAACCA-3' (F) 5'-CTCCACCAGTGTTCCCATCT-3' (R)	56.6	203
Survivin	5'-ACCAGGTGAGAAGTGAGGGA-3' (F) 5'-AACAGTAGAGGAGCCAGGGA-3' (R)	59	309

Table 3.1 Primer nucleotide sequences, Ta and amplicon length used for PCR experiments.

Thermal cycle conditions were as follows: 95°C for 15 min, 35 cycles of denaturation at 95°C for 1 min followed by annealing and extension at 72°C for 1 and 10 min, respectively. Detection of the RT-PCR products was performed by agarose gel electrophoresis and ethidium bromide staining. Real-time PCR was performed with SsoFast Eva Green Supermix (Ref. 172-5201, Bio-Rad, CA, USA). Samples were amplified using the following thermal profile: 95°C for 30 s, 40 cycles of denaturation at 95°C

15 s followed by annealing for 30 s and 72°C for 30 s, with a final step at 65°C for 5 s. β-actin and GAPDH were used as housekeeping genes.

3.2.6 Determination of nuclear morphology

Changes in nuclear morphology of A375 cells were assessed after treatment with AM251 or its vehicle for 48 h. Cells were fixed with 2% paraformaldehyde on 8-well chamber slides. After washing with PBS, cells were incubated with DAPI 300 nM (Invitrogen Life Technologies, CA, USA). Fluorescence analysis was realized with Eclipse E600FN Nikon microscope using λ_{ex} 360 nm and λ_{em} 460 nm (magnification 40 × WD).

3.2.7 Fluorescent microscope analysis of $[Ca^{2+}]_i$

Imaging of $[Ca^{2+}]_i$ was carried out in A375 cells grown on discs of 35 mm diameter. Fluo-3 AM (Ref. F-1242, Molecular probe, Life Technologies, CA, USA) was added to the culture medium, the cells were incubated for 30 min at 37°C dark and then washed with medium. After 30 min of de-esterification, fluorescence analysis was performed with Eclipse E600FN Nikon microscope (water dipping objective 40X, λ_{ex} 490 nm, λ_{em} 520 nm) during the perfusion with AM251 and 5 μM ionomycin (Calbiochem, Merck Millipore, Darmstadt, Germany) as positive control. The relative fluorescence $\Delta F/F_0$ was used as an indicator of $[Ca^{2+}]_i$ in regions of interest. To determine the $[Ca^{2+}]_i$ concentrations, Fura-2 AM (Ref. F1201, Molecular probe, Life Technologies, CA, USA) was added to the cells previously treated with AM251 or vehicle for 48 h, for 30 min at 37°C in the dark. After washing with medium and 30 min of de-esterification, fluorescence analysis was performed with Eclipse E600FN Nikon microscope. Loaded cells were alternatively excited at 340 and 380 nm while they were imaged at 510 nm. After background subtraction, ratio images were obtained by dividing, pixel by pixel, pairs of digitized images at 340 and 380 nm. Fluorescence values were converted into ion concentrations, according to Grynkiewicz et al. (1985).

3.2.8 Cell Cycle

The distribution of cells in the different cycle phases was performed using the Muse™ Cell Analyzer (Merck KGaA, Darmstadt, Germany). Briefly, A375 cells were treated with AM251 (5 μM) or its vehicle for 48 h. Asynchronous adherent cells were collected and centrifuged at 300 × g for 5 minutes. The pellet was washed with PBS (phosphate buffered saline) and re-suspended in 100 μl of PBS; finally cells were slowly added to 1 ml of ice cold 70% ethanol and maintained o/n at –20°C. Then, a cell suspension aliquot (containing at least 2×10^5 cells) was centrifuged at 300 × g for 5 minutes, washed once with PBS and suspended in the fluorescent

reagent (Muse™ Cell Cycle reagent). After incubation for 30 minutes at room temperature in the dark, measurements of the percentage of cells in the different phases were acquired.

3.2.9 Statistical analysis

All experiments were performed in triplicate and results were analyzed by GraphPad Prism 5 (GraphPad Software, San Diego, CA, USA). Data were shown as mean values ± standard error of the mean (SEM) obtained from at least three separate experiments. Statistical analyses were performed by Student's *t*-test or one-way ANOVA followed by the Bonferroni's multiple comparison test.

3.3 Results

3.3.1 Effect of AM251 on cell viability

AM251 at 0.1-50 µM for 24-72 h induced a concentration- and time-dependent cytotoxicity in A375 cells (Fig. 3.2). The IC50 mean value was 5.52 ± 1.08 µM and 1.79 ± 1.42 µM after 48 and 72 h, respectively, while after 24 h the IC50 was not reached. The IC50 of cisplatin (CisPt), the anticancer drug used as reference compound, was 4.33 ± 0.04 µM after 48 h-exposure.

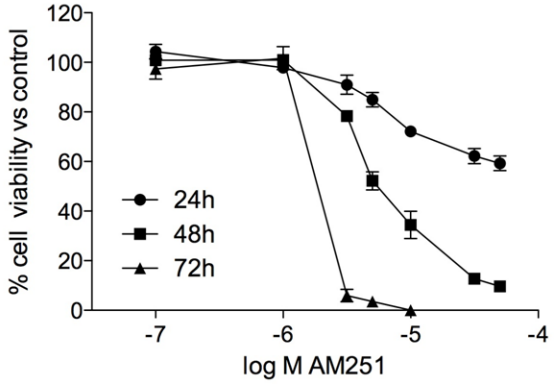

Figure 3.2 Concentration-dependent cell viability decrease to AM251, in A375 melanoma cells after 24, 48 and 72 h exposure to a single drug administration. Data are the mean ± SEM from three independent experiments.

Noteworthy, the IC50 was never reached in human dermal fibroblasts-adult, HDFa treated with AM251 at 0.1-50 µM for 48 and 72 h (Fig. 3.3).

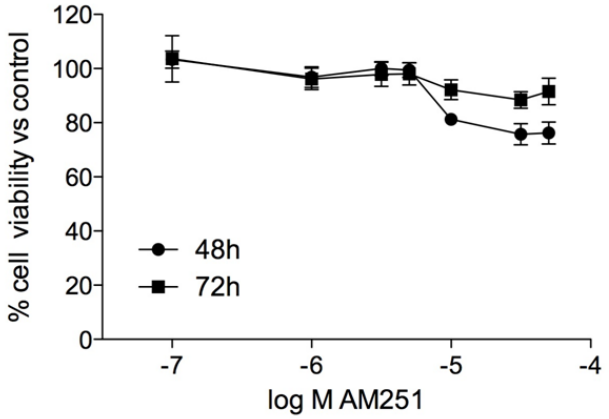

Figure 3.3 Concentration-response curves to AM251 in HDFa cells after 48 and 72h exposure. Data are the mean ± SEM from three independent experiments.

3.3.2 Effect of AM251 on apoptosis

The role played by the apoptotic process in the AM251-induced cytotoxicity was assessed measuring variation in gene expression of pro-/anti-apoptotic proteins and morphological changes in the cell nuclei by fluorescence microscopy. AM251 at 5 µM for 48 h increased Bax, decreased survivin and Bcl2 gene expression (Fig. 3.4), and induced DNA fragmentation and chromatin condensation in the cell nuclei (Fig. 3.5), compared to untreated cells.

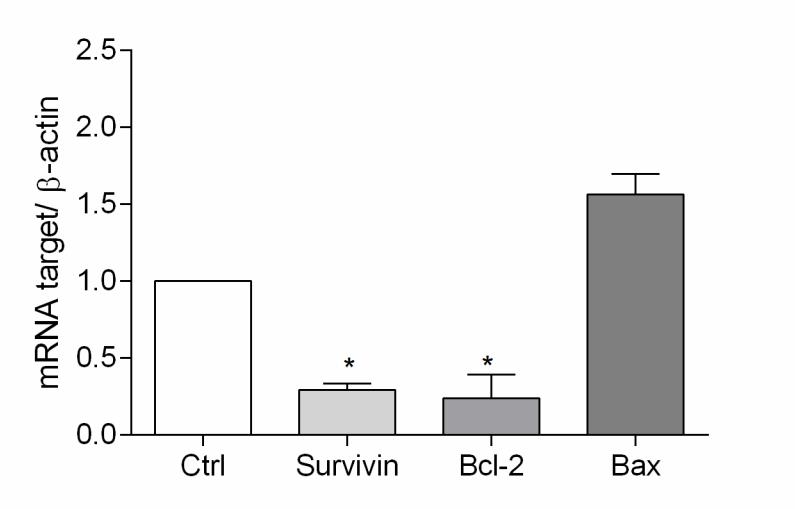

Figure 3.4 Real-time PCR for the three protein involved in apoptosis in A375 treated with AM251 for 48 h. Values were expressed as mean ± standard of the mean (SEM) from three separate experiments. *$p<0.05$ as compared with control (ctrl) (ANOVA followed by the Bonferroni's multiple comparison test).

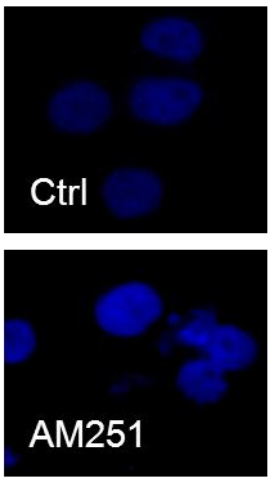

Figure 3.5 Nuclear morphology revealed by DAPI staining of A375 cells treated with AM251 or vehicle at 48 h.

The role of intracellular calcium in the pro-apoptotic effect induced by AM251 was investigated evaluating the effects of both short and long term treatment of A375 cells. A375 cells loaded with Fura-2 AM and treated with AM251 5 μM or vehicle for 48 h did not differ in their intracellular concentration of free calcium, as shown in Fig. 3.6.

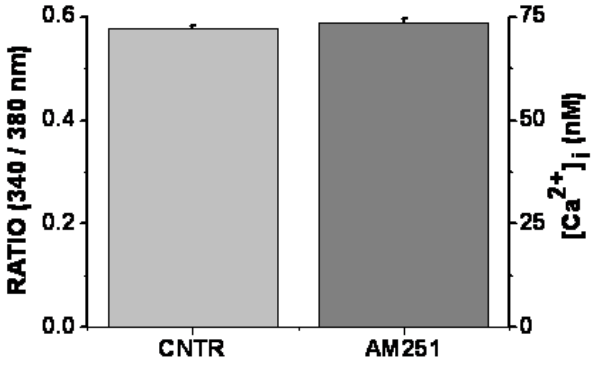

Figure 3.6 [Ca2+]i levels in Fura-2 AM loaded A375 cells after treatment for 48 h with AM251 or vehicle (CNTR). Mean values ± SEM (n = 160, P = 0.35 Student t test).

3.3.3 Effect of AM251 on cell cycle

The analysis of cell cycle phase distribution of asynchronous cells was assessed by flow cytometry. After treatment with AM251 at 5 μM for 48 h the proportion of cells in G0/G1, S and G2/M phases of the cell cycle was 59.2, 14.7 and 20.2%, respectively. The comparison with untreated cells revealed a significant increase of cells in the G2/M and S phases and a decrease of cells in G1/G0 phase (Fig. 3.7).

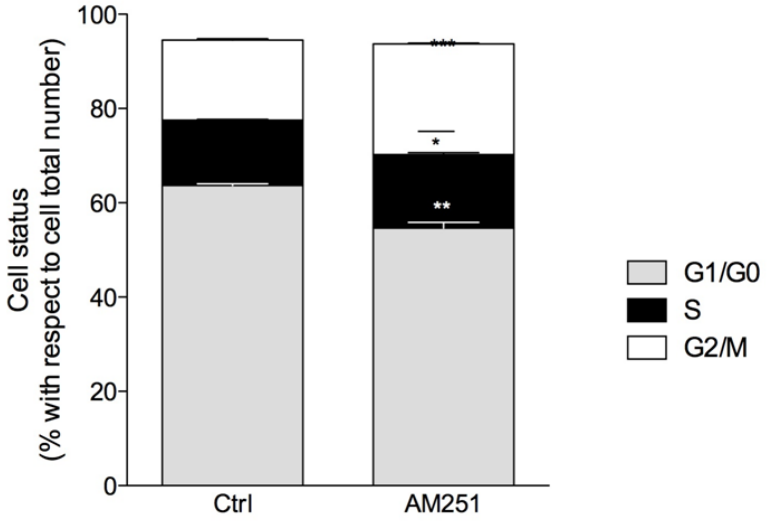

Figure 3.7 Cell cycle analyses for asynchronized A375 cells treated with AM251 or vehicle at 48 h. Representative cell cycle histograms of control and treated cells. The data are presented as percentage of cells in the different phases (G0/G1, G2 or S) versus total cell number. Data represent the mean ± SEM of three different experiments. *P < 0.05, ** P<0.01, *** P<0.001 from Student's *t*-test.

3.3.4 Effect of AM251 on GPR55 and TRPA1

The role of GPR55 on the mechanism of AM251 action was evaluated using gene silencing. 100 nM specific siRNA incubated for 24 and 48 h time-dependently reduced GPR55 mRNA expression by 40.9 and 72.8%, respectively, as compared with scrabbled siRNA treated cells (Fig. 3.8).

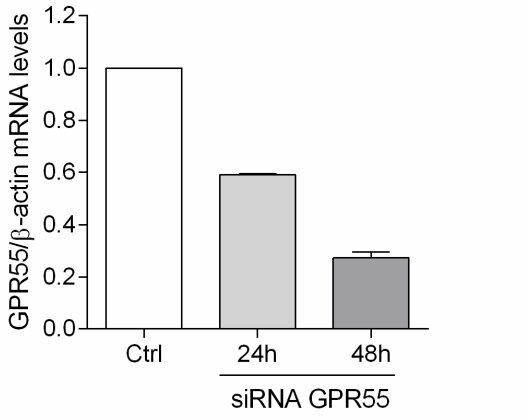

Figure 3.8 Real-time PCR results for GPR55 expression, referred to the housekeeping gene beta-actin, after 24 h and 48h after siRNA treatment compared to control siRNA-treated cells. *** P<0.001 from ANOVA and Bonferroni test.

No change was induced by siRNA on AM251-induced cytotoxicity (Fig. 3.9).

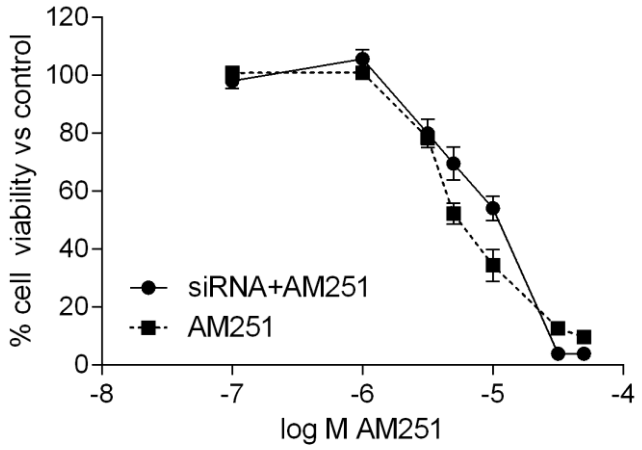

Figure 3.9 Concentration-response curve to AM251 in non-treated cells and in cells silenced with GPR55 siRNA.

Treatment with the potent endogenous GPR55 agonist LPI or the selective GPR55 antagonist, CID16020046, up to 30 μM for 48h did not significantly affect cell viability

TRPA1 (Transient receptor potential channel A1) is expressed in A375 cells (Oehler et al., 2012) and could be a possible target for AM251 (Patil et al., 2011). After confirming the presence of TRPA1 by RT-PCR analysis (Fig. 3.10), the role of TRPA1 in the AM251-induced cytotoxicity was investigated recording calcium changes immediately after treatment in Fluo 3-AM loaded cells.

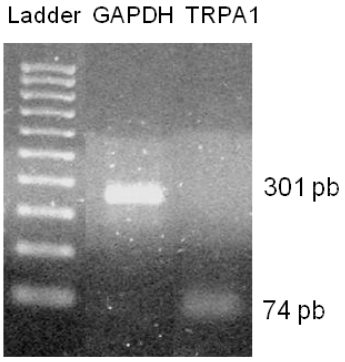

Figure 3.10 Ethidium-bromide stained agarose gel revealing TRPA1 gene espression (74pb band) in A375 cells.

Cells loaded with Fluo-3 did not exhibit detectable changes of fluorescence during treatment with AM251 at concentrations 0.1-10 μM, while they responded to ionomycin 5 μM, as shown in Fig. 3.11.

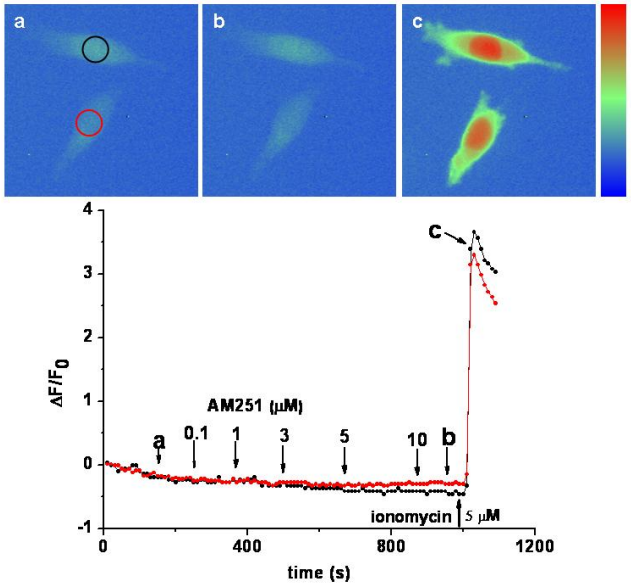

Figure 3.11 Absence of changes in Fluo 3-AM fluorescence during treatment with AM251 (0.1-10 μM) and increase of signal after calcium loading induced by ionomycin 5 μM. The black and red traces indicate the mean pixel values in the regions of interest marked by circles. On the pseudocolor scale blue represents 0 and red 255.

3.3.5 Role of COX-2 in AM251-induced cytotoxicity

We previously reported that COX (cyclooxygenase) enzymes are expressed in A375 cells (Adinolfi et al., 2013). In the current study, we found that treatment of A375 cells with the selective COX-2 (cyclooxygenase-2) inhibitor celecoxib at 0.1-100 μM for 48 h induced cytotoxicity with an IC50 of 35.64 ± 1.03 (Fig. 3.12).

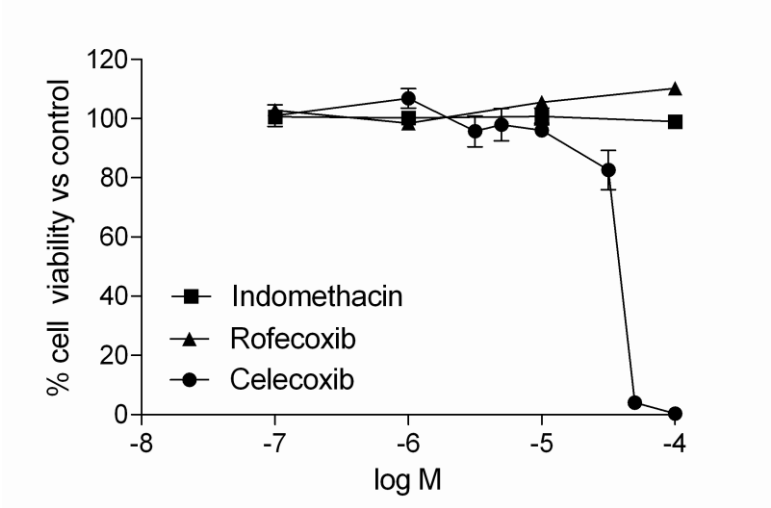

Figure 3.12 Concentration-response curves to celecoxib, rofecoxib and indomethacin in A375 cells after 48h exposure. Data are the mean ± SEM from three independent experiments.

At variance with this, no effect on cell viability was observed when cells were exposed to rofecoxib (selective COX-2 inhibitor) or indomethacin (non-selective COX inhibitor) (Fig. 3.12).

3.4 Discussion

In the current study, we demonstrated that AM251 exerted a remarkable cytotoxic effect against A375 human melanoma cells with potency comparable to that observed for cisplatin. AM251, in the concentration range tested against melanoma cells, did not significantly affect the viability of proliferating human fibroblasts, suggesting that the compound may exhibit some selectivity for cancer cells. To explore in more detail the underlying mechanism of AM251, we assessed whether genes encoding for Bcl-2, Bax and survivin were a target of AM251. Bax and Bcl-2 are two members of the Bcl-2 family that regulates, with opposite effects, the release of cytochrome c in mitochondria-dependent apoptosis (Elmore, 2007), whereas survivin is a member of the IAP family, which inhibits caspase-9 activation, a typical enzyme involved in the intrinsic apoptotic pathway. In our experimental conditions, the pro-/anti-apoptotic balance drifted to the pro-apoptotic side after treatment of A375 cells with AM251. Specifically, AM251 reduced the expression of anti-apoptotic Bcl-2 and survivin proteins and increased transcription levels of pro-apoptotic Bax. Furthermore, AM251, at a concentration that approximate the IC50 value obtained in cell viability experiments (i.e., 5 μM) induced characteristic features of apoptosis, including DNA fragmentation and chromatin condensation. Using real-time imaging with the single-wavelength intensity-modulating dye Fluo 3, we did not find changes of intracellular Ca^{2+} in A375 cells during treatment with AM251 at 0.1-10 μM.

Moreover, dual-wavelength ratiometric indicator Fura-2 allowed us to measure the $[Ca^{2+}]_i$ concentrations in cells treated for 48 h with AM251 5 μM or vehicle, assessing the maintenance of the intracellular calcium homeostasis in both experimental conditions. These findings suggest that AM251 can induce apoptosis by a specific Ca^{2+}-independent mechanism of action. Interesting to note, Gogvadze and co-workers demonstrated a Ca^{2+}-independent mechanism of mithocondria release of cytochrome c via the pro-apoptotic protein Bax (Gogvadze et al., 2001) and data of the current study showed that AM251 significantly increased Bax expression in A375 cells. Apoptotic cell death is generally linked to alterations in cell cycle program. The percentage of G0/G1 phase cells was considerably decreased by AM251 and the parallel increase in the proportion of cells in S-phase and G2/M-phase, in treated *versus* untreated cells, suggests a cell cycle arrest at this level. In line with this, drug-induced arrest in the G2 or M

phases may be followed by apoptotic cell death (DiPaola, 2002) and a pro-apoptotic G2 arrest has been already described in A375 melanoma cells treated with various agents (Wei et al., 2014; Huang et al., 2014; Das et al., 2012; Huang et al., 2012).

Several orphan G-protein coupled receptors have been proposed to act as endocannabinoid receptors (Brown, 2007; Pertwee et al., 2010). Among these, GPR55 has been recognized as the possible "third" cannabinoid receptor (Ryberg et al., 2007; Moriconi et al., 2010) with a role in tumorigenesis and metastasis (Pineiro et al., 2011; Andradas et al., 2011; Paul et al., 2014). Although AM251 has been recognized to act as agonist/partial agonist at GPR55 (Kapur et al., 2009; Sharir and Abood, 2010; Anavi-Goffer et al., 2012), our findings clearly exclude the involvement of GPR55 in the mechanism of AM251 action. Indeed, the potent endogenous GPR55 agonist, LPI (Yamashita A et al., 2013) did not affect A375 cell viability and no difference in AM251 activity was observed in GPR55-silenced cells, compared to controls. AM251 has been also reported to activate the transient receptor potential A1 (TRPA1) in sensory neurons (Patil et al., 2011) and TRPA1 was found to be expressed in A375 cells (Oehler et al., 2012), a condition that has also been confirmed in the current study. We therefore investigated whether TRPA1 could be a possible target involved in the AM251-induced cancer cell death. Our findings demonstrated no early rise in $[Ca^{2+}]_i$ basal levels after treatment of A375 cells with AM251. Since TRPA1 is a non-selective Ca^{2+} permeable channel, the anticancer effect of AM251 was probably independent of TRPA1 channel activation. Furthermore, data showing that ionic currents through TRPA1 are unlikely responsible for the anti-tumour effects of highly potent TRPA1-activating compounds in A375 cells (Oehler et al., 2012), suggest that this receptor type does not have a major role in determining the phenotype of human melanoma cells.

Taking into account the high levels of cyclooxygenase (COX)-2 expressed in A375 cells (Adinolfi et al., 2013), we tried to understand whether COX-2 could play a role in AM251 cytotoxicity. While celecoxib induced cytotoxicity in A375 cells, with a potency lower than that observed for AM251, other selective and non-selective COX-2 inhibitors did not. It is interesting to note that COX-2-inhibitory function is not required for celecoxib-mediated apoptosis, which seems to be associated to the unbalance between pro- e anti-apoptotic proteins, the activation of intrinsic apoptotic pathway, and the delayed progression of cells through the G2/M phase of the cell cycle (Grösch et al., 2006). Our findings are in line with the previously reported celecoxib-AM251 molecular similarity (Fogli et al.,

2006), which may represent the basis for further investigation on the molecular mechanism of AM251 (Fig. 3.13).

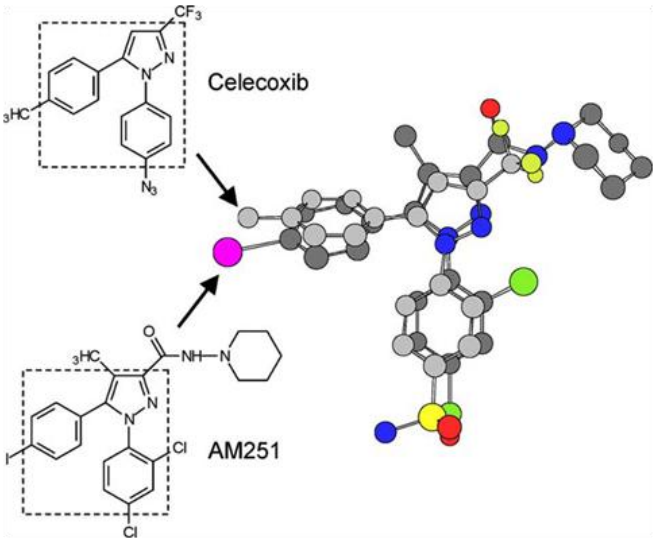

Figure 3.13 Celecoxib-AM251 molecular similarity (Fogli et al., 2006).

Overall, the results of the current study suggest that AM251 could be a prototypical compound for the development of promising diarylpyrazole derivatives in human cutaneous melanoma.

Nomenclature

501-Mel	Metastatic melanoma cell line
A375	Metastatic melanoma cell line
AJCC	American Joint Committee on Cancer
Akt	Protein kinase B (PKB)
AM251	(N-(Piperidin-1-yl)-5-(4-iodophenyl)-1-(2,4-dichlorophenyl)-4-methyl-1H-pyrazole-3-carboxamide)
AMP	Adenosine monophosphate
AMPK	AMP-activated protein kinase
AP-1	Activator protein 1
APC	Antigen-presenting cell
ATP	Adenosine triphosphate
Bad	Bcl-2-associated death promoter
Bax	Bcl-2-associated X protein
Bcl-2	B-cell lymphoma 2
BSMC	Human Bronchial Smooth Muscle Cells
CB1R	Cannabinoid receptor subtypes 1
CB2R	Cannabinoid receptor subtypes 2
CD271	Low affinity nerve growth factor receptor
CD28	Cluster of Differentiation 28
CDK	Cyclin dependent kinase
CDK2	Cyclin dependent kinase type 2
CDK4	Cyclin dependent kinase type 4
CDK6	Cyclin dependent kinase type 6
CDKN2A	Cyclin-dependent kinase inhibitor 2A
CisPt	Cisplatin
CK2	Protein kinase 2 or casein kinase II
CKII	Casein kinase II or protein kinase 2
c-KIT	Tyrosine-protein kinase or CD117
COX	Cyclooxygenase
COX-2	Cyclooxygenase-2
CREB	cAMP response element-binding protein
CSC	Cancer stem cells
CTLA-4	Cytotoxic T-Lymphocyte Antigen 4
CTRL	Control
DAPI	4',6-diamidino-2-phenylindole
DIC	Differential interference contrast
DMEM	Dulbecco's modified Eagle's medium
DMSO	Dimethyl sulfoxide

DTX	Docetaxel
ECS	Endocannabinoid system
EGFR	Epidermal growth factor receptor
ELISA	Enzyme-linked immunosorbent assay
EMA	European Medicine Agency
ERK	Extracellular signal-regulated kinases
ERK1	Extracellular signal-regulated kinase 1
ERK2	Extracellular signal-regulated kinase 2
FBS	Fetal bovine serum
FDA	US Food and Drug Administration
GAPDH	Glyceraldehyde 3-phosphate dehydrogenase
GDP	Guanosine diphosphate
GPR55	G protein-coupled receptor 55
GSK3	Glycogen synthase kinase 3
GTP	Guanosine -5'triphosphate
GβL	G protein β-like
HDFa	Adult Human Dermal Fibroblasts
HIF1	Hypoxia-inducible factor-1
HSP90	Heat-shock protein 90
IAP	Inhibitor of apoptosis
IGF	Insulin-like growth factor
IkB	Nuclear factor of kappa light polypeptide gene enhancer in B-cells inhibitor
IKK	Inhibitor of nuclear factor kappa-B kinase
IL-2	Interleukin-2
INF-α2b	Interferon alpha 2b
Jak	Janus kinase
JNK	Jun N-terminal kinases
LPI	L-α-lysophosphatidylinositol
MAPK	Mitogen-activated protein kinase
MB	Molecular beacon oligodeoxyribonucleotides
MC1R	Melanocortin 1 receptor
MDM2	Mouse double minute 2
MIMIC	Malignant melanoma-initiating cell
MITF	Microphthalmia-associated transcription factor
mTOR	Mammalian target of rapamycin
mTORC1	Mammalian target of rapamycin complex 1
mTORC2	Mammalian target of rapamycin complex 2
NA	Numerical aperture
NCCN	National Comprehensive Cancer Network

NF-κB	Nuclear factor kappa-light-chain-enhancer of activated B cells
NIK	NF-kappa-B-inducing kinase
OS	Overall survival
$p14^{ARF}$	ARF tumor suppressor
$p16^{INK4}$	Cyclin-dependent kinase inhibitor 2A
p21	Cyclin-dependent kinase inhibitor 1
$p27^{KIP1}$	Cyclin-dependent kinase inhibitor 1B
p38	Mitogen-activated protein kinases
p53	Cellular tumor antigen p53
p65	Transcription factor p65
PBS	Phosphate buffered saline
PCR	Polymerase chain reaction
PD-1	Programmed death-1 or programmed cell death-1
PDGF	Platelet-derived growth factor
PDK1	Phosphoinositide dependent protein kinase-1
PD-L1	Programmed death-ligand 1
PD-L2	Programmed death-ligand 2
PI3K	Phosphatidylinositol-3-kinase
PIP2	Phosphatidylinositol-4,4-bisphosphate
PIP3	Phosphatidylinositol-3,4,5-triphosphate
PKA	Protein kinase A
PKB	Protein kinase B
PKC	Protein kinase C
POD	Horseradish peroxidase
PTEN	Phosphatase and tensin homolog
RAPTOR	Regulatory-associated protein of mTOR
Rb	Retinoblastoma
RICTOR	Rapamycin-insensitive companion of mammalian target of rapamycin
RTK	Receptor tyrosine kinase
RT-PCR	Reverse transcriptase polymerase chain reaction
SCF	Stem cell factor
SDS	Sodium dodecyl sulfate
SEM	Standard error of the mean
siRNA	Small or short interfering RNA
SLNB	Sentinel lymph node biopsy
SOS	Son of sevenless
STAT	Signal transducer and activator of transcription
Ta	Annealing temperature
TBE	Buffer tris-borate-EDTA

TNF	Tumor necrosis factor
TNFR	Tumor necrosis factor receptor
TNM	Tumor-Node-Metastasis
TRAF	Tumor necrosis factor receptor associated factor
TRPA1	Transient receptor potential channel A1
VEGF	Vascular endothelial growth factor
WST-1	4-(3-(4-iodophenyl)-2-(4-nitrophenyl)-2H-5-tetrazolium)-1,3-benzene disulfonate
$\Delta\Psi m$	Mitochondrial membrane potential

Bibliografy

Adinolfi B, Romanini A, Vanni A, Martinotti E, Chicca A, Fogli S, et al. (2013). Anticancer activity of anandamide in human cutaneous melanoma cells. Eur J Pharmacol 718: 154-159.

Aguado T, Carracedo A, Julien B, Velasco G, Milman G, Mechoulam R et al., (2007) Cannabinoids induce glioma stem-like cell differentiation and inhibit gliomagenesis. J Biol Chem. 282:6854-62.

Aiom-airtum, I numeri del cancro in Italia 2014, Aviable: [http://www.registri-tumori.it/cms/it/node/3412] Accessed December 12, 2014.

Aitken J, Welch J, Duffy D, Milligan A, Green A, Martin N et al. (1999) CDKN2A variants in a population-based sample of Queensland families with melanoma. J Natl Cancer Inst. 91:446-452.

AJCC, Cancer staging. Available: [https://cancerstaging.org/references-tools/Pages/What-is-Cancer-Staging.aspx] Accessed December 12, 2014.

Altieri DC (2008) Survivin, cancer netwoks and pathway-directed drug discovery. Nat Rev Cancer 8:61-70.

Altieri DC, Grossman D (2001) Drug Resistance in Melanoma: Mechanisms, Apoptosis, and New Potential Therapeutic Targets. Cancer Metastasis Rev 20:3-11.

Ambrosini G, Adida C, Altieri DC (1997) A novel anti-apoptosis gene, survivin, expressed in cancer and lymphoma. Nat med 3:917-21.

Amiri KI, Richmond A (2005) Role of nuclear factor-kappa B in melanoma. Cancer Metastasis Rev. 24:301-313.

Anavi-Goffer S et al., (2012) Modulation of L-α-lysophosphatidylinositol/GPR55 mitogen-activated protein kinase (MAPK) signaling by cannabinoids. J Biol Chem 287(1):91-104.

Anavi-Goffer S, Baillie G, Irving AJ, Gertsch J, Greig IR, Pertwee RG, et al. (2012). Modulation of L-α-lysophosphatidylinositol/GPR55 mitogen-activated protein kinase (MAPK) signaling by cannabinoids. J Biol Chem. 287: 91-104.

Andradas C, Caffarel MM, Pérez-Gómez E, Salazar M, Lorente M, Velasco G, et al. (2011). The orphan G protein-coupled receptor GPR55 promotes cancer cell proliferation via ERK. Oncogene 30: 245-252.

Baur R, Gertsch J, Sigle E (2012). The cannabinoid CB1 receptor antagonists rimonabant (SR141716) and AM251 directly potentiate GABA(A) receptors. Br J Pharmacol 165: 2479-2484.

Bhatia S, Tykodi SS, Thompson JA (2009) Treatment of metastatic melanoma: an overview. Oncology (Williston Park) 23:488-496.

Blázquez C, Carracedo A, Barrado L, Real PJ, Fernández-Luna JL, Velasco G, et al. (2006). Cannabinoid receptors as novel targets for the treatment of melanoma. FASEB J 20: 2633-2635.

Blázquez C, Carracedo A, Barrado L, Real PJ, Fernández-Luna JL, Velasco G et al., (2006) Cannabinoid receptors as novel targets for the treatment of melanoma. FASEB J. 20(14):2633-5.

Boiko AD, Razorenova OV, Van de Rijn M, Swetter SM, Johnson DL, Ly DP et al. (2010) Human melanoma-initiating cells express neural crest nerve growth factor receptor CD271. Nature 466:133–7.

Brahmer JR, Drake CG, Wollner I, Powderly JD, Picus J, Sharfman WH et al., (2010) Phase I study of single-agent anti-programmed death-1 (MDX-1106) in refractory solid tumors: safety, clinical activity, pharmacodynamics, and immunologic correlates. 28:3167-3175.

Brown A (2007). Novel cannabinoid receptors. Br J Pharmacol 152: 567-575.

Cantwell-Dorris ER, O'Leary JJ, Sheils OM (2011) BRAFV600E: implications for carcinogenesis and molecular therapy. Mol Cancer Ther.10:385-394.

Capiod T (2011). Cell proliferation, calcium influx and calcium channels. Biochimie 93: 2075-2079.

Carnero A (2002) Targeting the cell cycle for cancer therapy. Br. J.Cancer. 87:129-133.

Carrasco RA, Stamm B, Marcusson E, Sandusky G, Iversen P, Patel BK (2011) Antisense inhibition of survivin expression as a cancer therapeutic. Mol Cancer Ther 10: 221-232.

Chakravarti B, Ravi J, Ganju RK (2014) Cannabinoids as therapeutic agents in cancer: current status and future implications. Oncotarget. 5:5852-72.

Chambers CA, Kuhns MS, Egen JG, Allison JP (2001) CTLA-4-mediated inhibition in regulation of T cell responses: mechanisms and manipulation in tumor immunotherapy. Annu. Rev. Immunol. 19:565-594.

Chapman PB, Hauschild A, Robert C, Haanen JB, Ascierto P, Larkin J et al. (2011) Improved survival with vemurafenib in melanoma with BRAF mutation. N. Engl. J. Med. 364: 2507-2516.

Cheever MA, Higano CS (2011) PROVENGE (Sipuleucel-T) in prostate cancer: the first FDA-approved therapeutic cancer vaccine. Clin Cancer Res 17:3520–6.

Chen N, Gong J, Chen X, Meng W, Huang Y, Zhao F, et al. (2009) Caspases and inhibitor of apoptosis proteins in cutaneous and mucosal melanoma: expression profile and clinicopathologic significance. Hum Pathol 40:950-956.

Cheung CHA, Huang CC, Tsai FY, Lee JYC, Cheng SM, Chang YC, et al. (2013) Survivin-biology and potential as a therapeutic target in oncology. Onco Targets Ther 6:1453-1462.

Chin L (2003) The genetics of malignant melanoma: lessons from mouse and man. Nature Reviews Cancer 3:559-570.

Cho RW, Clarke MF (2008) Recent advances in cancer stem cells. Curr Opin Genet Dev. 18:48–53.

Compagnucci C, Di Siena S, Bustamante MB, Di Giacomo D, Di Tommaso M, Maccarrone M et al. (2013) Type-1 (CB1) cannabinoid receptor promotes neuronal differentiation and maturation of neural stem cells. PLoS One 8:5427.

Cully M, You H, Levine AJ, Mak, TW (2006) Beyond PTEN mutations: the PI3K pathway as an integrator of multiple inputs during tumorigenesis. Nat. Rev.Cancer. 6:184-192.

Currais A, Hortobágyi T, Soriano S (2009) The neuronal cell cycle as a mechanism of pathogenesis in Alzheimer's disease. Aging (Albany NY). 1:363-371.

Dancey J (2010) mTOR signaling and drug development in cancer. Nature Reviews Clinical Oncology 7:209-219.

Dankort D, Curley DP, Cartlidge RA, Nelson B, Karnezis AN, Damsky WE et al., (2009) Braf(V600E) cooperates with Pten loss to induce metastatic melanoma. Nat. Genet. 41:544-552.

Das S, Das J, Samadder A, Boujedaini N, Khuda-Bukhsh AR (2012). Apigenin-induced apoptosis in A375 and A549 cells through selective action and dysfunction of mitochondria. Exp Biol Med 237: 1433-1448.

Datta SR, Brunet A, Greenberg ME (1999) Cellular survival: a play in three Akts. Genes Dev. 13:2905–27.

Davis MI, Ronesi J, Lovinger DM. (2003) A predominant role for inhibition of the adenylate cyclase/protein kinase A pathway in ERK activation by cannabinoid receptor 1 in N1E-115 neuroblastoma cells. J Biol Chem. 278:48973-80.

DiPaola RS (2002). To arrest or not to G(2)-M Cell-cycle arrest : commentary re: A. K. Tyagi et al., Silibinin strongly synergizes human prostate carcinoma DU145 cells to doxorubicin-induced growth inhibition, G(2)-M arrest, and apoptosis. Clin cancer res 8: 3311-3314.

Dirks P (2010) Cancer stem cells: invitation to a second round. Nature 466:40–41.

Dohi T, Beltrami E, Wall NR, Plescia J, Altieri DC (2004) Mitochondrial survivin inhibits apoptosis and promotes tumorigenesis. J Clin Invest 114:1117-1127.

Dummer R, Hauschild A, Guggenheim M, Keilholz U, Pentheroudakis G, on behalf of the ESMO Guidelines Working Group (2012) Cutaneous melanoma: ESMO Clinical Practice Guidelines for diagnosis, treatment and follow-up *Ann Oncol* 23:vii86-vii91.

Eisenmann KM, VanBrocklin MW, Staffend NA, Kitchen SM, Koo HM.(2003) Mitogen-activated protein kinase pathway-dependent tumor-specific survival signaling in melanoma cells through inactivation of the proapoptotic protein bad. Cancer Res 63:8330-7.

Elmore S (2007). Apoptosis: a review of programmed cell death. Toxicol Pathol 35: 495-516.

Fargnoli MC, Argenziano G, Zalaudek I, Peris K. (2006) Highandlow-penetrance cutaneous melanoma susceptibility genes. Expert Rev Anticancer Ther. 6:657-670.

Fiori JL, Sanghvi M, O'Connell MP, Krzysik-Walker SM, Moaddel R, Bernier M (2011). The cannabinoid receptor inverse agonist AM251 regulates the expression of the EGF receptor and its ligands via destabilization of oestrogen-related receptor α protein. Br J Pharmacol 164: 1026-1040.

Fogli S, Nieri P, Chicca A, Adinolfi B, Mariotti V, Iacopetti P et al. (2006). Cannabinoid derivatives induce cell death in pancreatic MIA PaCa-2 cells via a receptor-independent mechanism. FEBS Lett 580: 1733-1739.

Follin-Arbelet V, Hofgaard PO, Hauglin H, Naderi S, Sundan A, Blomhoff R et al. (2011). Cyclic AMP induces apoptosis in multiple myeloma cells and inhibits tumor development in a mouse myeloma model. BMC Cancer 11: 301.

Gajewski TF, Schreiber H, Fu YX (2013) Innate and adaptive immune cells in the tumor microenvironment. Nat Immunol. 14(10):1014-22.

Galve R, Chiurchiù V, Díaz-Alonso J, Bari M, Guzmán M, Maccarrone M (2013) Cannabinoid receptor signaling in progenitor/stem cell proliferation and differentiation. Prog Lipid Res. 52:633-50.

Gandini S, Sera F, Cattaruzza MS, Pasquini P, Zanetti R, Masini C et al. (2005) Meta-analysis of risk factors for cutaneous melanoma: I. Common and atypical naevi. Eur J Cancer. 41:28–44.

Gandini S, Sera F, Cattaruzza MS, Pasquini P, Zanetti R, Masini C et al. (2005) Meta-analysis of risk factors for cutaneous melanoma: II. Sun exposure. Eur J Cancer. 41:45–60.

Gandini S, Sera F, Cattaruzza MS, Pasquini P, Zanetti R, Masini C et al. (2005) Meta-analysis of risk factors for cutaneous melanoma: III. Family history, actinic damage and phenotypic factors. Eur J Cancer. 41:2040–2059.

Garber K (2010) Industry makes strides in melanoma. Nature Biotechnology 28:763–764.

Giannetti A, Tombelli S, Baldini F (2013) Oligonucleotide optical switches for intracellular sensing. Anal Bioanal Chem 405:6181-6196.

Giles N, Pavey S, Pinder A, Gabrielli B (2012) Multiple melanoma susceptibility factors function in an ultraviolet radiation response pathway in skin. Br. J. Dermatol. 166:362-371.

Girouard SD, Murphy GF (2011) Melanoma stem cells: not rare, but well done Lab. Invest. 91:647-64.

Globacan 2012, (2014) Available: [http://globocan.iarc.fr/old/pie_site.asp?selection=16120&title=Melanoma+of+skin&sex=0&type=0&populations=0&window=1&join=1&submit=%C2%A0Execute%C2%A0] Accessed December 12, 2014.

Goggins WB, Tsao H. (2003) A population-based analysis of risk factors for a second primary cutaneous melanoma among melanoma survivors. Cancer. 97:639-643.

Gogvadze V, Robertson JD, Zhivotovsky B, Orrenius S (2001). Cytochrome c release occurs via Ca2+-dependent and Ca2+-independent mechanisms that are regulated by Bax. J Biol Chem 276: 19066-19071.

Graziani G, Tentori L, Navarra P. (2012) Ipilimumab: a novel immunostimulatory monoclonal antibody for the treatment of cancer. Pharmacol. Res. 65:9-22.

Groner B. Weiss A (2014) Targeting survivin in cancer: novel drug development approaches. BioDrugs 28:27-39.

Grösch S, Maier TJ, Schiffmann S, Geisslinger G (2006). Cyclooxygenase-2 (COX-2)-independent anticarcinogenic effects of selective COX-2 inhibitors. J Natl Cancer Inst 98: 736-747.

Grossman D, McNiff JM, Li F, Altieri DC (1999) Expression and targeting of the apoptosis inhibitor, survivin, in human melanoma. J Invest Dermatol 113:1076-1081.

Grynkiewicz G, Poenie M, Tsien RY (1985). A new generation of Ca2+ indicators with greatly improved fluorescence properties. J Biol Chem 260: 3440–3450.

Gudbjartsson DF, Sulem P, Stacey SN, Goldstein AM, Rafnar T, Sigurgeirsson B et al. (2008) ASIP and TYR pigmentation variants associate with cutaneous melanoma and basal cell carcinoma. Nat Genet. 40:886-91.

Guertin DA, Sabatini DM (2009) The Pharmacology of mTOR Inhibition. Sci Signal. 2 (67):24.

Gustafsson SB, Wallenius A, Zackrisson H, Popova D, Plym Forshell L, Jacobsson SO (2013) Effects of cannabinoids and related fatty acids upon the viability of P19 embryonal carcinoma cells. Arch Toxicol. 87:1939-51.

Halaban R (2005) Rb/E2F: a two-edged sword in the melanocytic system. Cancer Metastasis Rev. 24:339-356.

Han SX, Jia X, Ma JL, Zhu Q (2013) Molecular beacons: a novel optical diagnostic tool. Arch Immunol Ther Exp 61:139-148.

Hanaizi Z, Van Zwieten-boot B, Calvo G, Lopez AS, Van Dartel M, Camarero J et al. (2012). The European Medicines Agency review of ipilimumab (Yervoy) for the treatment of advanced (unresectable or metastatic) melanoma in adults who have received prior therapy: summary of the scientific assessment of the Committee for Medicinal Products for Human Use. Eur. J. Cancer. 48:237-242.

Hardin, Bertoni, Kleinsmith (2012) Principles of Cell Biology Aviable: [http://www.mun.ca/biology/desmid/brian/BIOL2060/BIOL2060-19/19_39.jpg] Accessed December 12, 2014.

Harland M, Cust AE, Badenas C, Chang YM, Holland EA, Aguilera P (2014) Prevalence and predictors of germline CDKN2A mutations for melanoma cases from Australia, Spain and the United Kingdom. Hereditary Cancer in Clinical Practice. 12:20.

Hartman MM, Czyz M (2013) Anti-apoptotic proteins on guard of melanoma cell survival. Cancer Lett 331: 24-34.

Haskó J, Fazakas C, Molnár J, Nyúl-Tóth Á, Herman H, Hermenean A et al., (2014) CB2 Receptor Activation Inhibits Melanoma Cell Transmigration through the Blood-Brain Barrier. Int. J. Mol. Sci. 15(5):8063-8074.

Helfand M, Mahon S, Eden K. (2001) Screening for Skin Cancer [Internet]. Rockville (MD): Agency for Healthcare Research and Quality (US); Report No.: 01-S002.U.S. Preventive Services Task Force Evidence Syntheses, formerly Systematic Evidence Reviews.

Hennessy BT, Smith DL, Ram PT, Lu Y, Mills GB (2005) Exploiting the PI3K/AKT Pathway for Cancer Drug Discovery. Nature Reviews Drug Discovery 4:988-1004.

Herrera-Gonzalez NE (2013) Interaction Between the Immune System and Melanoma, in Recent Advances in the Biology, Therapy and Management of Melanoma. Eited Lester MD.

Hocker T, Tsao H (2007) Ultraviolet radiation and melanoma: a systematic review and analysis of reported sequence variants. Hum. Mutat. 28: 578-588.

Holderfield M, Deuker M, McCormick F, McMahon M (2014). Targeting RAF kinases for cancer therapy: BRAF-mutated melanoma and beyond. Nat Rev Cancer 14: 455-467.

Huang H, Wang X, Ding X, Xu Q, Hwang SK, Wang F et al. (2014). Effect and mechanism of tacrolimus on melanogenesis on A375 human melanoma cells. Chin Med J (Engl) 127: 2966-2971.

Huang SH, Wu LW, Huang AC, Yu CC, Lien JC, Huang YP et al. (2012). Benzyl isothiocyanate (BITC) induces G2/M phase arrest and apoptosis in human melanoma A375.S2 cells through reactive oxygen species (ROS) and both mitochondria-dependent and death receptor-mediated multiple signaling pathways. J Agric Food Chem 60: 665-675.

Hu-Lieskovan S, Robert L, Homet Moreno B, Ribas A (2014). Combining targeted therapy with immunotherapy in BRAF-mutant melanoma: promise and challenges. J Clin Oncol 32: 2248-2255.

Ibrahim N, Haluska FG (2009) Molecular pathogenesis of cutaneous melanocytic neoplasms. Annu. Rev. Pathol. 4:551-579.

Ikeguchi M, Liu J, Kaibara N (2002) Expression of survivin mRNA and protein in gastric cancer cell line (MKN-45) during cisplatin treatment. Apoptosis 1:23-9.

Jemal A, Saraiya M, Patel P, Cherala SS, Barnholtz-Sloan J, Kim J et al. (2011) Recent trends in cutaneous melanoma incidence and death rates in the United States, 1992-2006. J Am Acad Dermatol. 65:S17-25.

Johns DG, Behm DJ, Walker DJ, Ao Z, Shapland EM, Daniels DA, et al. (2007). The novel endocannabinoid receptor GPR55 is activated by atypical cannabinoids but does not mediate their vasodilator effects. Br J Pharmacol 152: 825-831.

Johnson JD, Young B (1996) Demographics of brain metastasis. Neurosurg Clin N Am.7:337-44.

Kaneko N, Yamanaka K, Kita A, Tabata K, Akabane T, Mori M (2013) Synergistic antitumor activities of sepantronium bromide (YM155), a survivin suppressant, in combination with microtubule-targeting agents in triple-negative breast cancer cells. Biol Pharm Bull 36:1921-7.

Kanwar JR, Kamalapuram SK, Kanwar RK (2013) Survivin signaling in clinical oncology: a multifaceted dragon. Med Res Rev. 33:765-89.

Kapur A, Zhao P, Sharir H, Bai Y, Caron M, Barak L, et al. (2009). Atypical responsiveness of the orphan receptor GPR55 to cannabinoid ligands. J Biol Chem 284: 29817-29827.

Kapur A, Zhao P, Sharir Y, Caron M, Barak L, Abood M (2009) Atypical responsiveness of the orphan receptor GPR55 to cannabinoid ligands. J Biol Chem 284(43):29817-27.

Karbowniczek M, Spittle CS, Morrison T, Wu H, Henske EP (2008) mTOR is activated in the majority of malignant melanomas. J. Invest. Dermatol. 128:980-987.

Kauffmann RM, Chen SL (2014) Workup and staging of malignant melanoma. Surg Clin North Am. 94:963-72.

Kolpashchikov DM (2012) An elegant biosensor molecular beacon probe: challenges and recent solutions. Scientifica 2012:1-17.

Krzysik-Walker S, González-Mariscal I, Scheibye-Knudsen M, Indig F, Bernier M (2013). The biarylpyrazole compound AM251 alters mitochondrial physiology via proteolytic degradation of ERRα. Mol Pharmacol 83: 157-166.

Lasithiotakis K, Leiter U, Meier F, Eigentler T, Metzler G, Moehrle M et al. (2008) Age and gender are significant independent predictors of survival in primary cutaneous melanoma. Cancer. 112:1795-1804.

Lee N, Barthel SR, Schatton T (2014) Melanoma Stem Cells and Metastasis: Mimicking Hematopoietic Cell Trafficking? Lab Invest. 94:13–30.

Li G, Chang H, Zhai YP, Xu W. (2013) Targeted silencing of inhibitors of apoptosis proteins with siRNAs: a potential anti-cancer strategy for hepatocellular carcinoma. Asian Pac J Cancer Prev. 14(9):4943-52.

Li H, Niederkon JY, Neelam S, Alizadeh H (2006) Downregulation of survivin expression enhances sensitivity of cultured uveal melanoma cells to cisplatin treatment. Exp Eye Res 83:176-182.

Ligresti A, Petrosino S, Di Marzo V (2009) From endocannabinoid profiling to 'endocannabinoid therapeutics'. Curr. Opin. Chem. Biol. 13:321–331.

Madhunapantula SV, Robertson GP (2009) The PTEN-AKT3 signaling cascade as a therapeutic target in melanoma. Pigment Cell Melanoma Res. 22: 400-419.

Madonna G, Ullman CD, Gentilcore G, Palmieri G, Ascierto PA (2012) NF-kappaB as potential target in the treatment of melanoma. J. Transl. Med. 10:53.

Martí RM, Sorolla A, Yeramian A (2012) New therapeutic targets in melanoma. Actas. Dermosifiliogr. 103: 579-590.

McKenzie JA, Liu T, Goodson AG, Grossman D (2010) Survivin enhances motility of melanoma cells by supporting Akt activation and {alpha}5 integrin upregulation. Cancer Res 70:7927-7937.

McKenzie JA, Liu T, Jung JY, Jones BB, Ekiz HA, Welm AL, et al. (2013) Survivin promotion of melanoma metastasis requires upregulation of α5 integrin. Carcinogenesis 34:2137-2144.

Melero I, Hervas-stubbs S, Glennie M, Pardoll DM, Chen L (2007) Immunostimulatory monoclonal antibodies for cancer therapy. Nature Reviews Cancer. 7:95-106.

Merriam-Webster. Melanoma. Available: [http://www.merriam-webster.com/medical/melanoma] Accessed December 12, 2014

Meyle KD, Guldberg P. (2009) Genetic risk factors for melanoma. Hum Genet. 126:499-510.

Mihic LL, Bulat V, Situm M, Krolo I, Seserko A (2010) The role of apoptosis in the pathogenesis of malignant melanoma. Coll. Antropol. 34:303-306.

Miller DM, Flaherty KT, Tsao H (2014) Current status and future directions of molecularly targeted therapies and immunotherapies for melanoma. Semin Cutan Med Surg. 33:60-7.

Mita AC, Mita MM, Nawrocki ST, Giles FJ (2008) Survivin: key regulator of mitosis and apoptosis and novel target for cancer therapeutics. Clin Cancer Res 14:5000-5005.

Molckovsky A, Siu LL (2008) First-in-class, first-in-human phase I results of targeted agents: highlights of the 2008 American society of clinical oncology meeting. J. Hematol. Oncol. 29:1-20.

Moriconi A, Cerbara I, Maccarrone M, Topai A (2010). GPR55: Current knowledge and future perspectives of a purported "Type-3" cannabinoid receptor. Curr Med Chem 17: 1411-1429.

Mouawad R, Sebert M, Michels J, Bloch J, Spano JP, Khayat D.(2010) Treatment for metastatic malignant melanoma: old drugs and new strategies. Crit Rev Oncol Hematol 74:27-39.

Na YR, Seok SH, Kim DJ, Han JH, Kim TH, Jung H et al., (2009) Isolation and characterization of spheroid cells from human malignant melanoma cell line WM-266-4. Tumor Biology 30:300-309.

National Cancer Istitute. Melanoma Anatomy. Available: [https://visualsonline.cancer.gov/details.cfm?imageid=8284] Accessed December 12, 2014.

National Cancer Istitute. Melanoma. Available: [http://www.cancer.gov/cancertopics/types/melanoma] Accessed December 12, 2014 NCCN Guidelines–Melanoma –Version 1.2015.

Neri T, Cordazzo C, Carmazzi Y, Petrini S, Balìa C, Stefanelli F, Brunelleschi S, Breschi MC, Pedrinelli R, Paggiaro P, Celi A (2012) Effects of peroxisome proliferator-activated receptor-γ agonists on the generation of microparticles by monocytes/macrophages. Cardiovasc Res. 94:537-44.

Nitin N, Santangelo PJ, Kim G, Nie S, Bao G (2004) Peptide linked molecular beacons for efficient delivery and rapid mRNA detection in living cells. Nucleic Acids Res 32:58.

Oehler B, Scholze A, Schaefer M, Hill K (2012). TRPA1 is functionally expressed in melanoma cells but is not critical for impaired proliferation

caused by allyl isothiocyanate or cinnamaldehyde. Naunyn Schmiedebergs Arch Pharmacol 385: 555-563.

Ozao-Choy J, Lee DJ, Faries MB (2014) Melanoma vaccines: mixed past, promising future. Surg Clin North Am. 94:1017-30.

Patil M, Patwardhan A, Slas M, Hargreaves K, Akopian A (2011). Cannabinoid receptor antagonists AM251 and AM630 activate TRPA1 in sensory neurons. Neuropharmacology 61: 778-788.

Paul RK, Wnorowski A, Gonzalez-Mariscal I, Nayak SK, Pajak K, Moaddel R et al. (2014). (R,R')-4'-methoxy-1-naphthylfenoterol targets GPR55-mediated ligand internalization and impairs cancer cell motility. Biochem Pharmacol 87: 547-556.

Peng XH, Cao ZH, Xia JT, Carlson GW, Lewis MM, Wood WC, Yang L (2005) Real-time detection of gene expression in cancer cells using molecular beacon imaging: new strategies for cancer research. Cancer Res 65:1909-17.

Pennati M, Folini M, Zaffaroni N. Targeting survivin in cancer therapy (2008) Expert Opin Ther Targets 124:463-476.

Pertwee R (2010). Receptors and channels targeted by synthetic cannabinoid receptor agonists and antagonists. Curr Med Chem 17: 1360-1381.

Pertwee R, (2010) Receptors and channels targeted by synthetic cannabinoid receptor agonists and antagonists. Curr Med Chem 17(14):1360-81.

Picard M, Pham Dang N, D'Incan M, Mansard S, Dechelotte P, Pereira B et al. (2014). Is BRAF a prognostic factor in stage III skin melanoma? A retrospective study of 72 patients after positive sentinel lymph node dissection. Br J Dermatol 171: 108-114.

Piñeiro R, Maffucci T, Falasca M (2011). The putative cannabinoid receptor GPR55 defines a novel autocrine loop in cancer cell proliferation. Oncogene 30: 142-152.

Pisanti S, Picardi P, D'Alessandro A, Laezza C, Bifulco M (2013) The endocannabinoid signaling system in cancer. Trends Pharmacol. *Sci.* 34:273–82.

Platz A, Egyhazi S, Ringborg U, Hansson J (2008) Human cutaneous melanoma; a review of NRAS and BRAF mutation frequencies in relation to histogenetic subclass and body site. Mol. Oncol. 1:395-405.

Populo H, Soares P, Faustino A, Rocha AS, Silva P, Azevedo F et al. (2011) mTOR pathway activation in cutaneous melanoma is associated with poorer prognosis characteristics. Pigment Cell Melanoma Res. 24: 254-257.

Porta C, Paglino C, Mosca A (2014) Targeting PI3K/Akt/mTOR Signaling in Cancer. Front Oncol. 4:64.

Pucci M, Pasquariello N, Battista N, Di Tommaso M, Rapino C, Fezza F et al., (2012) Endocannabinoids stimulate human melanogenesis via type-1 cannabinoid receptor. J Biol Chem. 287(19):15466-78.

Quintana E, Shackleton M, Sabel MS, Fullen DR, Johnson TM, Morrison SJ (2008) Efficient tumour formation by single human melanoma cells. Nature. 456:593-598.

Raffa R, Ward S (2012). CB_1-independent mechanisms of Δ^9-THCV, AM251 and SR141716 (rimonabant). J Clin Pharm Ther 37: 260-265.

Repetto G, del Peso A, Zurita JL (2008) Neutral red uptake assay for the estimation of cell viability/cytotoxicity. Nat Protoc. 3(7):1125-31.

Ribas A, Kefford R, Marshall MA, Punt CJA, Haanen JB, Marmol M et al. (2013) Phase III Randomized Clinical Trial Comparing Tremelimumab With Standard-of-Care Chemotherapy in Patients With Advanced Melanoma. J Clin Oncol. 31:616-622.

Rigel DS (2010) Trends in dermatology: melanoma incidence. Arch Dermatol 146:318.

Ross R (2009) The enigmatic pharmacology of GPR55. Trends Pharmacol Sci 30(3):156-63.

Ryan MB, O'Donovan N, Duffy MJ (2009) Survivin: a new target for anti-cancer therapy. Cancer Treat Rev 35:553-562.

Ryberg E, Larsson N, Sjögren S, Hjorth S, Hermansson NO, Leonova J et al. (2007). The orphan receptor GPR55 is a novel cannabinoid receptor. Br J Pharmacol 152: 1092-1101.

Sánchez MG, Ruiz-Llorente L, Sánchez AM, Díaz-Laviada I (2003) Activation of phosphoinositide 3-kinase/PKB pathway by CB(1) and CB(2) cannabinoid receptors expressed in prostate PC-3 cells. Involvement in Raf-1 stimulation and NGF induction. Cell Signal. 15:851-9.

Santangelo P, Nitin N, Bao G (2006) Nanostructured probes for RNA detection in living cells. Ann biomed eng 34:39-50.

Santangelo PJ, Nix B, Tsourkas A, Bao G (2004) Dual FRET molecular beacons for mRNA detection in living cells. Nucleic Acids Res 32:57.

Santini R, Pietrobono S, Pandolfi S, Montagnani V, D'Amico M, Penachioni JY et al., (2014) SOX2 regulates self-renewal and tumorigenicity of human melanoma-initiating cells. Oncogene. 33:4697-708.

Santini R, Vinci MC, Pandolfi S, Penachioni JY, Montagnani V, Olivito B et al., (2012) Hedgehog-GLI signaling drives self-renewal and tumorigenicity of human melanoma-initiating cells. Stem Cells. 30:1808-18.

Sarbassov DD, Ali SM, Kim DH, Guertin DA, Latek RR, Erdjument-Bromage H et al. (2004) Rictor, a novel binding partner of mTOR, defines a rapamycin-insensitive and raptorindependent pathway that regulates the cytoskeleton. Curr Biol 14:1296–302.

Schatton T, Frank M.H.(2008) Cancer stem cells and human malignant melanoma. Pigment Cell Melanoma Res. 21:39-55.

Schwartzentruber DJ, Lawson DH, Richards JM, et al. (2011) gp100 peptide vaccine and interleukin-2 in patients with advanced melanoma. N Engl J Med. 364:2119–27.

Seely K Brents LK, Franks LN, Rajasekaran M, Zimmerman SM, Fantegrossi WE, et al. (2012). AM-251 and rimonabant act as direct antagonists at mu-opioid receptors: implications for opioid/cannabinoid interaction studies. Neuropharmacology 63: 905-915.

Sekulic A, Haluska PJr, Miller AJ, Genebriera De Lamo JES, Pulido JS et al. (2008) Malignant melanoma in the 21st century: the emerging molecular landscape. Mayo. Clin. Proc. *83:*825-846.

Shakhova O (2014) Neural crest stem cells in melanoma development. Curr Opin Oncol. 26:215-221.

Sharir H, Abood M (2010) Pharmacological characterization of GPR55, a putative cannabinoid receptor. Pharmacol Ther 126(3):301-13.

Sharir H, Abood M (2010). Pharmacological characterization of GPR55, a putative cannabinoid receptor. Pharmacol Ther 126: 301-313.

Shi W, Li J, Bao Q, Wu J, Ge L, Zhu L, Wang Y, Zhu W (2014) Survivin mRNA expression in blood as a predictor of the response to EGFR-tyrosine kinase inhibitors and prognosis in patients with non-small cell lung cancer. Med Oncol 31:893.

Siegel R, Ma J, Zou Z, Jemal A (2014) Cancer statistics, 2014. CA Cancer J Clin. 64:9-29.

Sinha R, Kim GJ, Nie S, Shin DM (2006) Nanotechnology in cancer therapeutics: bioconjugated nanoparticles for drug delivery. Mol Cancer Ther 5:1909-17.

Smalley KS (2010) Understanding melanoma signaling networks as the basis for molecular targeted therapy. J. Invest. Dermatol. 130:28-37.

Sosman J, Unger J, Liu P, et al. (2002) Adjuvant immunotherapy of resected, intermediate-thickness, node-negative melanoma with an allogeneic tumor vaccine: impact of HLA class I antigen expression on outcome. J Clin Oncol. 20:2067–75.

Stahl JM, Cheung M, Sharma A, Trivedi NR, Shanmugam S, Robertson GP (2003) Loss of PTEN promotes tumor development in malignant melanoma. Cancer Res. 63:2881-2890.

Stahl JM, Sharma A, Cheung M, Zimmerman M, Cheng JQ, Bosenberg MW et al. (2004) Deregulated Akt3 activity promotes development of malignant melanoma. Cancer Res. 64:7002-7010.

Stecca B, Santini R, Pandolfi S, Penachioni JY (2013) Culture and isolation of melanoma-initiating cells. Curr Protoc Stem Cell Biol. 3,6

Sullivan RJ, Flaherty KT (2013) Resistance to BRAF-targeted therapy in melanoma. Eur J Cancer. 49:1297-1304.

Szafer-Glusman E, Fuller M, Giansanti M (2011) Role of survivin in cytokinesis revealed by a separation of function allele. Mol Biol Cell 20:3779-2790.

Takeuchi H, Morton DL, Elashoff D, Hoon DSB (2005) Survivin expression by metastatic melanoma predicts poor disease outcome in patients receiving adjuvant polyvalent vaccine. Int J Cancer 117:1032-8.

Tarhini AA, Edington H, Butterfield LH, Sinha M, Moschos SJ, Tawbi H, Shuai Y (2011) Neoadjuvant ipilimumab in patients with stage IIIB/C melanoma: immunogenicity and biomarker analysis. J. Clin. Oncol. 29: 8536.

Tsao H, Atkins MB, Sober AJ. (2004) Management of cutaneous melanoma. N Engl J Med. 351:998–1012.

Tseng HW, Li WT, Hsieh JF (2013) Targeted Agents for the Treatment of Melanoma: An Overview, in Recent Advances in the Biology, Therapy and Management of Melanoma. Eited Lester MD.

Uzdensky AB, Demyanenko SV, Bibov MY (2013) Signal Transduction in Human Cutaneous Melanoma and Target Drugs. Curr Cancer Drug Targets. 13:843-866.

Vainio H, Miller AB, Bianchini F. (2000) An international evaluation of the cancer-preventive potential of sunscreens. Int J Cancer. 88:838-42.

Vong Q, Cao K, Li H, Iglesias P, Zheng Y (2005) Chromosome alignement and segregation regulated by ubiquitination of survivin. Science 310:1499-1505.

Wang Q, Chen L, Long Y, Tian H, Wu J (2013) Molecular beacons of xeno-nucleic acid for detecting nucleic acid. Theranostics 3:395-408.

Wei G, Wang S, Cui S, Guo J, Liu Y, Liu Y, et al. (2014). Synthesis and evaluation of the anticancer activity of albiziabioside A and its analogues as apoptosis inducers against human melanoma cells. Org Biomol Chem 12: 5928-5935.

Weinstock MA (2012) Reducing death from melanoma and standards of evidence. J Invest Dermatol. 132: 1311-1312.

Wolchok JD (2014) Melanoma Aviable: [http://www.cancerresearch.org/cancer-immunotherapy/impacting-all-cancers/melanoma] Accessed: December 12, 2014.

Woods D, Cherwinski H, Venetsanakos E, Bhat A, Gysin S, Humbert M et al. (2001) Induction of beta3-integrin gene expression by sustained activation of the Ras-regulated Raf-MEK-extracellular signal-regulated kinase signaling pathway. Mol. Cell. Biol. 21:319-3205.

Yamanaka K, Nakahara T, Yamauchi T, Kita A, Takeuchi M, Kiyonaga F, et al. (2011) Antitumor activity of YM155, a selective small-molecule survivin suppressant, alone and in combination with docetaxel in human malignant melanoma models. Clin Cancer Res 17:5423-5431.

Yamashita A, Oka S, Tanikawa T, Hayashi Y, Nemoto-Sasaki Y, Sugiura T (2013). The actions and metabolism of lysophosphatidylinositol, an endogenous agonist for GPR55. Prostaglandins Other Lipid Mediat 107: 103-116.

Yang H, Fu JH, Hu Y, Huang WZ, Zheng B, Wang G, et al. (2008) Influence of siRNA targetingsurvivin on chemosensitivity of H460/cDDP lung cancer cells. J Int Med Res 36:734-747.

Zhao Z, Yang J, Zhao H, Fang X, Li H. (2012) Cannabinoid receptor 2 is upregulated in melanoma. J Cancer Res Ther. 8(4):549-54.

Zheng W, Chen H, Yuan S, Wu L, Zhang W, Sun H, et al. (2012) Overexpression of βIII-tubulin and survivin associated with drug resistance to docetaxel-based chemotherapy in advanced gastric cancer. J Buon 17:284-290.

Zhou L, Chen Z, Wang F, Yang X, Zhang B (2013) Multifunctional triblock co-polymer mP3/4HB-b-PEG-b-lPEI for efficient intracellular siRNA delivery and gene silencing. Acta Biomater. 9(4):6019-31.